HUNGARIAN UNIVERSITY OF AGRICULTURE AND LIFE SCIENCES

Doctoral School of Animal Biotechnology and Animal Science

IMPACT OF ENVIRONMENTAL EXPOSURES ON EARLY HUMAN CARDIAC DIFFERENTIATION OF INDUCED PLURIPOTENT STEM CELLS

DOI: 10.54598/005140

Doctoral (PhD) dissertation

Federica Lamberto

Gödöllő

2024

The PhD program

Name: Doctoral School of Animal Biotechnology and Animal Science

Discipline: Animal Science

Leader of the school: Professor Dr. Miklós Mézes, D.V.M., Member of the HAS

Head of Department,

Hungarian University of Agriculture and Life Sciences, Institute of Physiology and Animal Nutrition, Department of Nutritional Safety

Supervisor: Professor Dr. András Dinnyés, D.V.M, D.Sc.

Hungarian University of Agriculture and Life Sciences, Institute of Physiology and Animal Nutrition, Department of Physiology and Animal Health

……..……

Approval of the PhD School leader

……..……

Approval of the Supervisor

TABLE OF CONTENTS

LIST OF ABBREVIATIONS

2D	Two-dimensional
3D	Three-dimensional
AR	Androgen receptor
ARE	Androgen response elements
Arh	Aryl hydrocarbon receptor
ART	Assisted reproductive technologies
ATP	Adenosine triphosphate
BM	Basement membrane
BMI	Body mass index
BMP-2	Bone morphogenetic protein 2
BPA	Bisphenol A
CAD	Coronary heart disease
CLARITY-BPA	Consortium Linking Academic and Regulatory Insights on BPA Toxicity
COL4A1	Collagen type IV α-1 chain
COL4A2	Collagen type IV α-2 chain
CTD	Comparative Toxicogenomic Database
CVDs	Cardiovascular diseases
DOHaD	Developmental origins of health and disease
DPBS	Dulbecco's phosphate-buffered saline
DRP1	Calcineurin (CnAβ)-dynamin-related protein 1
E2	17-β estradiol
EB	Embryoid body
EC50	Half maximal effective concentration
ECM	Extracellular matrix
EDC	Endocrine disrupting compound
EFSA	European Food Safety Authority
ER	Estrogen receptor
ErbB	Epidermal growth factor receptor family proteins
ERE	Estrogen response elements
ESC	Embryonic stem cell
GO	Gene Ontology
H/R	Hypoxia/reoxygenation
HEK293	Human Embryonic Kidney 293 cell line

hERG K^+	Human ether-a-go-go related gene potassium channel
hESC-CMs	Human embryonic stem-cell-derived cardiomyocytes
HFD	High-fat diet
hiPSC	Human induced pluripotent stem cell
hiPSC-CMs	Human induced pluripotent stem cell-derived cardiomyocytes
HPA	Human Protein Atlas
HSPG2	Perlecan
LAMA1	Laminin subunit α-1
LAMB1	Laminin subunit β-1
LAMC1	Laminin subunit γ-1
LC-MS/MS	Label-free liquid chromatography-tandem mass spectrometry analysis
mRNA	Messenger ribonucleic acid
MHC	Myosin heavy chain
NAM	New approach methodology
NCD	Non-communicable disease
NHANES	National Health and Nutrition Examination Survey
NID2	Nidogen-2
Oct3/4	Octamer-binding transcription factor 3/4
PC	Periconceptional
PFA	Paraformaldehyde
PPI	Protein-protein interaction
ROS	Reactive oxygen species
RT-qPCR	Quantitative reverse transcription polymerase chain reaction
SERBP1	Plasminogen activator inhibitor 1 RNA-binding protein
TDI	Tolerable daily intake
TNNC1	Troponin C1
TR	Thyroid hormone receptor
TUB33	Beta 3 tubulin

1 INTRODUCTION

The rise in chronic diseases (e.g., diabetes, obesity, cardiovascular diseases, neuronal disorders) is increasingly attributed to environmental factors. In the 1980s, Barker and colleagues hypothesised that late-life conditions might originate during the periconceptional (PC) period, the theory now known as Developmental Origins of Health and Disease (DOHaD) (Barker & Osmond, 1988; Barker, 1995; Barker et al., 1989). When the foetus is exposed to an adverse uterine environment, it responds by developing adaptations to survive, but in the long term, this state can cause irreversible changes in the development, structure and function of certain tissues and vital organs. Consequently, there is a significant risk of developing non-communicable diseases (NCDs), which can result in cardiovascular, metabolic, and neurological disorders in childhood, adolescence, and adulthood (Fleming et al., 2018). According to evidence from animal models and observational studies in humans, exposure to environmental factors, such as toxins, during the PC period can negatively impact organ development (Fleming et al., 2018).

Bisphenol A (BPA) is an endocrine-disrupting compound (EDC), frequently used in the production of plastics and epoxy resins. Due to its widespread use, BPA is pervasive within the environment and potentially harmful for human health, increasing the risk of metabolic disorders, cancer, cardiovascular and neurological diseases (Cimmino et al., 2020). Through interaction with consumer products, dietary intake, or inhalation, humans are exposed repeatedly to BPA (Ma et al., 2019). Therefore, BPA is commonly detected in human biological fluids (e.g., urine, maternal blood), and placental tissue (Fonseca et al., 2022). The BPA daily intake for humans is estimated between 1-5 µg/kg/day (Murata & Kang, 2018), and a safe tolerable daily intake (TDI) was set to 4 µg/kg/day in 2015 (University of Hertfordshire, 2021). However, according to the Endocrine Society, assumptions regarding a safe TDI are highly questionable, because BPA responses are typically non-monotonic, a trait of EDCs (Gore et al., 2015). Numerous effects of BPA on the heart and its development are documented (Fonseca et al., 2022; Gao & Wang, 2014). Epidemiological studies have connected the BPA's negative effects to the predisposition of cardiovascular diseases (CVDs) (Melzer et al., 2010, 2012; Moon et al., 2021). Studies conducted in zebrafish, rodents, and non-human primates, revealed that gestational BPA exposure increases the risk of heart developmental abnormalities, through molecular and structural alterations (Chapalamadugu et al., 2014; Chen et al., 2020; Fonseca et al., 2022; Lombó et al., 2019; Rasdi et al., 2020; Ross Brown et al., 2019; Yujiao et al., 2023). Despite several studies, the effects of BPA toxicity on foetal heart development are still largely unknown, and the current research mostly

comes from animal models, which have significant limitations, including inter-species physiological differences with humans (Daley, 2022; Fischer et al., 2020; Fonseca et al., 2022).

Recently, *in vitro* models have attracted considerable attention for the study of developmental toxicity, representing a valid tool for regulators to characterise and integrate new strategies for risk assessment of environmental chemicals (Niethammer et al., 2022; Xie et al., 2020). Because of this, the use of human induced pluripotent stem cells (hiPSCs) as a New Approach Methodology (NAM) for studying cardiac toxicity and development has gained considerable attention (Daley, 2022; Zink et al., 2020). The differentiation of hiPSCs into cardiomyocytes (hiPSC-CMs) *in vitro* provides a unique platform to investigate the cellular and molecular mechanisms of cardiomyocyte development and function (Burridge et al., 2014; Zhao et al., 2019). The use of hiPSC-CMs has allowed the study of cardiotoxicity *in vitro*, with a broad variety of chemicals (Burnett et al., 2021a). However, a vast majority of studies focus on the immediate effects of toxicants after acute treatment, while chronic exposure (repeated for several days to weeks) has only been investigated recently (Narkar et al., 2022). In this regard, BPA toxicity *in vitro* has been documented mainly after acute exposure, showing the effects of higher doses than those that are typically observed in an environmental pollution context. Concentrations above 3 μM represent the tolerable daily intake (TDI) of 50 μg/kg/day assumed to be "safe" before 2015 (Vom Saal & Vandenberg, 2021), while doses lower than 1 μM, correspond to the TDI of ≤ 4 μg/kg/day agreed after 2015 (University of Hertfordshire, 2021). Concentrations above 10 μM are part of supraphysiological range. Human iPSC-CMs treated with BPA doses above 10 μM mainly showed contractility alterations, reducing the amplitude and duration of field potential, and inhibiting ion channels and calcium currents in a dose-dependent manner (Hyun et al., 2021; Prudencio et al., 2021). In the work of O'Reilly *et al.*, the predominant voltage-gated Na^+ channel subtype in the human heart (hNav1.5), transiently expressed in HEK293 cell line, is blocked after BPA treatment (O'Reilly et al., 2012). In cardiac tissue, this effect reduces the rate of depolarization and slows cardiac conduction velocity (Ramadan et al., 2020). Due to its endocrine disruptor properties, high micromolar doses of BPA and 17β-estradiol (E2) showed similar toxicity effects on hiPSC-CMs, such as decreased depolarizing spike amplitude and shorter calcium transient duration (Cooper et al., 2023). Recently, acute exposure to environmentally relevant doses of BPA has been investigated. The results showed that, even after a short treatment (minutes to a few hours), nanomolar doses of the chemical caused significant functional alterations. For example, BPA at very low concentrations (1-10 nM) delayed the repolarization and prolonged the action potential duration through inhibition of the human ether-a-go-go related gene potassium (hERG K^+) channel in hiPSC-CMs (Kofron et al., 2021; Ma, et al., 2023). In the work of Cheng and colleagues, BPA at low doses

could induce cardiac hypertrophy via the calcineurin (CnAβ)-dynamin-related protein 1 (DRP1) signalling pathway by disrupting Ca^{2+} homeostasis, in human embryonic stem-cell-derived cardiomyocytes (hESC-CMs) (Cheng et al., 2020).

However, to better evaluate BPA's pleiotropic effects, as well as the extent of cardiac damage when compared to a single exposure, further research is needed to investigate the effects of BPA after repeated exposure during early human cardiomyocyte development. While it is crucial to conduct *in vitro* experiments over short durations, with the aim to provide effect and concentration-response information as input to hazard and risk assessment, potential chronic effects that occur over time are not usually considered. Thus, developing new model systems to mimic human chronic exposure and its effects is of the utmost importance to make *in vitro* methods more broadly useful in risk assessment. Only a limited number of studies evaluated the effects of BPA during *in vitro* cardiomyocyte differentiation. In this regard, mouse ESC-CMs or H9c2 rat embryonic cardiomyoblasts have been used (Escarda-Castro et al., 2021; Lee et al., 2019; Zhou et al., 2020). These studies reported that BPA altered the transcriptional levels of genes related to heart physiology (Lee et al., 2019; Zhou et al., 2020), or increased the percentage of DNA repair foci and decreased the levels of epigenetic marks (Escarda-Castro et al., 2021). That said, the effects of low doses and repeated exposure to BPA on human *in vitro* cardiomyocyte differentiation still require further investigation. Moreover, co-exposure with other endogenous and exogenous agents, which could easily occur during daily life and early development, is an additional confounding factor in understanding the impact of BPA on human health. For example, *in vitro* and *in vivo* studies investigated the interactions between BPA and factors such as dietary compounds, therapeutics, and other environmental compounds, or well-known stressors such as hypoxia (Sonavane & Gassman, 2019). For this reason, the integration of other stress factors can provide more robust study designs to evaluate BPA's toxicity.

In this study, we established an *in vitro* human-based iPSC-CM to assess early cardiac developmental toxicity of DOHaD-related chemical exposure. To increase the relevance of toxicity assessment *in vitro*, we mimicked, for the first time, a chronic exposure scenario to investigate the effects of environmental doses of BPA during human cardiomyocyte differentiation. Our model provided information of disturbances caused by BPA on functionality, molecular features, and cellular surrounding environment during early phases of human foetal cardiomyocyte development. Additionally, quantitative proteomics together with network mapping revealed BPA-induced molecular alterations that could be linked to hiPSC-CMs phenotypical alterations, and CVDs associations. Furthermore, the toxicity raised after BPA treatment was investigated exposing the hiPSC-CMs to a hypoxia-reoxygenation (H/R) insult.

Thus, our *in vitro* cardiotoxicity study can provide valuable supplementary information on environmental chemical risk assessment for regulators.

1.1 Objectives of the PhD

In this study, we aimed to investigate the molecular and functional alterations of environmentally relevant doses of BPA during early cardiomyocyte differentiation using a human induced pluripotent stem cell-derived model. For this purpose, firstly cardiomyocytes obtained from hiPSCs in a two-dimensional (2D) *in vitro* differentiation system were characterised by demonstrating the expression of key cardiac genes, their spontaneous beating activity, and the proteome profile. Next, to investigate the effects of BPA, we emulated a chronic exposure scenario, treating the cells starting from the pluripotency stage throughout the cardiac differentiation process. The treatment outcomes were evaluated using flow cytometry, contractility assay and quantitative proteomics. Finally, we aimed to analyse the effects raised after BPA treatment by exposing the hiPSC-CMs to a hypoxia-reoxygenation insult.

The overall aim of this study was to find answers to the following scientific questions:

- Do hiPSC-CMs represent a valid model to study chemical exposures during early cardiomyocyte development *in vitro*?
- Do low doses of BPA affect the efficiency of cardiomyocyte differentiation and their viability over time? Does the chemical cause alterations to cellular proliferation and DNA lesions?
- Is the functionality altered in hiPSC-CMs after 21-day treatment with BPA?
- Is the proteome profile different in hiPSC-CM treated with BPA? Does the BPA treatment reveal early biomarkers which can be linked to cardiomyocyte alterations and/or heart diseases?
- What impact does the repeated treatment with BPA have on the hiPSC-CMs, if exposed to additional stress such as hypoxia-reoxygenation? Are the hiPSC-CMs more vulnerable?

Specific objectives of the research:

- Establishment and maintenance of hiPSC-CM cultures and their characterisation by the expression of cardiac markers and their spontaneous beating activity.
- Validation of the hiPSC-CMs as a NAM to study chemical exposures *in vitro*.
- Evaluation of the effects of BPA during early stages of cardiomyocyte differentiation.
- Protein analysis of the hiPSC-CMs treated with environmentally relevant doses of BPA.
- Investigation of altered biomarkers and diseases association study.
- Evaluation of the effects of hypoxia-reoxygenation stress on the hiPSC-CMs treated with BPA.

2 LITERATURE OVERVIEW

2.1 DOHaD concept

There is solid evidence showing that offspring worldwide exhibit future disease risks associated with different exposures of their parents, including chemical, nutritional, and environmental stressors or other conditions like reproductive failure, adverse pregnancy outcome, diabetes, obesity and assisted reproductive technologies (ART) (Fleming et al., 2018; Velazquez et al., 2019). The most sensitive time window is represented by the PC period, which includes 5- to 6-month crucial steps, embracing oocyte growth, fertilization, gamete maturation and embryonic development up until week 10 of gestation (Velazquez et al., 2019). The Developmental Origins of Health and Disease (DOHaD) hypothesis, originally described by Barker and colleagues (Barker & Osmond, 1988; Barker et al., 1989), has significant implications for understanding the associations between environmental conditions and an individual status. The hypothesis postulates that, during critical periods in development, the organism exposed to environmental cues exhibits an enhanced adaptation to survival. This can be referred to as "reprogramming" developmental trajectories to adapt to novel conditions and diverse surroundings (Lacagnina, 2020). However, while this mechanism can confer immediate survival advantages, this can lead to irreversible changes in the development, structure, and function of some tissues and vital organs, affecting postnatal health (Fleming et al., 2015; Velazquez et al., 2019). As a result, individuals might be predisposed to non-communicable diseases (NCDs), including cardiovascular, metabolic, and neurological disorders (**Figure 1**) (Yajnik et al., 2016).

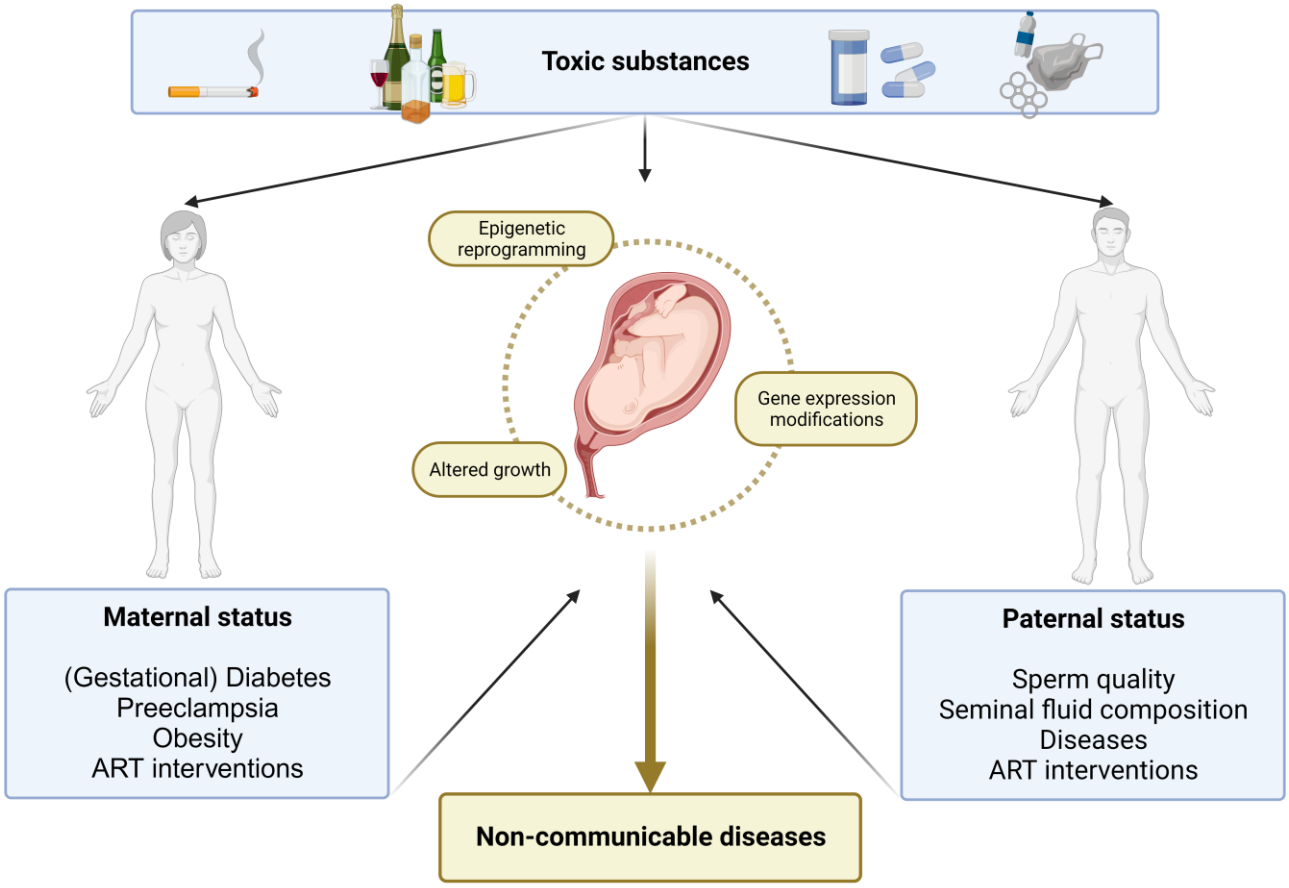

Figure 1: Toxic substances can negatively affect the health status of mother, father, and foetus. Additionally, stress factors, such as diseases or gametes status from the mother and/or father, can perturb the foetal status, leading to epigenetic reprogramming, altered growth and gene expression modifications. All these perturbations can ultimately predispose to the onset of NCDs. Figure created using BioRender.com.

In 2008, NCDs accounted for about 63% of all deaths globally (World Health Organization, 2011), increasing up to 74% in 2022, showing a continuously growing trend (WHO, 2022). Initially, NCDs were primarily associated with the elderly, but nowadays it is well known that these conditions also affect large numbers of younger people in low and middle-income countries (Hanson & Gluckman, 2014; Yajnik et al., 2016), accounting for who dies prematurely due to heart attacks, cancer, chronic respiratory diseases, diabetes, or mental disorders (Geneva: World Health Organization, 2020). Most of the evidence underpinning DOHaD concept comes from animal models and observational human studies, especially from children conceived via ART interventions, that make this population (over 6 million people worldwide) one of the largest well-defined clinical cohorts. According to these studies, the contribution of both maternal and paternal influence plays a pivotal role, especially the female reproductive fitness and male fertility (Feuer & Rinaudo, 2016; Fleming et al., 2018). From these cohorts, epigenetic mechanisms have been proposed to cover an important part in

DOHaD-related exposures and phenotypical alterations. For example, despite several millions of children conceived by ART being born healthy, growing numbers of studies suggest an association between ART and imprinting disorders (Lazaraviciute et al., 2014). Both parental and environmental factors (e.g., nutrition, exposure to toxins, diseases, and other environmental key drivers) have been demonstrated to modulate prenatal development through changes to the DNA methylation patterns, histone modifications, and/or non-coding RNA system (Zuccarello et al., 2022). Although genetic factors have a significant contribution, the non-genetic contributors (i.e., parental fertility's fitness, hormonal and nutritional status, toxin exposure, or other complications) cover a relevant role in the remodelling of phenotypic plasticity during prenatal development, thus determining long-term outcomes in the offspring (Zuccarello et al., 2022). The current challenge is to better understand the underlying mechanism of factors affecting embryo development, with an urgent need to develop models to investigate their characteristics and effects.

2.2 Early origins of cardiovascular disease risk factors

Cardiovascular diseases (CVDs) represent the most prevalent cause of death worldwide, accounting for almost half of all NCDs (17.9 million out of 41 million NCDs annually), and one-third of all global deaths (WHO; CVDs, 2021). CVDs are a group of disorders affecting the heart and blood vessels, including cerebrovascular disease, coronary heart disease, congenital heart defects, peripheral vascular disease, heart failure, atrial fibrillation, and other conditions. Noteworthy, the foetal cardiovascular system is vulnerable to adverse environmental insults, the reason why CVDs can originate from the early stages of life (Lurbe & Ingelfinger, 2021). There is growing evidence from human and animal studies showing an association between early life and later cardiometabolic risk factors. Morphological and functional changes during organogenesis, such as a stiffer vascular tree, endothelial dysfunction, small coronary arteries, and fewer cardiomyocytes may cause adverse cardiovascular "programming", which ultimately leads to CVDs in the adulthood (Blackmore & Ozanne, 2015; Lurbe & Ingelfinger, 2021).

2.2.1 Human studies

Several epidemiological data supporting DOHaD-related CVDs come from well-documented famines and historical cohorts (Barker & Osmond, 1986; Ravelli et al., 1998; Roseboom et al., 2006; Roseboom, 2019; Wang et al., 2012). From these and other studies, it has been demonstrated that the foetal cardiovascular system is susceptible to environmental factors and parental status mostly during early gestation. During the Dutch Hunger Winter of 1944/45, for example, mothers exposed to famine, especially during the earliest stages of gestation, gave birth to children with

higher risks of developing cardiometabolic and neurological abnormalities (Roseboom, 2019; Tobi et al., 2014). Similarly, children born from mothers who suffered the Chinese Great Famine (1959–61) during the first trimester of pregnancy had a four-fold increased risk of developing hypertension in adulthood compared to individuals exposed to the famine after birth (Wang et al., 2012). Although studies have focused mostly on the effect of low birth weight and its association with heart diseases (Lurbe & Ingelfinger, 2021; Pfab et al., 2006; Raisi-Estabragh et al., 2022), others indicated that high birth weight was also related to the development of CVDs, associated with maternal metabolic diseases. High maternal body mass index (BMI), obesity and type 2 diabetes mellitus during the PC period are adverse factors which influence neonatal adiposity and the cardiometabolic profile in the offspring (Godfrey et al., 2017; Longmore et al., 2019). Despite the well-known link between the mother's lifestyle and the health of her offspring, how paternal factors contribute to the risk of adverse birth outcomes remain far less understood. Nevertheless, studies showed the link between paternal conditions, such as sperm quality, epigenetic status and seminal fluid composition with the outcomes of the offspring's health status (Fleming et al., 2018; Velazquez et al., 2019). Notably, epidemiological studies have demonstrated that paternal exposures can influence the metabolic programming of offspring. Retrospective studies conducted on the population of Överkalix-Sweden, and their issues with food supply due to crop failures in the 19th century, identified that people who lived longer, and with lower risk of CVDs, had paternal grandparents with limited access to food during their youth. However, grandchildren of paternal grandparents who had abundant food supply were inclined to have diabetes and cardiometabolic diseases, which were correlated with a shorter lifespan (Bygren et al., 2001; Kaati et al., 2002; Pembrey et al., 2006). Interestingly, the data from Överkalix-Sweden population contradict those of the Chinese famine. There could be several reasons, including differences between maternal and paternal inheritance, or different maladaptation responses to abrupt food uptake changes of the individuals.

Alarmingly, industrialization has significantly changed the chemical exposome of humans over the past century. Estimates mention hundreds of thousands of chemicals produced in global commerce, and these contaminants can affect both the environment and humans (Wang et al., 2020). There is an extensive and ever-expanding body of literature reporting multiple statistically significant linkages between gestational exposure to drugs, toxins, and endocrine-disrupting compounds (EDC), that alter the post-natal development, leading the child to disease susceptibility. For example, an increased risk of neurodevelopmental disorders, disruption of metabolism, cardiovascular disorders, and altered reproductive maturation and function have been associated to EDCs exposure during foetal development (Ghassabian et al., 2022; Vinnars et al.,

2023). These findings suggest that foetus health may be adversely affected by environmental chemicals at current exposure levels, calling for better risk assessment and management.

2.2.2 Animal studies

Despite their inter-species physiological differences with humans, animal models are widely utilised to study and mimic complications of human pregnancies. Different species has been used (Dickinson et al., 2016; Symonds et al., 2007; Williams et al., 2014), but large mammals (e.g., ovine, bovine, and swine) represent those with higher similarities to human beings (Dickinson et al., 2016; Savoji et al., 2019). Some of them include the relatively long gestation time, the delivery of a single foetus, in most cases with a fairly similar size to a human infant, and numerous affinities in the structure and function of human organs. For instance, sheep have been used to model the effects of pre- and periconceptional undernutrition on cardiovascular development (Burrage et al., 2009; Torrens et al., 2009). Other studies used pigs and non-human primate models to study the effects of high-fat diet (HFD) during maternal gestation, showing impaired glucose metabolism, liver dysfunction and endothelial alteration in the offspring (Fainberg et al., 2014; Fan et al., 2013; McCurdy et al., 2009; Xu et al., 2016). Nevertheless, the main disadvantages of large animal models include the cost and the experimental length, the arduous genetic manipulation, and numerous ethical concerns, especially related to non-human primate models (Dickinson et al., 2016). For these reasons, the majority of DOHaD research has been conducted in rodent models, mostly with rats and mice, due to the ease of handling and housing, short gestation period, lower maintenance expenses and easier genetic manipulations (Dickinson et al., 2016; McMullen & Mostyn, 2009). Evidence showed blastocyst abnormalities and cardiovascular alterations followed by undernutrition or HFD in rodents (Blin et al., 2020; Watkins et al., 2008). Moreover, the effects of maternal stress, toxin exposure or hypoxia are widely studied in rodents as risk factors for the offspring to develop CVDs (Vuguin, 2007). Additionally, many important advancements to our knowledge of genomic imprinting have been obtained from mouse models, also due to the high conservation of imprinting mechanisms between humans and mice (Edwards & Ferguson-Smith, 2007). The epigenetic imprinting process investigated in mouse models may cover a pivotal role in the cardiovascular and metabolic health of the progeny, as observed in human studies too (Eberle et al., 2020; Sun et al., 2013; Watkins et al., 2020; Watkins & Sinclair, 2014). Despite numerous advantages, significant limitations of small animal models concern anatomy, physiology, and pathophysiology differences with humans. As a relevant example, rat or mouse heart operates fundamentally differently from the human ventricles (Bers, 2002). Large mammals are frequently used to cover these discrepancies in experimental cardiology (Nánási et al., 2020; Smith et al., 2022), however, the lack of human models (due to obvious reasons) is yet to be solved.

2.3 New approach methodologies: human induced pluripotent stem cells

Stem cells are undifferentiated or partially differentiated cells that can give rise to more than 200 cellular types (Rajabzadeh et al., 2019). Over the past 20 years, stem cell biology has gained attention in experimental research and cell therapy in both human and veterinary medicine (Doss & Sachinidis, 2019; Rajabzadeh et al., 2019; Sharma et al., 2020; Wu & Izpisua Belmonte, 2016). Several types of stem cells are used in this research field, but pluripotent stem cells (PSCs), including embryonic- and induced-PSCs (ESCs; iPSCs), are currently the most attractive tool for studying developmental biology and novel clinical applications (Wu & Izpisua Belmonte, 2016). The emergence of human ESCs (hESCs), derived from human blastocyst by Thomson and colleagues more than two decades ago (Thomson, 1998), quickly made them an advantageous tool for human developmental studies. In 2007, the pioneer study of Yamanaka and his group generated human iPSCs (hiPSCs), thus providing the opportunity of dedifferentiating any cell to a pluripotent state and, equally important, to obtain autologous, patient-specific cells bypassing the ethical concerns of hESCs (Takahashi et al., 2007). The use of hiPSCs led to the *in vitro* development of various cell types, such as pancreatic cells, neuronal cells, cardiac cells or even organs (Bellin et al., 2012). This customisable *in vitro* model creates an opportunity to study tissues and their precursors, diseases, or even patient-specific systems in a dish. Moreover, hiPSCs, referred to as NAM, provide a human-relevant platform for drug testing and *in vitro* toxicology models. The growing interest for NAMs aims to promote a high-throughput, mechanistic analysis of the molecular pathways of toxicity associated with adverse outcomes, also for challenging fields such as repeated dose toxicity and reproductive/developmental toxicity (Zink et al., 2020). However, while it is a major goal to replace, reduce, and refine animal experiments, it is still difficult to completely replace animal experiments for obvious reasons (Zink et al., 2020).

2.3.1 Modelling cardiac development with pluripotent stem cells: hiPSC-derived cardiomyocytes

During development, fast cell division and differentiation from early progenitor stages occur in the embryo to acquire cell- and tissue-specific identities that lead to fully functional organs at birth. Due to advancements in *in vitro* differentiation techniques, hiPSCs are becoming a convenient tool for studying human embryonic development, and for providing valuable supplementary information to study developmental deficiencies that arise due to environmental or genetic factors (Zhu & Huangfu, 2013). The differentiation of cardiomyocytes from hESCs (hESC-CMs) was first reported over 20 years ago (Kehat et al., 2001; Mummery et al., 2003). Since then, simpler protocols have been established to generate hiPSC-CMs (Burridge et al., 2012). The

cardiomyocyte differentiation method consists of the biphasic modulation of the Wnt/β-catenin pathway (**Figure 2**).

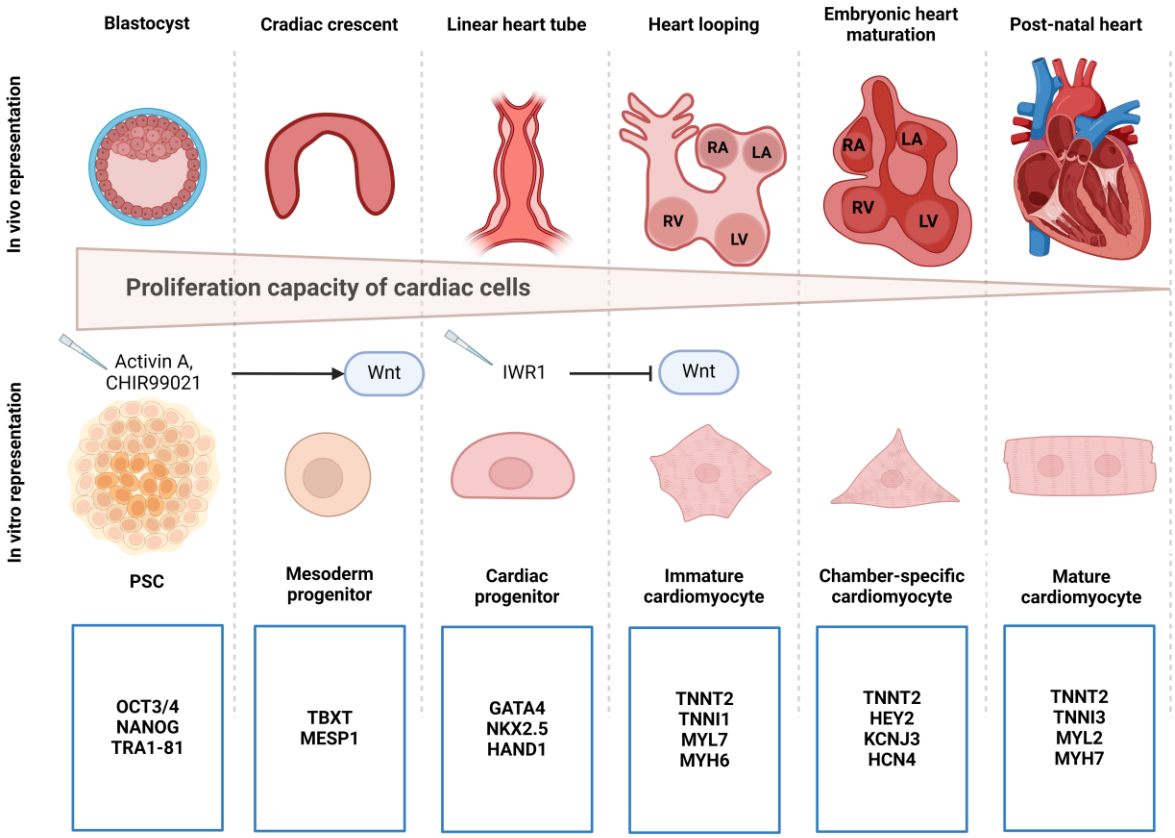

Figure 2: Schematic representation of cardiac development during prenatal days *in vivo*, compared with *in vitro* differentiation. Pluripotent stem cells (PSC) represent both induced and embryonic stem cells. Small molecules such as Activin A/CHIR99021 and IWR1 are used *in vitro* to initiate the cardiomyocyte differentiation, modulating the Wnt signalling. The proliferation capacity of cardiac cells decreases over the time. Key genes are also shown at each time-point. RA: right atrium; LA: left atrium; RV: Right ventricle; LV: Left ventricle. Figure created using BioRender.com.

Briefly, Wnt signalling activation is mediated by the administration of growth factors (e.g., Activin A, BMP-2) or small molecules (e.g., CHIR99021), which commit the cells to the mesodermal lineage (*NKX2.5*$^{+}$, *GATA4*$^{+}$, *MESP1*$^{+}$) (Burridge et al., 2012, 2014; Jha et al., 2015; Lian et al., 2013). During the second step, small molecules (e.g., dorsomorphin) or Wnt inhibitors (e.g., IWR-1, IWP-2) are utilised to enhance the cardiac lineage specification and differentiation (*TNNT2*$^{+}$, *MYH6*$^{+}$, *TNNI3*$^{+}$) (Burridge et al., 2012; Kattman et al., 2011; Lian et al., 2013). Following these conditions *in vitro*, ventricular-like cardiomyocytes (*HEY2*+, *MYL2*+) are more predominant than other cardiac cell types (Burridge et al., 2014; Hamad et al., 2019; Lian et al., 2012; Weng et al., 2014). Based on the research aim, there are also protocols to purify and isolate atrial-like cardiomyocytes (*KCNJ3*+, *KCNJ5*+, *CACNA1D*+), for example using retinoic acid or BMP

antagonist (e.g., Noggin, Gremlin 2), which upregulate atrial-specific genes (Devalla et al., 2015; Goldfracht et al., 2020; Tanwar et al., 2014; Zhang et al., 2011). Pacemaker-like cardiomyocytes are still difficult to obtain *in vitro*. To date, the most effective method to generate the sinoatrial node cell population (*HCN4*+, *TBX3*+, *TBX18*+) is the inhibition of neuregulin1β/ErbB signalling. More recently, it has been hypothesized that the Wnt signalling modulation through Nodal inhibition may promote the pacemaker cells fate (Liang et al., 2020; Yechikov et al., 2020; Zhu et al., 2010).

2.3.2 Current hurdles for in vitro heart muscle model: maturation of hiPSC-CMs

Currently available *in vitro* models of the human heart include a variety of setups, extensively reviewed by Campostrini *et al.*, such as simple 2D cultures on tissue culture plastic or polymers and hydrogels, and three-dimensional (3D) cultures, which include the generation of microtissues, engineered heart tissues, 'heart-on-chip' models (containing microfluidic channels that mimic the blood flow) and self-organising cardioids (Campostrini et al., 2021; Hofbauer et al., 2021). Although all these models yield hiPSC-CMs, the main challenge *in vitro* is to obtain fully matured cardiomyocytes, concerning their functional and physiological characteristics.

Mature and immature cardiomyocytes can be recognised based on morphological, transcriptional, and functional characteristics, as summarized in **Figure 3**.

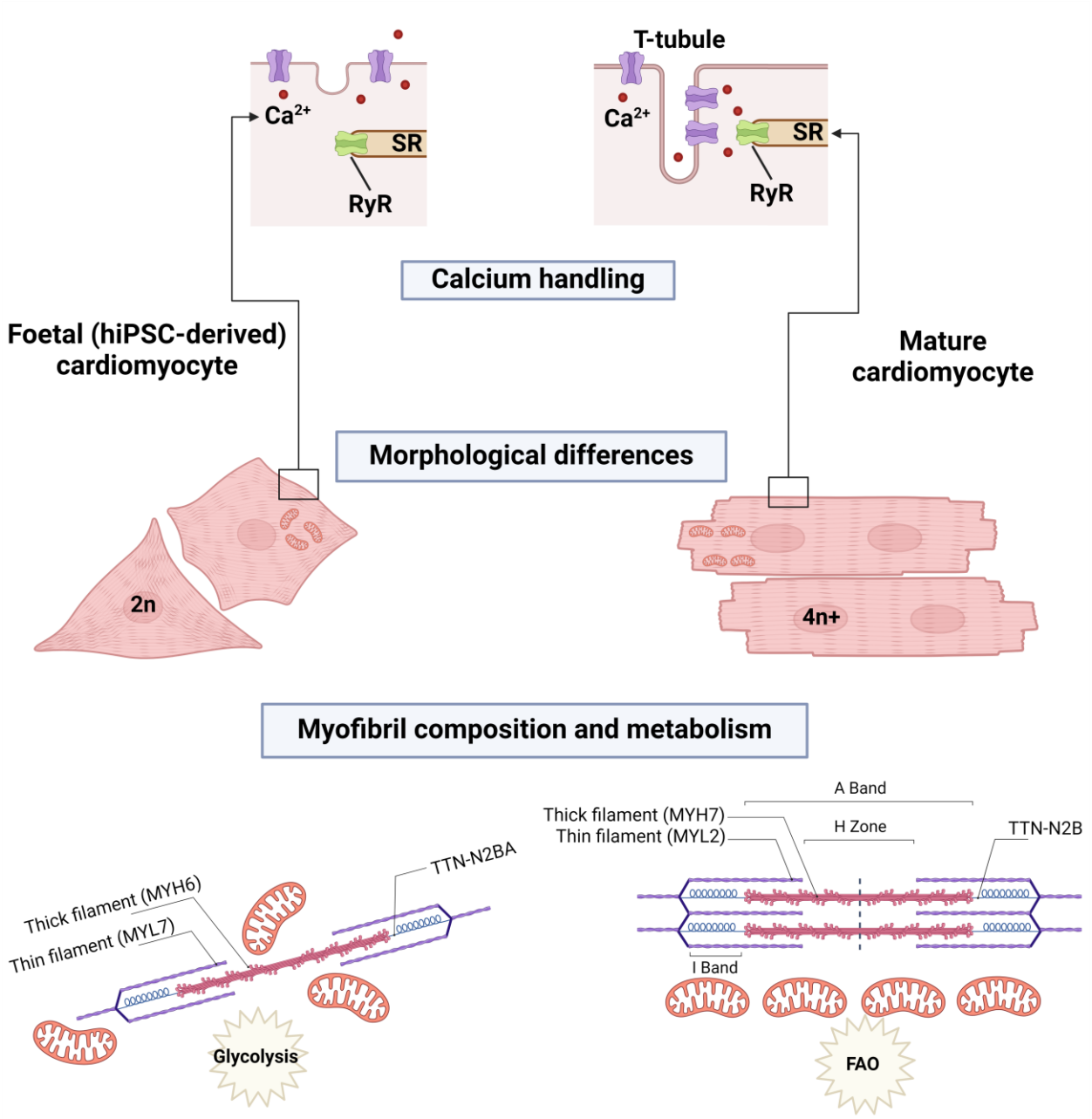

Figure 3: Main features of immature and mature cardiomyocytes. Foetal cardiomyocytes are round and mononucleated, while adult cardiomyocytes are mono/bi-nucleated and form a syncytium. The diploid (2n) and polyploid (4n+) nuclei of the immature and mature cardiomyocytes, respectively, are shown. In foetal cardiomyocytes, T-tubules are absent, and the sarcoplasmic reticulum (SR) is underdeveloped, while in adult cardiomyocytes T-tubules and SR are well-developed to regulate the calcium handling and the excitation-contraction coupling. L-type calcium channels are represented in purple, and ryanodine receptor (RyR) in green. The myofibrils are disorganised in foetal cardiomyocytes, with sparse mitochondria (orange), which rely on glucose as their source of energy. The foetal cardiomyocytes express cardiac protein isoforms that are typical of the foetal/neonatal heart (e.g., MYH6, MYL7, TTN-N2BA). In adult cardiomyocytes, muscle fibers are organised and aligned in sarcomeres, with the 'I bands' of thin filaments and 'A bands' where thin and thick filaments overlap. The protein isoforms expressed are typical of the adult heart (e.g., MYH7, MYL2, TTN-N2B). Mitochondria are aligned along the muscle fibers, and fatty acid oxidation (FAO) represents the main energy source. Figure created using BioRender.com.

Mature cardiomyocytes exit the cell cycle after birth, becoming hypertrophic, rod-shaped, and bigger compared to immature and hiPSC-derived cardiomyocytes (Bergmann et al., 2009; Porrello

et al., 2011). To some extent, immature cardiomyocytes continue to proliferate, and they are mainly mononucleated. In matured cardiomyocytes, the morphological differences are achieved to meet the increased workload and the formation of a functional "syncytium", in which the beating is triggered by the contraction of a neighbouring cell (eventually restricted to specialised pacemaker cells). By contrast, hiPSC-CMs spontaneously beat *in vitro,* and their morphology is characterised by sparse, disorganised myofibrils and the absence of transverse tubules (T-tubules) (Brette & Orchard, 2003; Mills et al., 2017). During early development and maturation, cardiomyocyte genes undergo a process called isoform switching while transitioning from one stage to another. For example, there is an increase in mature sarcomere components (Guo & Pu, 2020). Cardiac myosin heavy chain (MHC) switches from alpha-MHC (*MYH6*) to beta-MHC (*MYH7*), which is predominant in adult cardiomyocytes. Foetal and hiPSC-CMs express *TNNI1*, coding for the slow skeletal muscle isoform (ssTnI), while *TNNI3*, coding for cardiac troponin I (cTnI), predominates in adult cardiomyocytes (Bedada et al., 2014). Similarly, titin (*TTN*), which represents a major contributor to myocardial mechanics, is expressed in two main cardiac isoforms: stiff N2B and more flexible N2BA. The predominant titin isoform in hiPSC-CMs is N2BA, which is replaced by smaller-size N2BA isoforms and N2B in adult cardiomyocytes, reinforcing their sarcomeres (Krüger et al., 2006; Lahmers et al., 2004). The switch of sodium and calcium channel isoforms, coded by *SCN5A* and *CACNB2*, are pivotal for an efficient excitation-contraction coupling to evolve into a mature electrophysiological phenotype (Karbassi et al., 2020). Moreover, during post-natal development, metabolic reprogramming is crucial for cardiomyocytes. As the demand for energy increases during maturation, cardiomyocytes are forced to switch their metabolism from glycolysis to fatty acid oxidation, such that ATP is generated more efficiently (Lopaschuk & Jaswal, 2010). Consequently, higher expression of genes related to mitochondrial biogenesis, fatty acid oxidation, and oxidative phosphorylation (e.g., *PPARGC1A*, *PPARA*, *ESRRA*) are fundamental to drive the metabolic maturation of hiPSC-CMs (Karbassi et al., 2020).

2.3.3 Current models to enhance hiPSC-CM maturation

To date, several methods have been used to support and improve the maturation of hiPSC-CMs. Extended culture periods are effective in maturing hiPSC-CMs. However, this method is costly, line-to-line variable, and only enhances the maturation of some subset features in hiPSC-CMs (Snir et al., 2003; Veerman et al., 2017). More effective approaches are often based on recapitulating the biophysical, mechanical, and biochemical cues present in the native heart (**Figure 4**) (Campostrini et al., 2021).

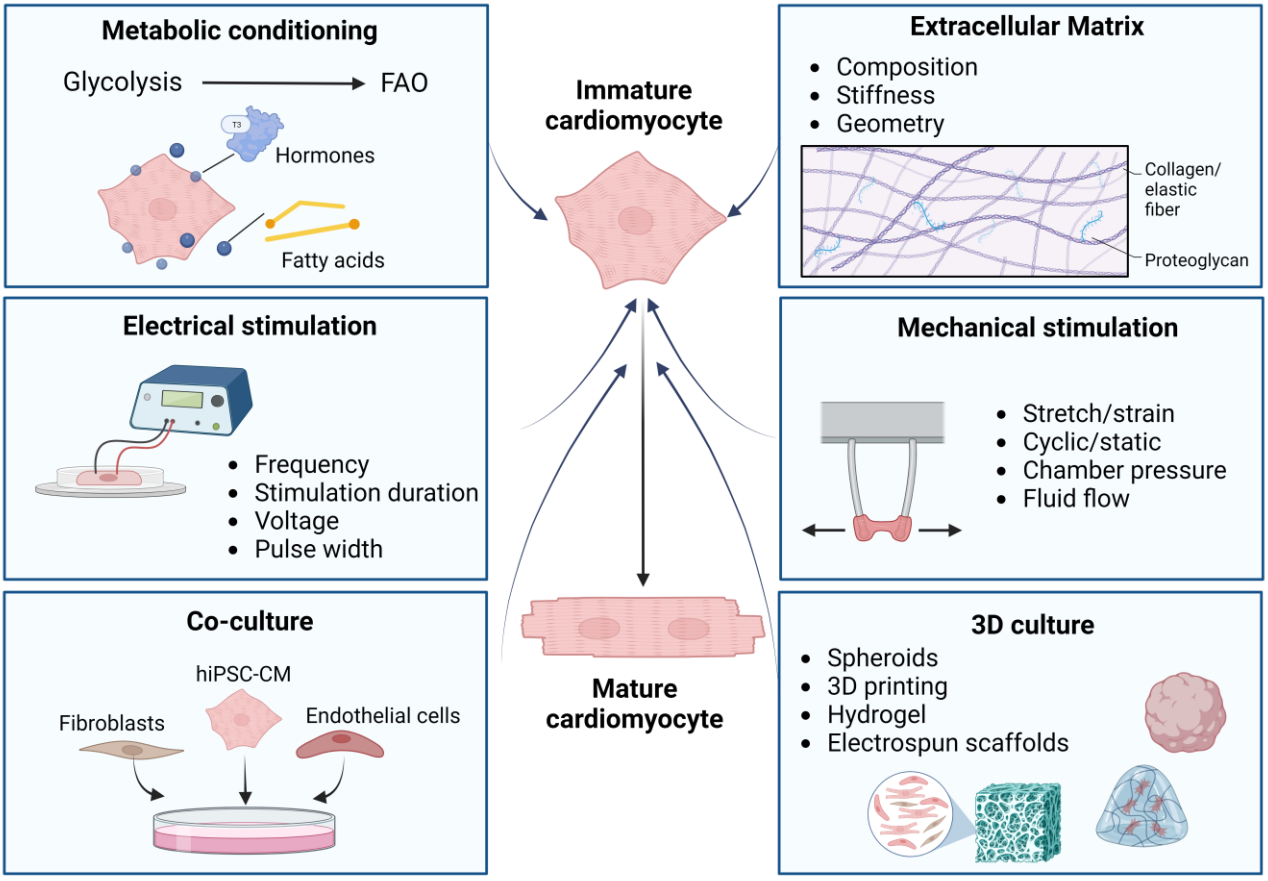

Figure 4: Methods to mature hiPSC-CMs. Metabolic conditioning, cellular interactions with a more complex extracellular matrix, electrical and mechanical stimulation, co-culture with different cell types, and 3D culture have all been utilized to increase hiPSC-CMs maturity in culture. The Figure was prepared based on (Ly et al., 2021). FAO: fatty acid oxidation. Figure created using BioRender.com.

For example, *in vitro* co-cultures with non-cardiomyocyte cellular types provide physical and functional support to the cardiac tissue, promoting cardiomyocyte maturation, too. Co-cultures with fibroblasts and endothelial cells have been used to enhance the maturity of engineered 3D cardiac tissues and 3D cardiac organoids (Giacomelli et al., 2017, 2020; Ieda et al., 2009; Tiburcy et al., 2017). Other methods modulate the surrounding extracellular matrix (ECM) proteins, such as laminins, collagens, and fibronectin, to improve functional cues of hiPSC-CMs, as the excitation-contraction coupling (Block et al., 2020; Ong et al., 2023). Functional maturation can be achieved also through mechanical and electrical stimulation. The application of synchronised electrical and mechanical stimulation to hiPSC-CMs improves the localization of N-cadherin in the cell membrane, sarcomere shortening, and decreases the transmembrane calcium current, all signs of a more mature phenotype (Kroll et al., 2017). Moreover, metabolic maturation can be obtained by supplementing the culture medium with fatty acids to lead to higher intracellular ATP production, increased oxygen consumption and reduced cell cycle activity in hiPSC-CMs (Correia

et al., 2017; Mills et al., 2017; Zhang et al., 2023). Methodological advancements employ these approaches in a more complex 3D environment with the fabrication of scaffold-free and scaffold-based 3D cardiac models, which can receive external stimuli (e.g., mechanical, electrical) to further enhance the maturation of hiPSC-CMs (Campostrini et al., 2021; Ottaviani et al., 2023). Nonetheless, the best model is one fitting for purpose: in many cases, it may be suitable to capture some (but not all) characteristics of the mature cardiomyocytes. For example, a more robust and reproducible hiPSC-CM model in 2D culture, though not entirely matured, has been shown to be highly predictive for cardiotoxicity (Saleem et al., 2020). Moreover, hiPSC-CMs have emerged as a promising platform for pharmacogenomics and drug development, also due to the ability to reproduce the main features of (genetic) disease phenotypes in 2D culture (Bellin et al., 2012; Hnatiuk et al., 2021).

2.4 In vitro cardiotoxicity models dedicated to environmental toxicity

Many NAMs developed for cardiotoxicity are optimized mainly for pharmaceutical applications (Daley, 2022; Gintant et al., 2019; Magdy et al., 2018). However, there is an urgent necessity to assess the cardiotoxicity risks of an increasing number of environmental chemicals (Judson et al., 2009). Several applications utilise hPSC-CMs as *in vitro* model to study morphological, physiological, and transcriptional changes of cardiomyocytes under the effects of toxicants related to DOHaD field (**Figure 5**).

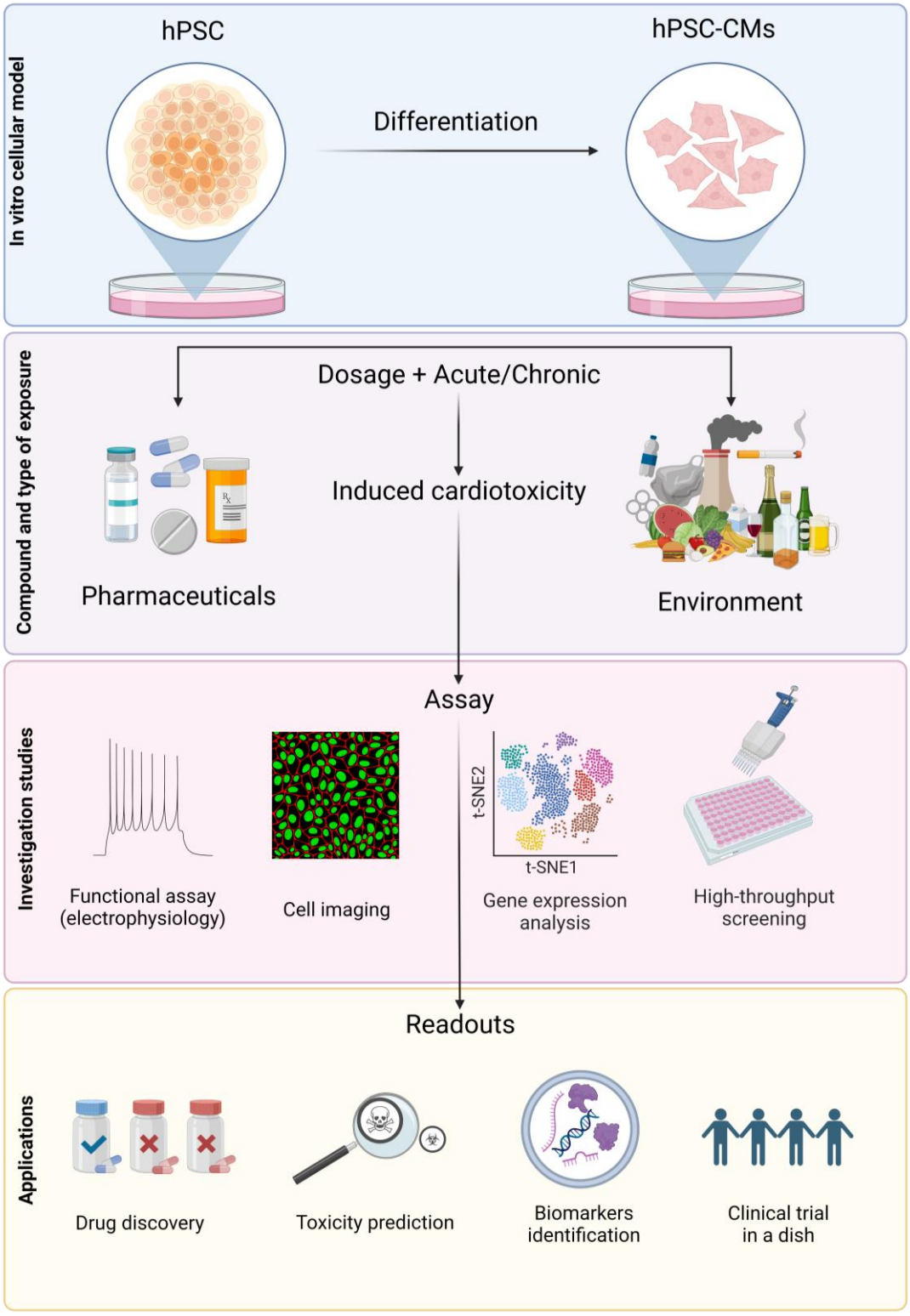

Figure 5: Overview of the workflow for the *in vitro* assessment of compound toxicity. It is important to identify the relevant duration and concentration of the desired compound, reflecting on the subsequent readouts and desired level of applications. hPSC: human pluripotent stem cells; hPSC-CM: human pluripotent stem cell-derived cardiomyocytes. Figure created using BioRender.com.

Nutritional exposures. Diet and nutrients play an important role during foetal development, and changes in myocardial metabolism may affect the cardiomyocyte function. If glucose uptake is not reduced in foetus just before birth, the nucleotide biosynthesis supported by high levels of glucose can inhibit cardiac maturation (Nakano et al., 2017). Therefore, the delay of the metabolic switch may lead to pathological remodelling of the neonatal heart, contributing to the onset of congenital heart defects. Nakano and colleagues described the impact of glucose exposure on cardiac differentiation using hESC-CMs cultured in media containing various glucose concentrations, which dose-dependently suppressed the expression of key cardiac markers (*TNNT2*, *NKX2.5*), as well as the mitochondrial marker PGC1/PPARα, required for postnatal maturation (Murphy et al., 2021; Nakano et al., 2017). In a 2D model which recapitulates the diabetogenic environment, hiPSC-CMs exposed to prolonged hyperglycemia revealed pathological hypertrophy and reduced contractility due to calcium cycling dysfunctions (Ng et al., 2018).

Alcohol and cigarette smoking exposures. Similarly, alcohol, and cigarette smoking, although often neglected in the context of DOHaD, remain a significant societal problem and can alter foetal development, leading to heart alterations and impaired postnatal cardiac function (Goh et al., 2011; Guo et al., 2019; Ko et al., 2019; Rodríguez-Rodríguez et al., 2018). Recent studies show that ethanol treatment of hiPSC-CMs resulted in overall decreased mitochondrial function and cellular viability, increased glycolysis, disrupted fatty acid oxidation, ROS overproduction, and impaired cardiac structural development (Hwang et al., 2023; Liu et al., 2021; Rampoldi et al., 2019). Upon ethanol exposure, markers related to calcium handling and contractility (e.g., *ATP2A2, KCNA4*, *SCN5A*) were mostly downregulated, and components of the surrounding ECM (e.g., *COL1A1*, *COL3A1*) were upregulated, which correspond to alterations observed in cardiac fibrosis, hypertrophy cardiomyopathy, and diastolic and systolic dysfunction (Bi et al., 2021). Similarly, nicotine exposure affects the calcium signalling in hESC-CMs, increasing the propensity to arrhythmia (Guo et al., 2019). Electronic and conventional cigarette smoking extracts impaired hiPSC-CMs function, such as slowing down the contraction time and increasing ROS-induced cell death (Basma et al., 2020). Notably, genes essential for normal heart function and response to stress (e.g., *MYLK*, *NPPA*, *TNNT2* and *TNNI3*) were mostly downregulated.

Environmental contaminants. Recent studies that looked at numerous environmental chemicals are used to highlight the concern of different chemical classes to various regulatory agencies in the United States, European Union, and other countries (Williams et al., 2017). The use of hiPSC-CMs is feasible when applied even to a broad range of chemicals, including environmental pollutants such as pesticides, flame retardants, polycyclic aromatic hydrocarbons, plasticisers, and industrial chemicals (Burnett et al., 2021a). In this context, hiPSC-CMs have been used to estimate

margins of safety (for pharmaceuticals) and margins of exposure (for environmental chemicals) (Blanchette et al., 2020; Burnett et al., 2021b; Sirenko et al., 2017), finding wide variation across different pharmaceutical compounds and between pharmaceutical and non-pharmaceutical compounds.

While there is a pressing need to assess the cardiotoxic risks of an increasing number of environmental chemicals (Judson et al., 2009), many of the existing cardiotoxicity models do not sufficiently account for the unique facets of these toxicants (Dix et al., 2007; Truskey, 2018). Above all, a vast majority of studies investigate the acute effects of toxicants *in vitro*, and chronic exposure (repeated for several days to weeks) has only been investigated recently (Narkar et al., 2022). Methods that mimic and model longer-term exposures to environmental toxicants, rather than acute biological effects, will be those best suited for integration into NAMs for environmental cardiotoxicity. Indeed, the examination of acute effects at relatively high doses limits the ability of hazard screening to inform policymakers of real environmental risk, because these screens do not incorporate data on actual toxicant exposures (i.e., concentration and duration) (Krewski et al., 2010). Therefore, the most straightforward approach is to apply representative, chronic dosing regimens to existing *in vitro* cardiotoxicity models. However, the lower "strength" of environmental toxicants makes the ability to detect meaningful biological outcomes more difficult under chronic conditions (Dix et al., 2007). For this reason, NAMs designed for the investigation of environmental cardiotoxicity will require the incorporation of different approaches to improve the sensitivity in detecting environmental exposures. For example, the need for a higher biological complexity of NAMs has increased the interest in higher content "omics-level" data (Moffat et al., 2017). Albeit more difficult to interpret, omics-level data can offer holistic and comprehensive information regarding interacting pathways of toxicity of environmental toxicants and suggest omics-level signatures of cardiotoxicity risks (Burnett et al., 2021b).

2.5 Bisphenol A

Of all the chemical exposures that individuals experience, organic pollutants such as bisphenols are considered environmental contaminants with well-known adverse effects on human health (Murata & Kang, 2018; Vom Saal & Vandenberg, 2021). Bisphenol A (BPA) is a synthetic organic compound widely used in the manufacturing of polycarbonate plastics and epoxy resins. Materials produced with BPA have excellent chemical and physical properties, including thermal stability, elasticity and resistance to acids and oils. For this reason, BPA has been used in the production of an uncountable number of different products, such as food and beverage containers, toys, cosmetics, cash receipts, DVDs, and water pipes (Vandenberg et al., 2007; Vom Saal &

Vandenberg, 2021). Due to its ubiquitous presence, humans are exposed repeatedly to BPA in several ways, such as direct contact, inhalation, or dietary intake (Ma et al., 2019). Therefore, BPA is commonly detected in human biological fluids (e.g., maternal blood, breast milk, urine) or tissues (e.g., placenta). Due to its endocrine disrupting effects on humans, BPA has become a major public health concern, resulting in health hazards for the reproductive system, metabolism, immune function, brain, cardiovascular system, as well as the growth and development of offspring (Cimmino et al., 2020; Fonseca et al., 2022; Ma et al., 2019; Welch & Mulligan, 2022).

Based on estimations, the BPA daily intake by humans ranges between 1 and 5 μg/kg/day (Murata & Kang, 2018), and 4 μg/kg/day was set as a safe tolerable daily intake (TDI) in 2015 (University of Hertfordshire, 2021). However, according to the Endocrine Society, assumptions regarding a safe TDI are difficult to judge, as the BPA responses are non-monotonic in most cases, a characteristic of EDCs (Gore et al., 2015). Notably, the TDI for humans changed from 4 μg/kg/day to 0.0025 μg/kg/day (0.2 ng/kg) in 2023, amount 20.000 times lower than the "safe" dose of BPA stated in 2015 by EFSA (EFSA CEF Panel, 2015; EFSA CEP Panel, 2023; Heindel et al., 2020; Vandenberg et al., 2019; Vom Saal & Vandenberg, 2021).

2.5.1 Mechanism of action of Bisphenol A

Similarly with other EDCs, BPA interacts with receptors activated by estrogens (ERs), androgens (ARs), thyroid hormones (TRs), and peroxisome proliferator (PPARs), acting either as an agonist or antagonist, due to its chemical structure.

Even if BPA's affinity to ERs is about 1.000-10.000 times lower than that of 17-β estradiol (E2), its endocrine disrupting effect is manifested even at low-doses (Alonso-Magdalena et al., 2012). Notably, depending on the tissue, cell type or specific subtype and distribution of ERs, low doses of BPA can promote estrogen-like activities similar to or stronger than E2, partially due to its rapid responses via non-classical estrogen pathways (Watson et al., 2005). Despite the BPA binding and mechanism of activation of ERs, the chemical can ultimately regulate gene expression by binding with estrogen response elements (ERE) (Ma et al., 2019). BPA is commonly considered an antagonist of the ARs, disrupting the normal function of androgen. Indeed, contrary of what observed for ERs pathway, BPA is unable to trigger androgen response elements (ARE), which won't be stimulated, affecting the reproductive function and development (Tan et al., 2015). Additionally, cell-based reporter gene assays revealed that BPA inhibits the beta isoform of TR, suggesting that the chemical can disrupt the action of thyroid hormone, consequently affecting the thyroid activity (Freitas et al., 2011; Sheng et al., 2012). Finally, BPA was also associated with the activation of PPARγ, whose alteration has been linked to the development of metabolic

diseases, such as type 2 diabetes. Indeed, low doses of BPA result in lipid accumulation and insulin dysfunction, also associated with an increased risk of obesity-related diseases (Ariemma et al., 2016).

The pathways discussed so far, together with others affected by BPA, but here not mentioned (e.g., aryl hydrocarbon receptor, estrogen-related receptor gamma, integrins, xenobiotic receptors), are ultimately involved in numerous intracellular responses, as shown in **Figure 6** (Ma et al., 2019). Through the interaction with specific pathways, BPA induces corresponding biological effects related to inflammation and oxidative stress (Cho et al., 2018), genotoxic mechanisms (Ramos et al., 2019), mitochondrial dysfunctions (Cheng et al., 2020), and epigenetic modifications, such as methylation alterations (Ye et al., 2019), histone modifications (Altamirano et al., 2017), or non-coding RNA regulations (Rodosthenous et al., 2019).

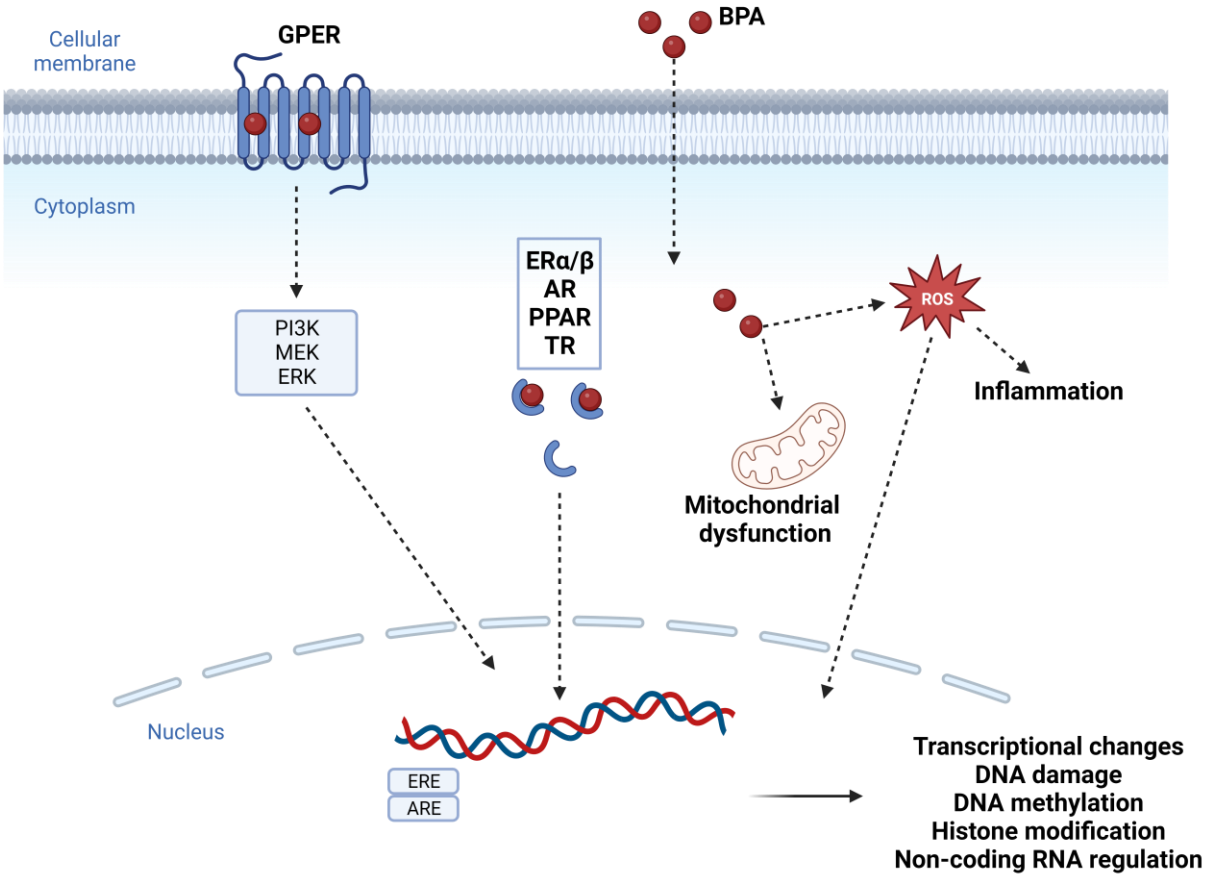

Figure 6. Schematic representation of the main BPA toxicity mechanisms. BPA mediates numerous biological effects by binding cell surface receptors (e.g., GPER), intracellular receptors (e.g., ERα, PPAR) or passing through the cellular membrane. Membrane receptors could mediate the activation of ERK pathways, as well as PI3K/AKT pathway, mainly regulating cell proliferation and migration. BPA can also affect the antioxidant system, leading to ROS accumulation, and it can impair mitochondrial functionality. Furthermore, BPA causes genetic toxicity, including DNA damage (e.g., double-strand breaks), and epigenetic changes, playing an important role in gene expression modifications. BPA: Bisphenol A; Erα/β: Estrogen receptor alpha/beta; AR: Androgen receptor; GPER: G protein-coupled estrogen receptor; PPAR: Peroxisome proliferator-activated receptor; TR: Thyroid hormone receptor; ROS: Reactive oxygen species;

PI3K: Phosphatidylinositol-3-kinases; MEK: MAPK/ERK kinase; ERK: Extracellular regulated protein kinases; ERE: estrogen response elements; ARE: androgen response elements. Figure created using BioRender.com.

2.5.2 Adverse cardiac effects after Bisphenol A exposure: Epidemiological studies

To assess the cardiotoxic effects of BPA, several epidemiological investigations have been developed. The evidence consistently associates BPA exposure with the increased prevalence of CVDs, for example, coronary heart disease (CAD) (Melzer et al., 2010), dilated cardiomyopathy (Xiong et al., 2015), peripheral artery disease (Shankar et al., 2012), myocardial infarction, and associated risk factors such as hypertension (Bae & Hong, 2015; Shankar & Teppala, 2012). Most epidemiological studies have been carried out from the National Health and Nutrition Examination Survey (NHANES) dataset, which investigated the relationship between urinary BPA levels of participants and CVDs. The first report to investigate this association was based on 2003-2004 NHANES data, showing that participants with elevated urinary BPA levels were diagnosed with CVDs, including CAD, angina pectoris and heart attack (Lang, 2008). Later, the same research group investigated the data set from 2005-2006 NHANES, finding that higher urinary BPA levels were still associated with CAD, although the urinary BPA concentrations were lower compared to 2003-2004 cohorts (Melzer et al., 2010). Due to the cross-sectional nature of NHANES, Melzer *et al.* performed a longitudinal study in 2012 to strengthen their findings and to assess the effects of BPA on the development of CAD, confirming this association (Melzer et al., 2012). In addition to CAD, other studies investigate BPA exposure with CVDs. For example, Lind *et al.* evaluated a possible relationship between atherosclerosis and BPA elevated urinary levels, which were related to the echogenicity of the plaques (Lind & Lind, 2011). More recently, in 2020, Cai *et al.* demonstrated a positive association between urinary BPA concentrations with heart failure, angina pectoris and myocardial infarction (Cai et al., 2020). Overall, NHANES dataset has been widely used to draw conclusions about BPA exposure and adverse cardiovascular outcomes. It should be underlined that a study from LaKind *et al.* observed that NHANES data may not be sufficient to conclude that BPA exposure is associated with CVDs (LaKind et al., 2012). Indeed, inconsistencies were noticed in terms of methods performed (e.g., exclusion criteria, definitions, and scoring systems), and, in this study, the authors showed no association between urinary BPA with CAD or heart attack in NHANES participants, highlighting that caution is needed to establish associations or cause-and-effect relationship between BPA concentrations and CVDs (LaKind et al., 2014).

Moreover, relevant to DOHaD field, BPA can cross the placenta (Schönfelder et al., 2002; Yamada et al., 2002), possibly affecting children's health. However, still little is known about the BPA

effects on foetal cardiac function and development. Bae *et al.* suggested that BPA exposure during midterm pregnancy (around 20 weeks) is associated with higher diastolic blood pressure in the children at age 4 (Bae et al., 2017). Recently, in a population-based prospective cohort study, Sol *et al.* evaluated the association between maternal urinary BPA levels during pregnancy and blood pressure in childhood. The authors observed that this association is sex-dependent, since higher blood pressure was found in boys, after foetal BPA exposure (Sol et al., 2020). However, further studies are needed to unravel the underlying mechanisms and long-term outcomes of BPA exposure and early cardiovascular alterations.

2.5.3 Adverse cardiac effects after Bisphenol A exposure: Experimental studies

Several experimental studies *in vivo* and *in vitro* have been performed to study the effects of BPA exposure on cardiac tissue and to identify possible pathways of toxicity. Due to non-monotonic responses of BPA, timing of exposure, as well as low and high doses of the chemical have been investigated. Low-dose BPA studies focus on environmentally relevant concentrations, common for human exposure, while studies using higher (supraphysiological) doses of BPA are relevant to better identify its toxicological actions and targets in case of occupational exposures or specific poisoning conditions.

The study by Pant *et al*. showed that high doses of BPA (1-100 μM) decreased atrial contraction rate and force by 90% through the NO-cGMP system (Pant et al., 2011). In the work of Posnack *et al*., BPA concentrations (0.1–100 μM) delayed the cardiac electrical conduction in the hearts of female rats, already after 15-minute exposure (Posnack et al., 2014). Additionally, the risk of developing myocarditis and cardiac fibrosis was increased in female mice exposed to high doses of BPA, due to the raise of inflammatory mediators (e.g., caspase-1, TLR4, IL-1β) in the heart (Bruno et al., 2019). Several studies have shown that high-dose BPA also alters the functioning of ion channels. For example, Asano *et al.* reported that high BPA doses (10-100 μM) activated the large conductance Ca^{2+}/voltage-sensitive K channels (Maxi-K) in canine and human coronary artery smooth muscle cells, suggesting that BPA might act as a coronary vasodilator (Asano et al., 2010). O'Reilly *et al.* examined that the steady-state inactivation of human heart sodium channels (hNav1.5) was shifted to more hyperpolarized potentials under BPA treatment (100 μM), blocking the sodium flux (O'Reilly et al., 2012). Additionally, Deutschmann *et al*. reported that high doses of BPA inhibited the L-type Ca^{2+} channels in isolated mouse ventricular myocytes in a dose-dependent manner (Deutschmann et al., 2013).

Even low-dose exposure to BPA (0.001 μM) resulted in cardiac electrical rhythm alterations in adult female rats (Yan et al., 2011). Soon after 15 minutes, BPA treatment promoted triggered

activities, a term used to indicate aberrant spontaneous excitation of cardiomyocytes, representing key mechanisms of cardiac arrhythmogenesis. In female, but not male hearts, acute exposure to BPA (0.001 μM) following ischemia injury resulted in a marked increase in the duration of sustained ventricular arrhythmias (Yan et al., 2013). The underlying mechanisms of the rapid actions of BPA in the heart might be mediated, at least in part, by rapid alteration of cardiomyocyte Ca^{2+} handling (Gao et al., 2013; Yan et al., 2011), which plays a key role in cardiac arrhythmogenesis (Bers, 2002). Interestingly, in a study by Liang *et al*., the most effective dose of BPA's cardiac actions was around 0.001 μM to 0.01 μM, overlapping with the reported human exposure levels (Liang et al., 2014). Different effects were observed if low doses of BPA were given for longer periods (i.e., chronic exposure). For instance, Patel *et al.* demonstrated that low-dose BPA (5 μg/kg/day) lifelong exposure induced cardiac concentric remodelling in male but not female mice, while it increased systolic and diastolic pressures in female but not in male mice (Patel et al., 2013). The expression levels of Ca^{2+} handling proteins were altered by BPA in a sex-specific way, differently from other *in vitro* studies using isolated rat ventricular cardiomyocytes (Gao et al., 2013; Yan et al., 2011), also reflecting the different impact of long-term and acute exposure. Numerous experimental studies *in vivo* using zebrafish, rodents, and non-human primates, showed that gestational BPA exposure elevates the risk of heart developmental alterations, through molecular and structural alterations (Chapalamadugu et al., 2014; Chen et al., 2020; Fonseca et al., 2022; Lombó et al., 2019; Rasdi et al., 2020; Ross Brown et al., 2019; Yujiao et al., 2023). Relevant for human studies, Chapalamadugu *et al*. found that maternal BPA exposure significantly altered transcript expression profiles in the foetal heart of rhesus monkeys. Here, the significant downregulation of *MYH6* and upregulation of *ADAM12* in foetal ventricles were both related to cardiovascular pathologies, such as cardiac hypertrophy (Chapalamadugu et al., 2014).

The extent of BPA toxicity on the human heart, as well as its effects during foetal cardiac development, is still largely unexplored. As a promising *in vitro* cardiomyocyte model, hPSC-CMs have been used to study the BPA cardiotoxicity on a human-based system. BPA treatment (≥10 μM) on hiPSC-CMs mainly showed contractility alterations, such as reduced amplitude and duration of the field potential, and inhibition of ion channels and calcium currents, in a dose-dependent manner (Hyun et al., 2021; Prudencio et al., 2021). Interestingly, 17β-estradiol (E2) and BPA at high micromolar concentrations showed similar toxicity effects on hiPSC-CMs, resulting in decreased depolarizing spike amplitude, shorter calcium transient duration, and decreased contractility (Cooper et al., 2023). Using very low concentrations (1-10 nM), BPA treatment delayed the repolarization through inhibition of the hERG K+ channel in hiPSC-CMs (Kofron et al., 2021; Ma et al., 2023). Additionally, hESC-CMs treated with BPA at low doses showed cardiac

hypertrophy features by disrupting Ca^{2+} homeostasis via the DRP1 signalling pathway (Cheng et al., 2020). Nevertheless, investigations into the effects of BPA exposure during *in vitro* cardiomyocyte differentiation are limited to a small number of studies. The studies in account utilise mouse embryonic stem cell-derived cardiomyocytes or H9c2 rat embryonic cardiomyoblasts (Escarda-Castro et al., 2021; Lee et al., 2019; Zhou et al., 2017, 2020, 2021). It has been reported that low doses of BPA treatment on developing cardiomyocytes altered the transcriptional levels of genes related to heart physiology (Lee et al., 2019; Zhou et al., 2020), or decreased the levels of mesoderm markers (Zhou et al., 2017, 2021). Notably, low doses of BPA promoted the expression of collagen mRNAs (e.g., type I collagen), which may cause abnormal cardiac hypertrophy during development, and lead to abnormal heart development (Zhou et al., 2020, 2021). Moreover, supraphysiological doses (≥ 10 μM) of BPA during the differentiation of H9c2 rat embryonic cardiomyoblasts increased the percentage of DNA repair foci and decreased the levels of epigenetic marks (Escarda-Castro et al., 2021). Nonetheless, the effects of low doses and repeated exposure to BPA on human cardiomyocyte differentiation still require further investigation.

3 MATERIALS AND METHODS

3.1 Chemicals and plasticware

Chemicals were obtained from Sigma-Aldrich (St Louis, MO, USA). Except when otherwise specified, all plasticware, reagents and devices for cell culture experiments were purchased from Thermo Fisher Scientific Inc. (Waltham, MA, USA).

3.2 hiPSC line

The human iPS cell line (hiPSC; SBAD2 clone) used in this study originated from Normal Adult Human Dermal Fibroblasts (NHDF-Ad) cells (51-year-old Caucasian male, Lonza #CC-2511), reprogrammed using non-integrative Sendai virus transduction. The cell line was provided during the IMI-funded StemBANCC project (Morrison et al., 2015). BD Matrigel (BD Biosciences #354277) was used for plate coating and cells were cultured with mTeSR™1 medium (Stem Cell Technologies #85870) supplemented with 1% Penicillin-Streptomycin. Cells were maintained in vitro at 37°C in a humidified atmosphere containing 5% CO_2. For routine passages, Versene® (EDTA) (0.02%, Lonza #BE17-711E) was used according to the manufacturer's protocol. Routine screening for mycoplasma was carried out using the Venor®GeM-Advance (Minerva Biolabs #11-7024) Mycoplasma Detection Kit, according to the manufacturer's instructions.

3.3 Pluripotency test

After single cell dissociation with Accutase® (#A6964), cells were cultured in suspension for five days in mTeSR™1. They formed embryoid bodies (EBs), which were plated on 0.1% gelatin (Merck) coated surface in differentiation medium (DMEM, 20% FBS, 1% MEM Non-Essential Amino Acid Solution (100×), 0.1 mM β-mercaptoethanol, 1% Pen/Strep). After 14 days of spontaneous differentiation, the cells were fixed with 4% paraformaldehyde (PFA) solution and evaluated for the 3 germ layer markers by immunocytochemistry.

3.4 Cardiomyocyte differentiation from hiPSC

For cardiomyocyte differentiation, the PSC Cardiomyocyte Differentiation Kit (#A2921201) was used according to the manufacturer's protocol. Plates were coated with Geltrex™ (#A14133) and the hiPSC were plated after Accutase® (#A6964) induced single-cell dissociation. Cells were seeded at a density of 1.25×10^4 cells/cm^2 in mTeSR™1 medium supplemented with RevitaCell™ (#A2644501). When the hiPSC confluency reached 70-80%, the mTeSR™1 medium was

aspirated and slowly replaced with Medium A. Two days later, the medium was substituted with Medium B, and two days after the medium was replaced with Maintenance Medium (**Figure 8**). Cells were maintained in a humidified atmosphere containing 5% CO_2 at 37°C, and the Maintenance Medium was replaced every other day. On sampling days, cells were collected after dissociation with TrypLE™ Select Enzyme (10X) (# A1217702).

3.5 Immunocytochemistry

Cells on glass coverslips were fixed with 4% PFA at room temperature (RT) for 15 minutes. Then, the samples were rinsed three times with DPBS and permeabilized using 0.2% Triton X-100 in DPBS. Afterwards, the cells were blocked in a buffer solution containing 5% bovine serum albumin (BSA) in DPBS for 1 h at RT, and then stained with primary antibodies (**Supplementary table 1**) and incubated overnight at 4 °C. The following day, cells were washed three times with DPBS and incubated for 2 hours in the dark with secondary antibodies (**Supplementary table 2**) in 1% BSA solution. Next, cells on coverslips were mounted with ProLong™ Diamond Antifade Mountant (#P36961) containing DAPI. The slides were analysed with a fluorescence microscope (Axio Imager system with ApoTome; Carl Zeiss MicroImaging GmbH, Göttingen, Germany) controlled by AxioVision 4.8.1 software (Carl Zeiss MicroImaging GmbH).

3.6 Reverse-transcription quantitative PCR (RT-qPCR)

Total RNA was isolated from hiPSC and hiPSC-CMs through digestion with Proteinase K (QIAGEN #19131) using the RNeasy Plus Mini Kit (QIAGEN #74134) following the manufacturer's instructions. One microgram of RNA was used for cDNA synthesis through the Maxima First Strand cDNA Synthesis Kit for RT-qPCR (#K1641). The QIAgility liquid handling robot along with the Rotor-Gene Q cycler (QIAGEN) were used for the experimental set-up and the RT-qPCR reaction, respectively. The amplification was carried out in a total of 15 µL using SYBR Green JumpStart Taq ReadyMix (#S4438). Oligonucleotide primers (**Supplementary table 3**) were designed with Primer 3 software (Untergasser et al., 2012) and blasted on the human reference genome on Ensembl (Cunningham et al., 2022). All RT-qPCR reactions were normalized using *GAPDH* as a housekeeping gene and analysed using the comparative $2^{-\Delta\Delta Ct}$ method by normalising hiPSC-CMs and hiPSC to human adult heart reference RNA (Takara #636532).

3.7 Cellular viability assay

On day 18 of the differentiation, hiPSC-CMs were seeded into a 96-well plate with a density of $2x10^5$ cell/cm^2. After three days (day 21), the cells were exposed to increasing concentrations of compounds (Doxorubicin, Menadione, Acrylamide and Bisphenol A) for different time periods (24-96 hours). CellTiter-Glo® Luminescent Cell Viability Assay (Promega #G7570) was used to perform the ATP viability assay following the manufacturer's protocol. The luminescent signal was recorded using the Varioskan Flash Multimode Reader. Cell survival was calculated by assigning 100% viability for untreated controls and 0% viability for cells killed by exposure to water.

3.8 Oxidative stress detection

Cells on glass coverslips were treated for 24 hours with Doxorubicin, Menadione, or Acrylamide at the chosen concentrations. To measure reactive oxygen species in hiPSC-CM cultures, the cells were treated with 5 mM CellROX™ Deep Red (#C10422) for 1h at 37°C (excitation/emission: 644/665 nm). Cells were then fixed with 4% PFA and mounted with ProLong™ Diamond Antifade Mountant (#P36961) containing DAPI. The images were acquired with a fluorescence microscope (Axio Imager system with ApoTome; Carl Zeiss MicroImaging GmbH, Göttingen, Germany) controlled by AxioVision 4.8.1 software (Carl Zeiss MicroImaging GmbH). The signal quantification was performed using ImageJ software (Schneider et al., 2012).

3.9 Bisphenol A repeated treatment

Bisphenol A (BPA) (Merck, #239658, CAS No. 80-05-7) stocks were prepared by dissolving the compound in DMSO to a final concentration of 100 mM and stored at -20 °C. BPA was further diluted to the chosen concentrations selected based on typical levels of human environmental exposure (Murata & Kang, 2018), and in accordance with the guidance of the European Food Safety Authority (EFSA) and the Consortium Linking Academic and Regulatory Insights on BPA Toxicity (CLARITY-BPA) (Heindel et al., 2020; University of Hertfordshire, 2021; Vandenberg et al., 2019; Vom Saal & Vandenberg, 2021). For the repeated treatment, cells were exposed to 0.1% DMSO (vehicle) or BPA at selected concentrations (0.01 μM, 0.1 μM, 1 μM), starting from day 0 until day 21 of cardiomyocyte differentiation. For this process, a fresh differentiation medium containing BPA at the designated treatment concentrations was added every two days after completely removing the spent medium.

3.10 Flow Cytometry

After single-cell dissociation using TrypLE™ Select Enzyme (10X), the collected cells were washed with DPBS and moved into flow cytometry tubes (Beckman Coulter, #2523749) for staining. Firstly, the cells were stained with the Fixable Viability Dye eFluorTM 660 (eBioscienceTM #65-0864) for 30 minutes at 2-8 °C, protected from light. Then, the samples were rinsed with 1% BSA solution and centrifuged at 300-400xg at RT for 10 minutes. The True-Nuclear^{TM} Transcription Factor Buffer Set (BioLegend #424401) was used for staining, following the manufacturer's instructions, with the antibodies listed in **Supplementary table 4**. Samples were processed using the Flow Cytometer Cytomics FC 500 (Beckman Coulter), and data analysis was conducted with FlowJo (BD Bioscience, V10.8.1).

3.11 Contractility assay

The contractile motion of hiPSC-CMs was recorded through phase contrast video-microscopy using the Olympus IX71 microscope equipped with a DP21 camera (Olympus) and its CellSens software (Olympus; V1.11). Videos lasting a minimum of 10 seconds and running at 12 frames/second were analysed using the Pulse analysis platform (Curibio) (Maddah et al., 2015).

3.12 Quantitative proteomics

3.12.1 Sample preparation

Using a Sonopuls HD3200 (Bandelin, Berlin, Germany), cells were ultrasonically lysed (18 cycles of 10 s) in 8 M urea/0.5 M NH_4HCO_3. Protein quantification was performed with the Pierce 660 nm Protein Assay (Thermo Fisher Scientific, Rockford, IL, USA). A total of 20 µg of protein was processed for digestion. Briefly, disulfide bonds were reduced using 45 mM dithiothreitol/20 mM tris(2-carboxyethyl) phosphine for 30 minutes at 56°C, and cysteine residues were alkylated (100 mM iodoacetamide, 30 min, room temperature), followed by quenching the excess of iodoacetamide with dithiothreitol (90 mM, 15 min, room temperature). Proteins were digested with modified porcine trypsin (Promega, Madison, WI, USA) for 16 h at 37°C (1:50 enzyme to protein ratio).

3.12.2 Nano-liquid chromatography–tandem mass spectrometry (LC-MS/MS) analysis and statistics

The sample (1 µg) was injected into an UltiMate 3000 nano-LC system connected online to a Q-Exactive HF-X mass spectrometer operated in data-dependent acquisition (DDA) mode. Then, peptides were transferred to a PepMap 100 C18 trap column (100 µm×2 cm, 5 µM particles) and separated using a PepMap RSLC C18 analytical column (75 µm×50 cm, 2 µm particles) at a flow rate of 250 nl/min, with a gradient of 5-20% of solvent B used for 80 minutes followed by a 9-minute increase to 40%. Formic acid 0.1% in water and acetonitrile were used as solvents A and B, respectively. Raw data were processed using MaxQuant (version 1.6.7.0) (Tyanova et al., 2016). The human SwissProt reference proteome (downloaded in October 2022) was used for all searches. The dataset has been submitted to the ProteomeXchange Consortium via the PRIDE partner repository (Perez-Riverol et al., 2022) with the dataset identifier PXD042046. Statistics and data visualization were performed in R using custom scripts. Reverse peptides, contaminants, and identifications only by site were excluded from quantification. Proteins with at least two peptides with a minimum of three replicate measurements in each condition were quantified using MS-EmpiRe pipeline (Ammar et al., 2019) as described previously (Flenkenthaler et al., 2021). Peptides with complete measurements in one condition but insufficient measurements in the other condition were inputed from a normal distribution (downshift = 1.8, scale = 0.3). Proteins with a Benjamini-Hochberg-adjusted p-value < 0.05 and a fold change above 1.3 were considered as significantly changed. The ComplexHeatmap R package (Gu et al., 2016) generated the heatmap, which was segregated into homogeneous regions using the k-means method. WebGestaltR package (Liao et al., 2019) and the functional category ‘GO Biological Process nonRedundant’ were used to perform over-representation analysis.

3.13 Human Protein-Protein Interactions (PPI) network construction and analysis

The human PPI network was constructed using publicly available resources (Alanis-Lobato et al., 2017; Luck et al., 2020; Menche et al., 2015), resulting in 18,816 proteins and 478,353 physical interactions. Proteins with a fold change (|FC|)>1.5 were mapped onto this network, and their connectivity was analysed by computing a z-score of the largest connected component (lcc) size for each protein group compared with 10,000 randomly selected protein sets of identical size. The global perturbation of each condition and the proteins that were up- and down-regulated were analysed. To create a connected core from the sparse network, a random walk with restart algorithm was used. The algorithm used a restarting parameter (alpha) of 0.9 to keep the propagation closer to the initial seed genes. Furthermore, only nodes with high expression levels

in the heart were included at each step. The Human Protein Atlas (HPA) (https://www.proteinatlas.org/) was used to extract this information. The resulting list contained 36 tissue enriched proteins (|FC|heart>4*|FC|any tissue), 129 group enriched proteins (|FC|heart>4*|FC|any tissue-4), and 257 tissue enhanced proteins (|FC|heart>4*|FC|average(all tissues)), totalling 452 proteins.

3.14 Protein enrichment analysis

The biological characterization of the core and expanded modules was carried out via enrichment analyses for the three main branches of the Gene Ontology (GO) (Ashburner et al., 2000): biological processes (BP), molecular functions (MF), and cellular components (CC), as well as KEGG pathway (Kanehisa & Goto, 2000) using GSEApy (Fang et al., 2023).

3.15 Disease relationship

Diseases-gene associations (GDA) were acquired from DisGeNet (Piñero et al., 2015). To retrieve data for 11,099 disorders, we only chose relationships having a GDA score >0.3. To determine the relationship between each differentially abundant protein set (s1) and set of disease proteins (s2), two methods were applied. Firstly, the Jaccard index (intersection (s1,s2)/union(s1,s2)) was calculated, and secondly, network proximity was used, which compares the distance between the two protein sets against 10,000 random sets with similar topological features (Guney et al., 2016). This enabled the correction for interactome biases, including the heavy-tail degree distribution and the discretization of other common network distances. Moreover, only heart diseases with a false discovery rate (FDR)<0.01 (n=1096) were considered and grouped into 9 phenotypic categories. The created network incorporated the shortest molecular path and the shortest hub-preferential path between the BPA-unified core and those heart diseases, based on heart transcriptomic protein expression. To achieve this, a random walk with a restart algorithm was applied to the 452 proteins elevated in the heart, obtained from HPA database, to obtain a heart-specific interactome. This network was then used to determine both the shortest and the hub-preferential path between the given gene sets.

3.16 Hypoxia and reoxygenation model

The hypoxia/reoxygenation (H/R) model was established according to the previously published method (Häkli et al., 2021), and using a HeraCellTM Vios 250i CO_2 incubator. Briefly, one day prior to hypoxia treatment, hiPSC-CMs were cultured in serum- and glucose-free medium (RPMI

1640 without glucose) containing 1% MEM NEAA, 1% GlutaMAX and 0.5% Penicillin-Streptomycin. The following day, hiPSC-CMs were subjected to a hypoxic environment of 1% O_2 and 5% CO_2 gas for a duration of 8 hours. After this period, hiPSC-CMs were supplied with Maintenance Medium (containing glucose) and maintained in the standard cell culture environment to simulate the reperfusion phase for 15 hours. For control conditions, cells were cultured in serum- and glucose-free medium followed by Maintenance Medium in the standard culture environment (referred to as "normoxia").

3.17 Analysis of apoptosis and mitochondrial activity

To monitor apoptosis and active mitochondria of hiPSC-CMs, Caspase 3/7 Green Dye (Incucyte®, Sartorius # 4440) and MitoTracker™ Deep Red (#M22426) were used, respectively, according to the recommended protocols. The fluorescent signal was assessed using the IncuCyte S3 Live-Cell Analysis Instrument (Sartorius AG). Each biological experiment included three wells (technical repeats), with a total of sixteen images captured per well using a 10× objective. The images were analysed using the IncuCyte Basic Software (Sartorius), with the acquisition times for the green and red channels being 300ms and 100ms, respectively. The Green or Red Mean Intensity Object Average metric was used to quantify the signal.

3.18 Statistical analysis

All data were analysed using Prism 8 (GraphPad Software, La Jolla, CA, USA) and handled in Microsoft Excel (Redmond, WA, USA) unless otherwise specified. The "n" value refers to the number of biological replicates, and the data analysis is presented as the mean ± standard error of the mean (SEM). The significance of the data was determined using one-way ANOVA or two-way ANOVA with Dunnett's post hoc test, as indicated in the figures' legend.

4 RESULTS

4.1 Characterisation of hiPSC (SBAD2 clone)

In the current study, SBAD2 hiPSC line was used to generate the 2D *in vitro* cardiomyocyte differentiation model. An important consideration when culturing hiPSCs is the maintenance of pluripotency. To confirm the pluripotency state and multilineage differentiation ability of our hiPSC line, a qualitative assessment of stem cell characteristics has been evaluated. The hiPSCs formed distinctive colonies (**Figure 7A**), which are positively stained for the typical pluripotency markers Oct4, Nanog and TRA1-81, supported by flow cytometry analysis showing more than 95% of $Oct4^{+}$/$Nanog^{+}$ expressing cells (**Figure 7B, C**). Additionally, SBAD2 hiPSC line can form 3D aggregates defined as EBs (**Figure 7D**), which contain the combination of the three germ layers. Following the formation and the maintenance of the EBs for 14 days, the cells were able to differentiate into endodermal (GATA4), mesodermal (BRACHUYRY) and ectodermal (NESTIN, TUBB3) lineages under spontaneous differentiation, thus confirming their pluripotent status in our *in vitro* setting (**Figure 7E**).

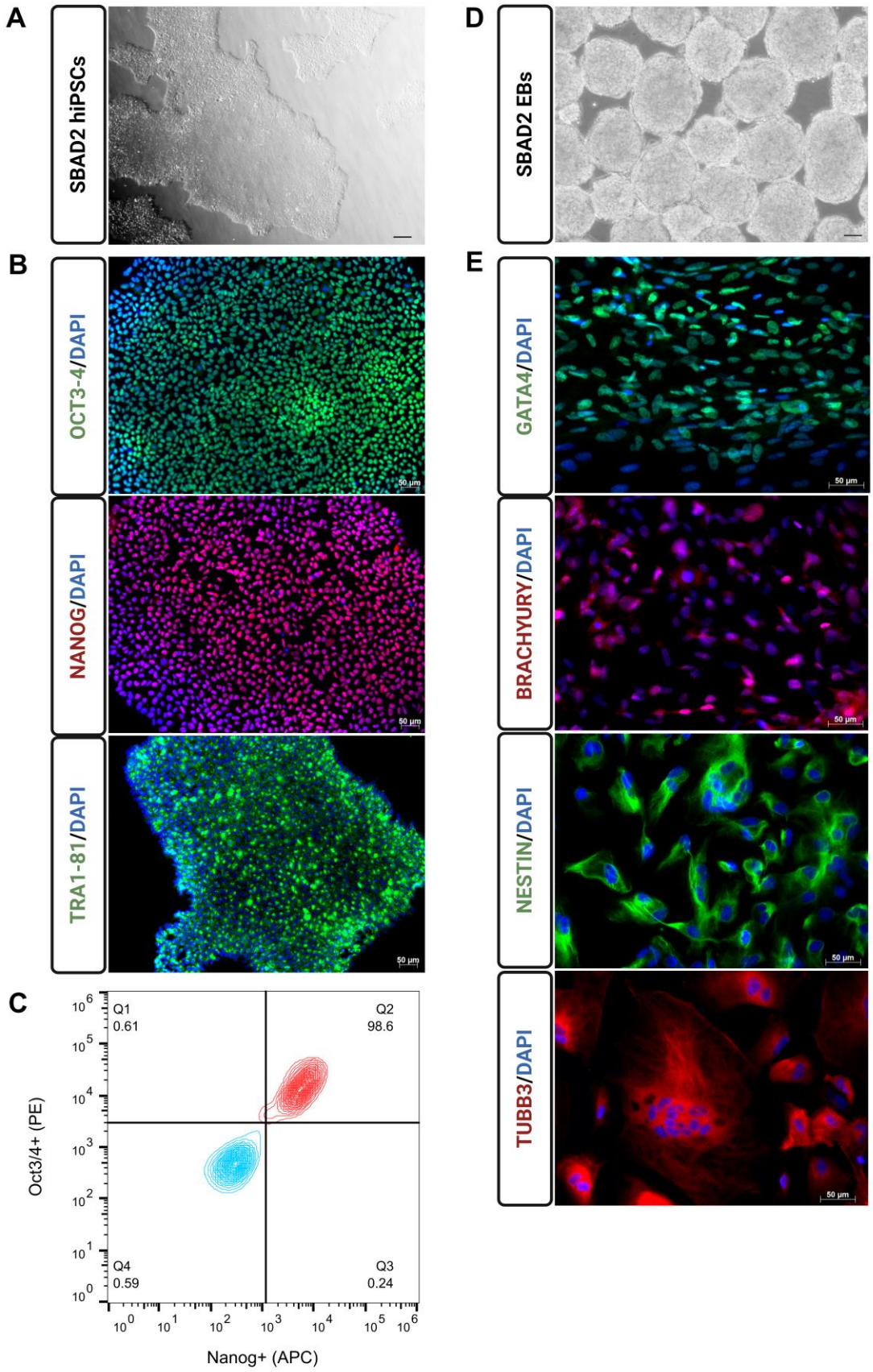

Figure 7. **Characterization of SBAD hiPSCs in culture**. (**A**) and (**D**) Phase contrast images of SBAD2 hiPSCs in 2D culture (4x magnification) and after embryoid bodies (EBs) formation (10x magnification). (**B**) Immunofluorescence staining of pluripotency markers OCT3-4 (AlexaFluor 488), NANOG (AlexaFluor 594) and TRA1-81 (AlexaFluor 488) in 2D culture. Nuclei were counterstained with DAPI

(blue). Scale bar, 50 µm. (**C**) Flow cytometry representation of SBAD2 hiPSC population double-positive for OCT3-4 (PE) and NANOG (APC). The light-blue peak represents the blank control sample. (E) Multilineage differentiation potential was confirmed by immunostaining for GATA4 (AlexaFluor 488), BRACHYURY (AlexaFluor 594), NESTIN (AlexaFluor 488) and TUBB3 (AlexaFluor 594) to observe the formation of the three germ layers. Nuclei were labeled with DAPI (in blue). Scale bar, 50 µm.

4.2 Characterisation of hiPSC-derived cardiomyocytes

SBAD2 hiPSC were differentiated in cardiomyocytes through the classic two-step protocol, consisting of the Wnt signalling activation, allowing the mesodermal induction, followed by the Wnt signalling inhibition to enhance the cardiac lineage specification and differentiation, as schematically represented in **Figure 8**.

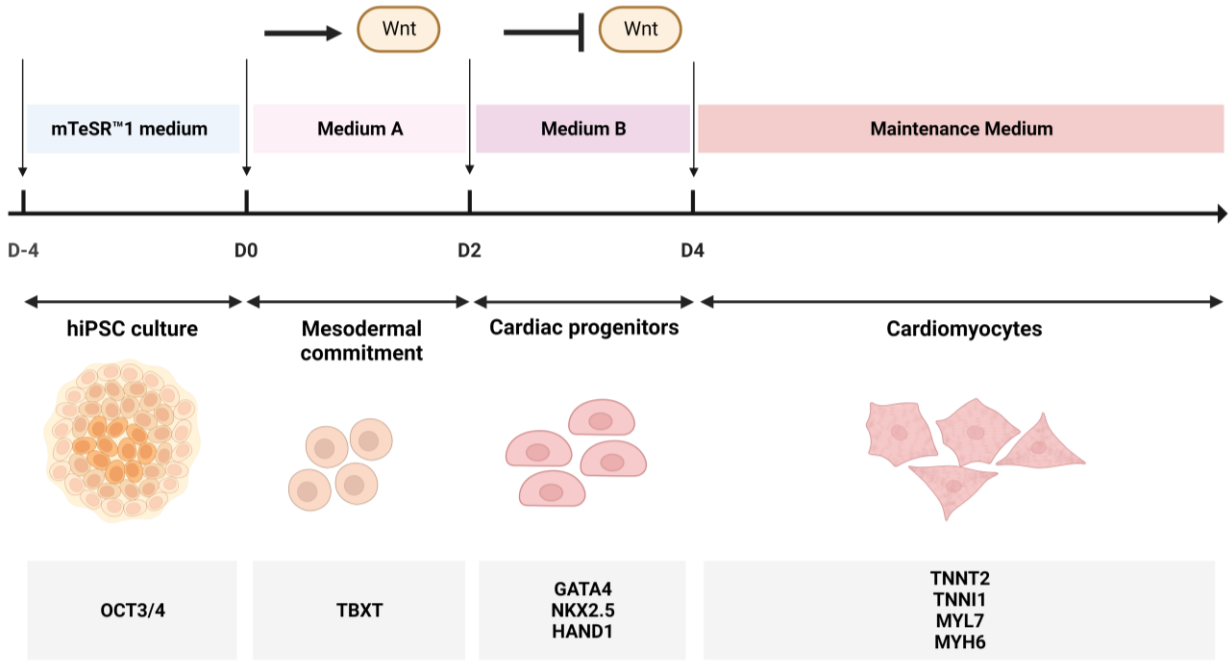

Figure 8. Schematic illustration of cardiomyocytes differentiation protocol from hiPSC. Pluripotency is maintained for 4 days (D-4) in mTeSR™1 medium to reach the targeted cellular confluence. Then, Wnt signalling pathway is activated following the medium A during the first 2 days of differentiation (D0-D2). Subsequently, Wnt signalling pathway is blocked following the medium B during day 2 (D2) and day 4 (D4) of differentiation. Afterwards, maintenance medium is used to culture the cells till desired level of maturity. Figure created using BioRender.com.

To monitor the progression of the cardiomyocyte differentiation, we analysed the mRNA levels of lineage-specific genes at time points corresponding to pivotal developmental transitions, including the pluripotency state, mesodermal specification, cardiac progenitor, and cardiomyocyte formation (**Figure 9**).

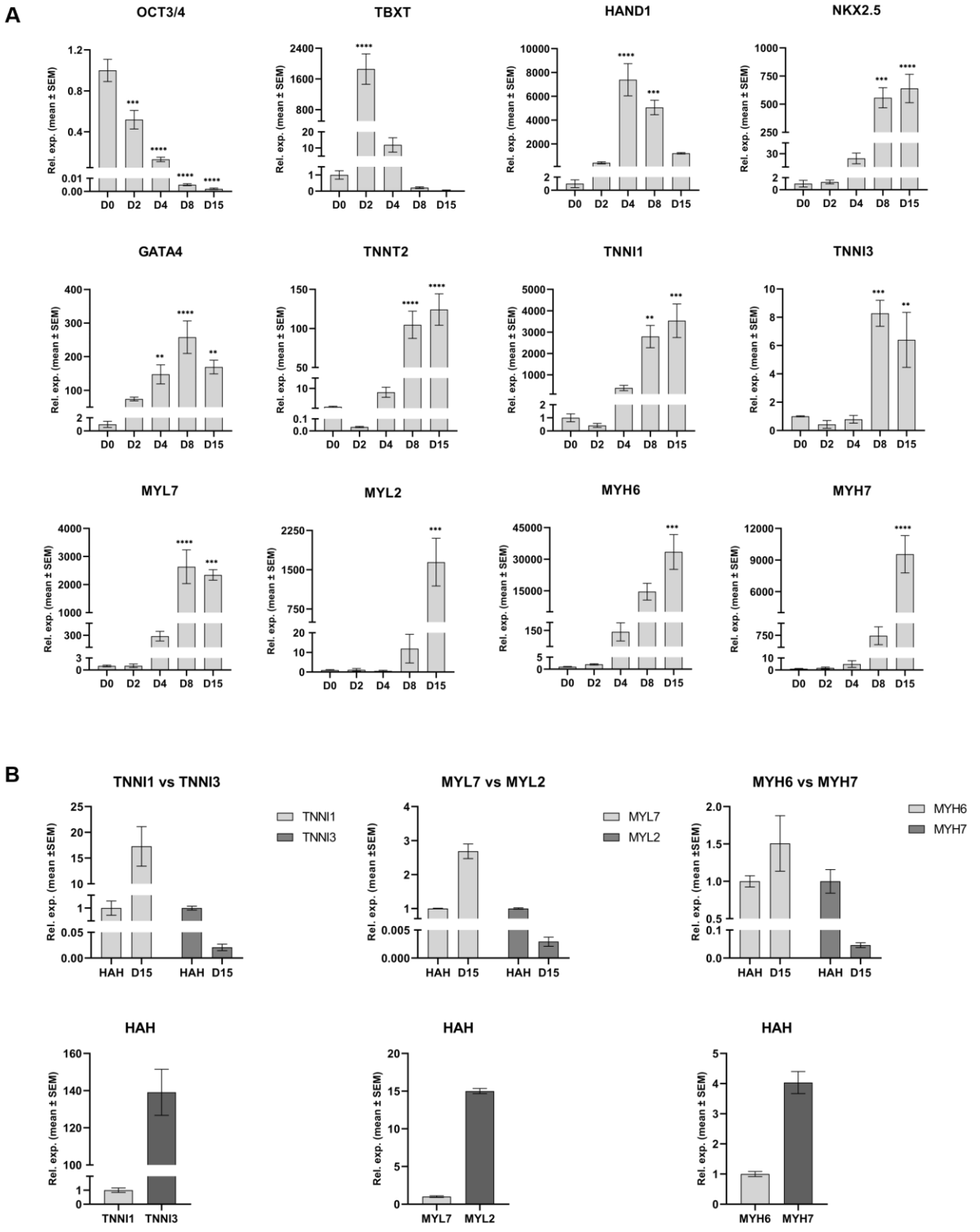

Figure 9. **Gene expression analysis during in vitro cardiomyocyte differentiation**. (**A**) mRNA expression levels during the cardiomyocyte differentiation, measured by RT-qPCR. (**B – upper panel**) mRNA expression levels comparison of early (MYH6, MYL7, TNNI1) and late (MYH7, MYL2, TNNI3) cardiac structural markers at day 15 (D15) of differentiation, and (**B – lower panel**) early vs late gene expression comparison in the human adult heart (HAH) RNA. Results show independent experiments (n = 4). Data were normalized using GAPDH as a housekeeping gene and the human adult heart (HAH) reference RNA (Takara Bio Inc.). Error bars represent ±SEM. One-way ANOVA with Dunnett's post-hoc test was used for comparisons between the hiPSC stage (D0) and the other time points (adjusted p-value *< 0.05, **< 0.01, ***< 0.001, ****< 0.0001.).

The pluripotency marker *OCT3/4* was rapidly downregulated from the second day of differentiation (D2), and cells expressed *TBXT*, which represents a key gene of mesodermal commitment (**Figure 9A**). Following the expression of *HAND1* and *GATA4* markers, the generation of cardiac progenitors started from the fourth day (D4), followed by the later expression of *NKX2.5* peaking by day 8. Spontaneous beating activity was observed already after one week of differentiation, together with the increase of myofilament genes, such as *TNNT2*, *TNNI1*, *MYH6* and *MYL7*. Higher mRNA expression of foetal troponin I (*TNNI1*) compared to the adult isoform (*TNNI3*) was observed, together with higher levels of *MYH6* and *MYL7*, compared to *MYH7* and *MYL2*, respectively (**Figure 9B**). Qualitative evaluation of the cells with immunocytochemistry labelling revealed that hiPSC-CMs exhibit an immature structure, shown by the misaligned localization of cardiac troponin T (cTnT) and MLC2a/MLC2v (**Figure 10A, B**). Flow cytometry analysis displayed that ~80% of the population is represented by hiPSC-CMs after 21 days of differentiation (**Figure 10C**). Accordingly, flow cytometry analysis showed higher expression of MLC2a (74.8%) compared to MLC2v (45.5%) (**Figure 10C**).

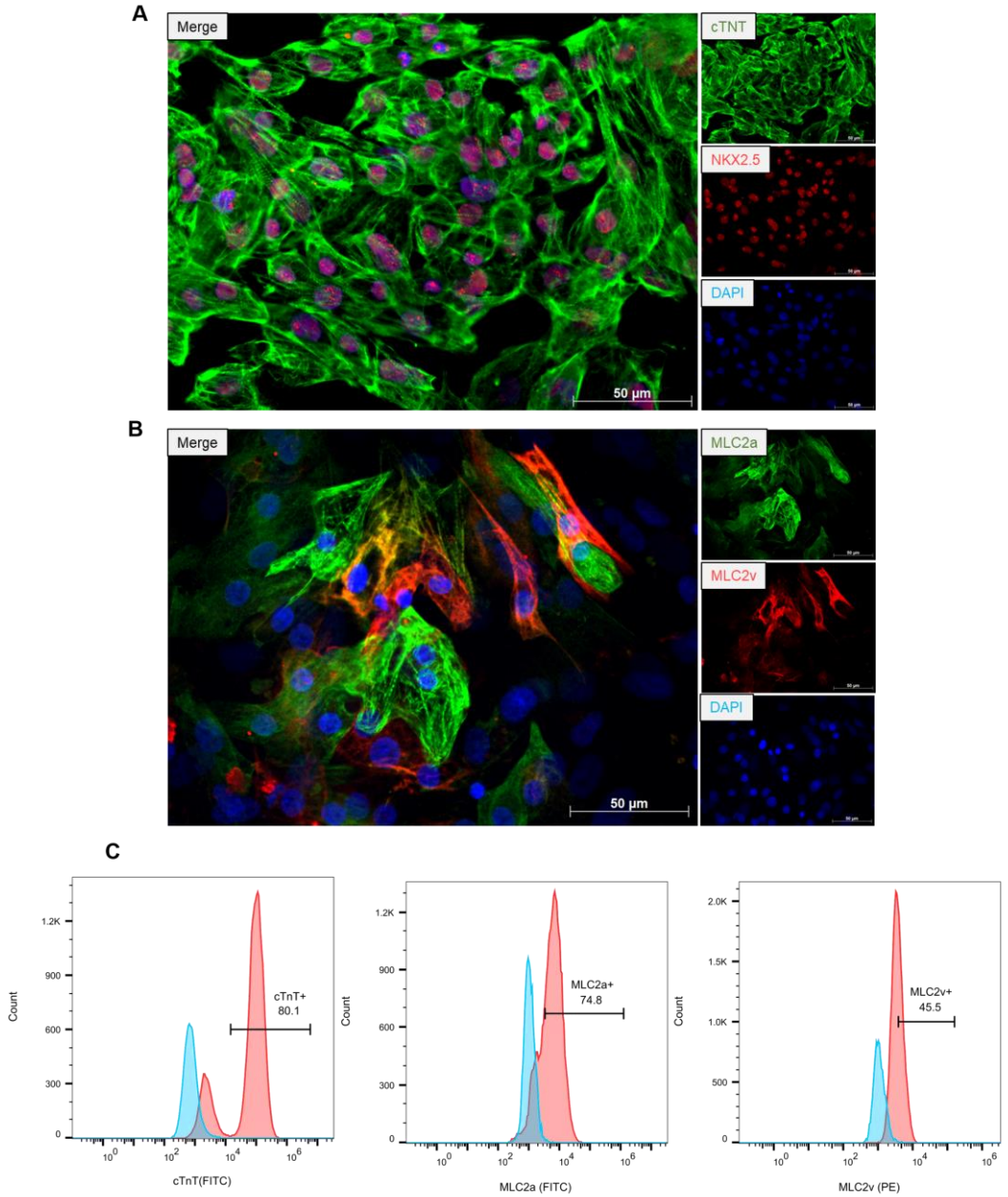

Figure 10. **Qualitative and quantitative analysis of key cardiac structural markers**. (**A**) and (**B**) Immunofluorescence staining of hiPSC-CMs at day 15 of differentiation for cardiac troponin T (cTnT; AlexaFluor 488), NKX2.5 (AlexaFluor 594), MLC2a (AlexaFluor 488) and MLC2v (AlexaFluor 594). Nuclei were stained with DAPI (blue). Scale bar, 50 µm. (**C**) Flow cytometry representation of hiPSC-CMs population after 21 days of differentiation for cardiac troponin T (cTnT; FICT), MLC2a (FICT) and MLC2v (PE). The light-blue peak represents the blank control sample.

Moreover, the proteome profiles of hiPSC-CMs have been characterized by LC-MS/MS, comparing the hiPSC stage (D0) and the hiPSC-CMs after 21 days of differentiation (D21). With high confidence (false-discovery rate < 0.01) 1922 proteins were identified, of which ~73 % were significantly altered at D21 compared to D0 (**Figure 11A**). The two clusters showed distinct protein changes, in line with the cardiac differentiation (**Figure 11B**). Gene Ontology (GO)

analysis revealed the increase of proteins being part of heart morphogenesis and cardiomyocyte differentiation in D21, while defining characteristics of stemness, such as cell cycle checkpoint and DNA replication, were decreased. Also, typical cardiomyocyte structural markers, such as multiple myosin isoforms (e.g., MYL7, MYL3 and MYL4) and troponins (e.g., TNNT2 and TNNI1), and heart metabolic markers (e.g., FABP3) were significantly increased in abundance in differentiated cells, confirming the correct route of cardiac differentiation process (**Figure 11C**).

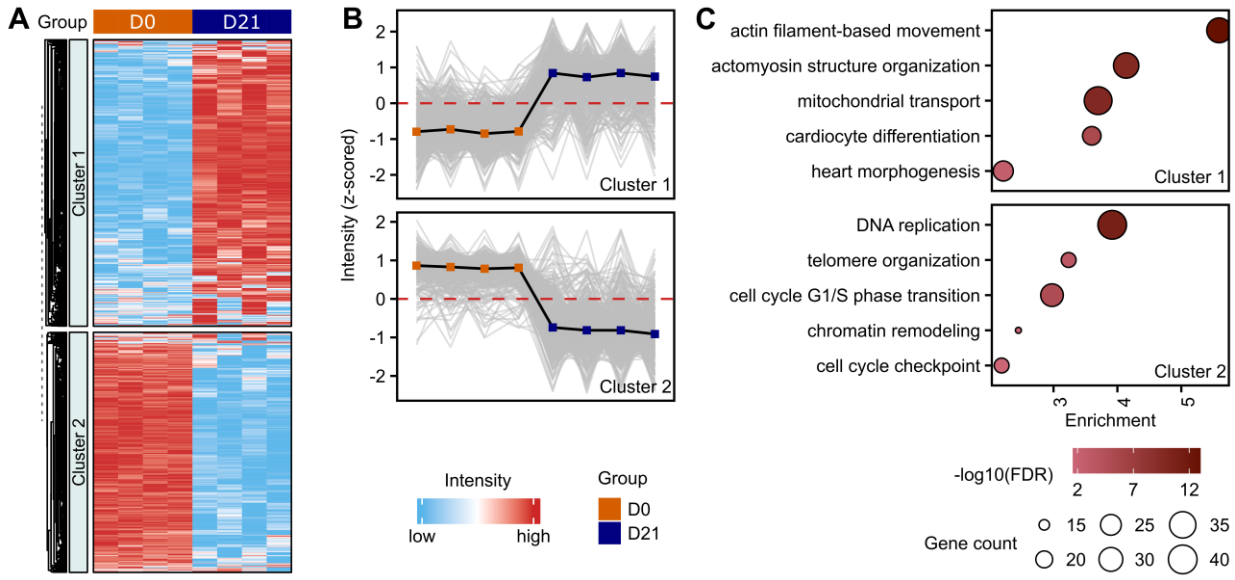

Figure 11. **Proteome changes after 21 days of cardiomyocyte differentiation**. (**A**) Heatmap of proteins significantly changed in abundance (adjusted p-value < 0.05, fold-change > 1.3) between D0 and D21. Z-scored protein abundance values are shown in red and light blue for high and low abundance, respectively. Heatmap rows were segregated into homogenous regions using K-means method (k = 2). (**B**) Profile plots with mean values (solid black line) of two clusters showing distinct alteration of proteins with respect to the day of differentiation. (**C**) Gene ontology enrichment analysis of proteins from each cluster. The colour of the bubble indicates the significance of the enrichment, and the size of the bubble indicates the corresponding number of differentially abundant proteins (referred to as gene count in the figure). Enrichment shows the magnitude of over-representation.

4.2.1 Validation of hiPSC-CMs as a cardiotoxicity model and experimental set up for the repeated treatment with Bisphenol A

To assess the suitability of our hiPSC-CMs model for investigating the toxicity of environmental chemicals on early developing cardiomyocytes *in vitro*, ATP-release based viability assay was performed to generate dose-response curves of doxorubicin, menadione and acrylamide. Already after 24-hour treatment, and even more extended after 48 hours and 96 hours, the viability of hiPSC-CMs significantly decreased under doxorubicin and menadione exposure in a dose-dependent manner (**Figure 12A, B**). Acrylamide was significantly less toxic after 24- and 48-hour treatment, even in high concentrations. After 96-hour treatment, supraphysiological doses of acrylamide significantly decreases the cellular viability **(Figure 12C**).

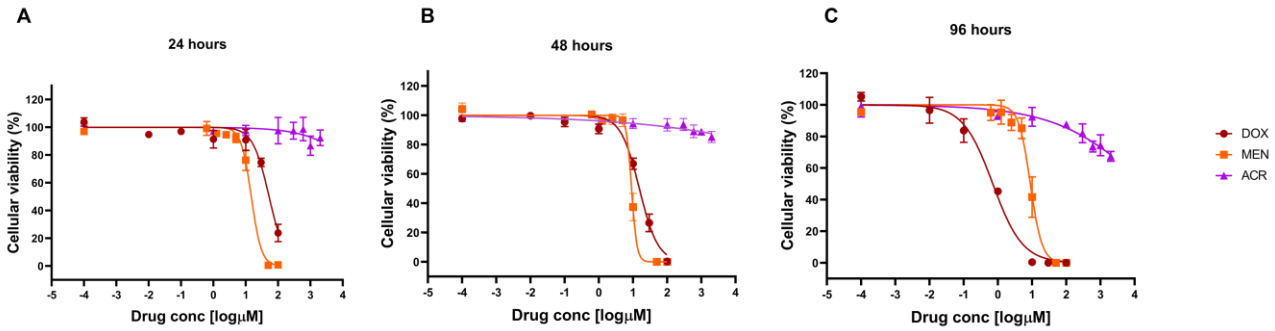

Figure 12. Cellular viability results of hiPSC-CMs 21-day differentiated treated with increasing concentrations of doxorubicin (DOX), menadione (MEN) and acrylamide (ACR) for 24 (**A**), 48 (**B**) and 96 hours (**C**). Standard error bars are shown (n=3).

The cytotoxicity model produced repeatable dose-responses, identifying specific half maximal effective concentration (EC50) for each compound (values not shown), according to the treatment duration. Subsequently, we investigated whether the compounds were able to generate ROS in hiPSC-CM cultures already after 24-hour treatment at chosen doses, ranging below the EC50. Using the CellROX assay, we performed a qualitative and quantitative detection of ROS, observing a positive fluorescent signal that increased in a dose-dependent manner (**Figure 13A**), although without significant differences after acrylamide treatment (**Figure 13B-D**).

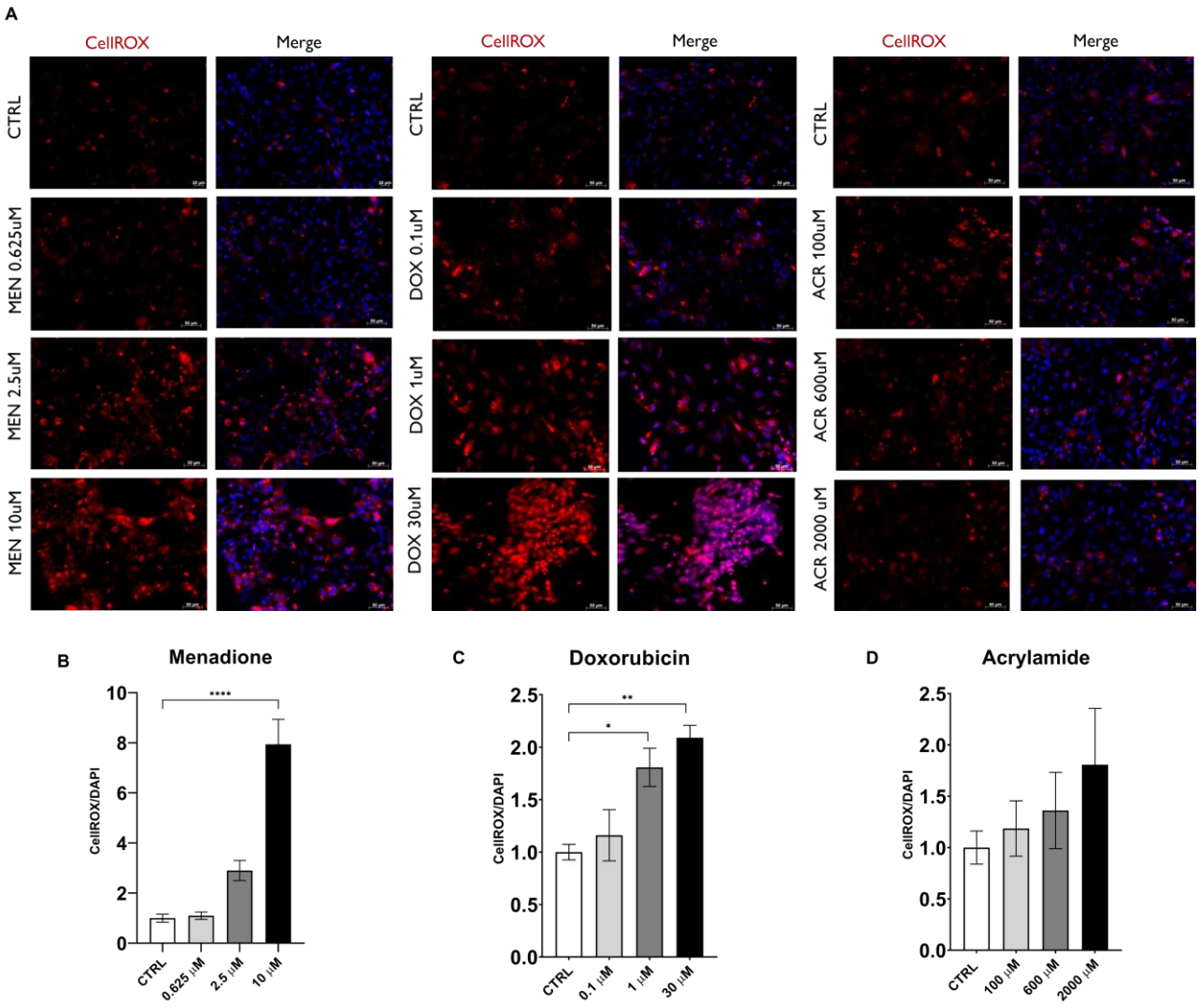

Figure 13: ROS detection after 24-hour treatment with menadione (0-10 µM), doxorubicin (0-30 µM) or acrylamide (0-2000 µM). (**A**) Immunofluorescence staining was acquired by CellROX Deep Red dye. The fluorescence signal was quantified for (**B**) menadione (n = 4), (**C**) doxorubicin (n = 4), and (**D**) acrylamide (n = 4). Error bars represent ±SEM. One-way ANOVA with Dunnett's post-hoc test was used for comparisons between untreated control (CTRL, 0 µM) and the other compound concentrations (adjusted p-value *< 0.05, **< 0.01, ***< 0.001, ****< 0.0001.).

Once the model was tested and validated on well-known toxic compounds, the experimental set up for the repeated treatment with BPA was designed. Firstly, a range of BPA concentrations was chosen according to the aim of the study. For this purpose, a broader concentration gradient was set for low doses. Specifically, concentrations of 3 µM and 5 µM were selected according to the tolerable daily intake (TDI) of 50 µg/kg/day assumed to be "safe" before 2015 (Vom Saal & Vandenberg, 2021), while the two highest concentrations (10 µM and 100 µM), were selected for the evaluation of the dose-response curve in the supraphysiological range. Concentrations between 0.01 µM and 1 µM represent the target range of this study, corresponding to the TDI of ≤ 4 µg/kg/day agreed after 2015 (University of Hertfordshire, 2021). Then, to assess the potential

cytotoxicity effects after acute treatment, the 21-day differentiated hiPSC-CMs were exposed to BPA (0.01–100 µM) for 24 and 72 hours (**Figure 14A**).

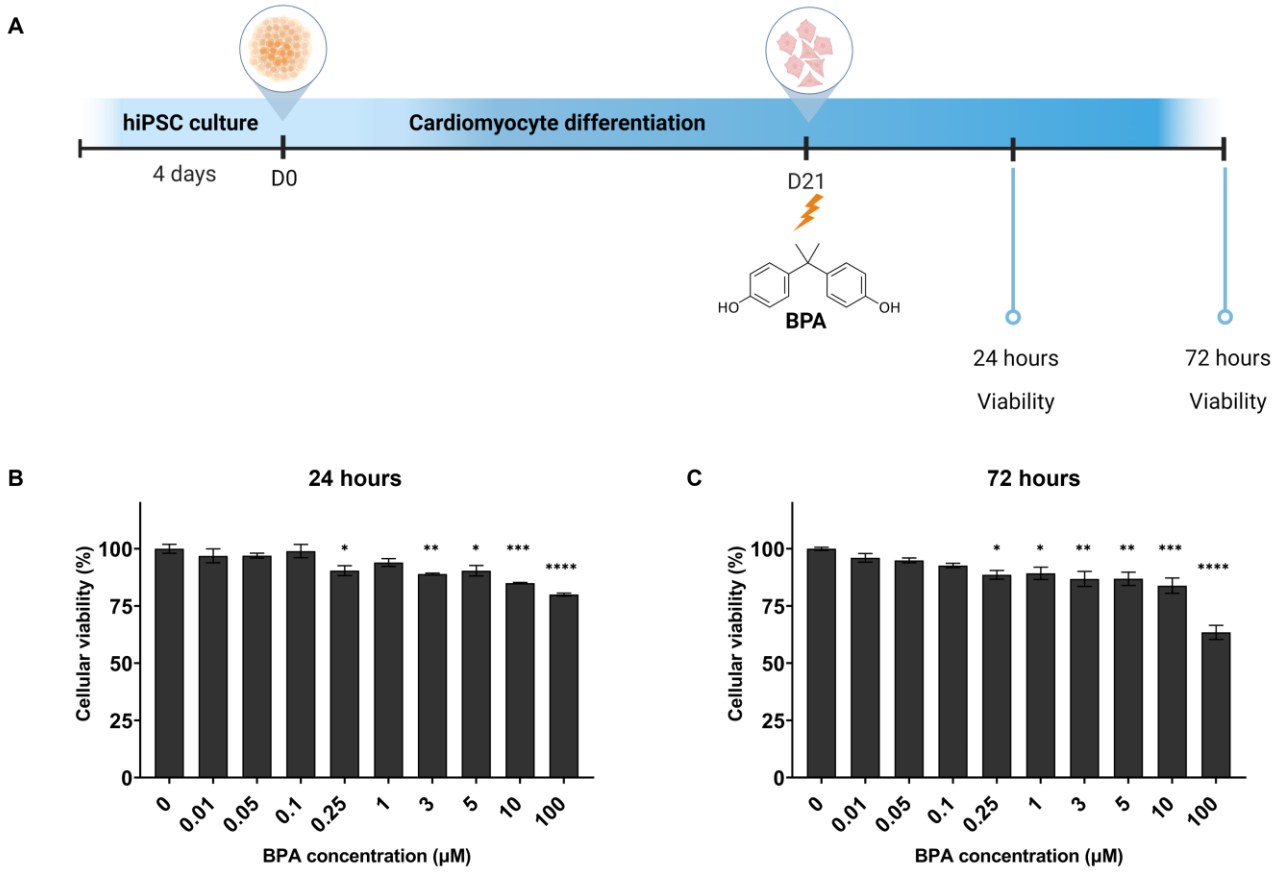

Figure 14: Acute BPA exposure on hiPSC-CMs. (**A**) Schematic overview of acute exposure with BPA on hiPSC-CMs; cellular viability was measured after 24- and 72-hour treatment. (**B, C**) Cellular viability of hiPSC-CMs (n = 3) 21-day differentiated after 24 hours and 72 hours of treatment with BPA in varying concentrations (0–100 µM). Error bars represent ±SEM. One-way ANOVA with Dunnett's post-hoc test was used for comparisons between untreated control (0 µM) and the other BPA concentrations (adjusted p-value *< 0.05, **< 0.01, ***< 0.001, ****< 0.0001.). Panel (**A**) is created using BioRender.com.

After 24 hours, the viability of hiPSC-CMs was affected at concentrations above 0.25 µM, even if the cellular mortality was not particularly extended. Around 90-85% viable cells were observed up to 10 µM, while 80% viability was measured at 100 µM concentration (**Figure 14B**). Similarly, after three days, the viability of hiPSC-CMs was affected starting from 0.25 µM, with the highest value of cellular death (35%) observed at 100 µM BPA (**Figure 14C**). According to these results, three physiologically relevant concentrations of BPA (0.01 µM, 0.1 µM, 1 µM) were chosen for the repeated treatment during the cardiomyocyte differentiation. A schematic representation of the repeated treatment with BPA is shown in **Figure 15A**, where cells were exposed to BPA every second day, starting from the pluripotency stage at day 0.

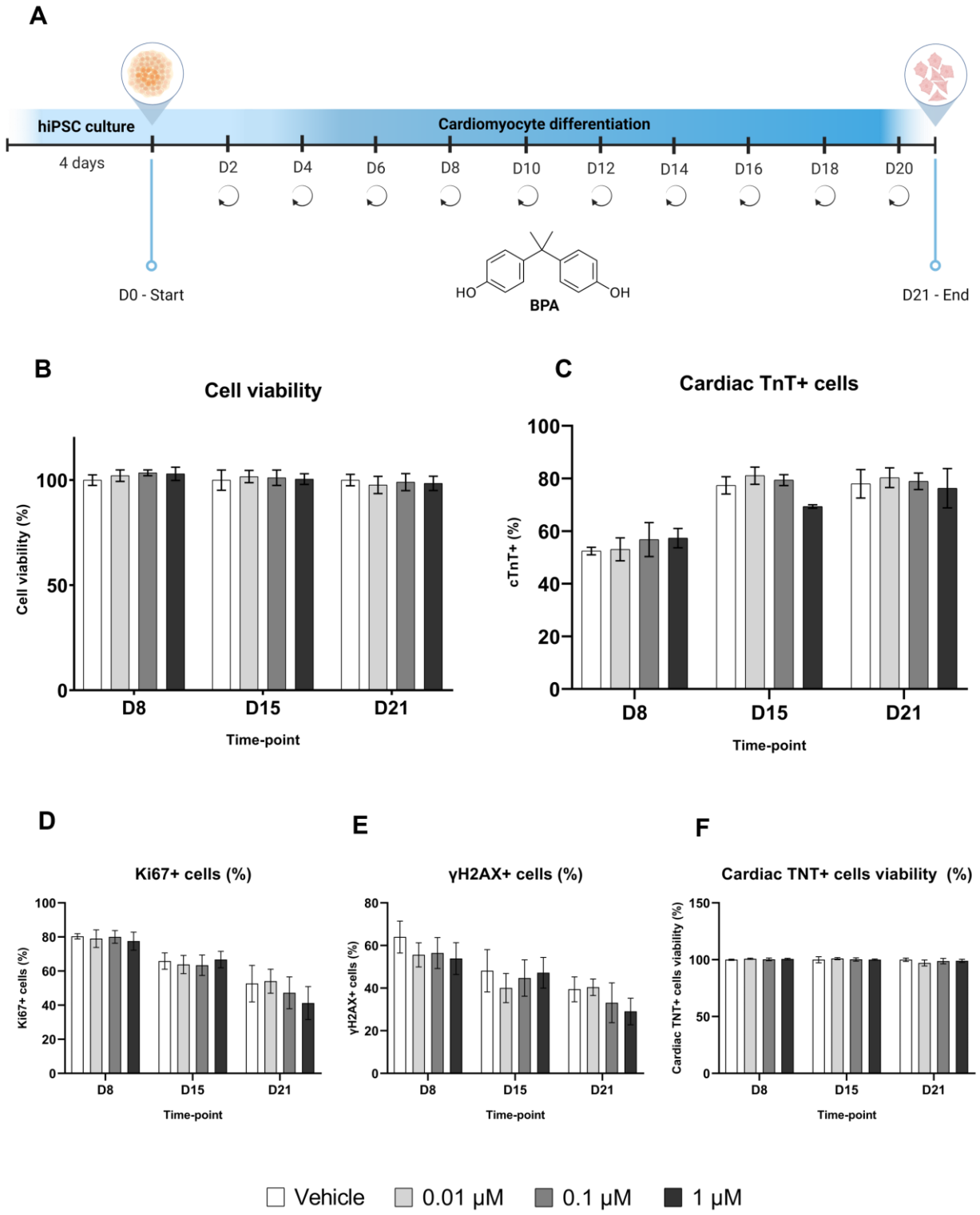

Figure 15. **Repeated exposure with BPA**. (**A**) Schematic overview of repeated exposure with BPA during cardiomyocyte differentiation. (**B**) Viability of the whole cellular population was measured by flow cytometry using Fixable Viability Dye eFluor™ 660 after repeated BPA exposure during cardiomyocyte differentiation. (**C**) Cardiac troponin T-positive (cTnT+) cells were measured by flow cytometry at different time points. Flow cytometry measurement of proliferation (**D**) with Ki67 and DNA double-strand breaks (**E**) using γH2AX in the whole cellular population. (**F**) Flow cytometry measurement of viability in cardiac TnT+ cells. Results show independent experiments (n = 3), and error bars represent ±SEM. Two-way ANOVA with Dunnett's post-hoc test was used for comparisons between untreated control (vehicle) and the three BPA concentrations. Panel (**A**) is created using BioRender.com.

Flow cytometry analysis showed that the viability of the whole cell population was not affected by BPA treatment over the duration of the differentiation (**Figure 15B**). As the differentiation progresses, the cell proliferation capacity (percentage of Ki67-positive cells) decreased, however, no significant differences were observed in the number of Ki67-positive cells in BPA-treated cells compared to vehicle control. Similarly, the amount of DNA double-strand breaks (percentage of γH2AX-positive cells) was not significantly altered upon BPA treatment (**Figure 15D, E**). According to the cardiomyocyte commitment, the proportion of hiPSC-CMs increased during the first two weeks of differentiation (**Figure 15C**). However, the percentage of cardiac troponin T-positive ($cTnT^{+}$) cells and their viability was mostly unchanged upon BPA treatment (**Figure 15C, F**).

4.3 Bisphenol A altered the contraction properties of hiPSC-CMs after 21 days of differentiation

After 21 days of BPA treatment, the contraction properties of hiPSC-CMs were investigated. As the interplay of contraction's parameters and their temporal relationship are essential for the proper functioning of hiPSC-CMs, we assessed the BPA effects on the cellular spontaneous contraction using the software platform Pulse (Curibio), which performed the motion analysis using phase-contrast videos. The beating force, together with the cell shortening, here expressed as peak height (arbitrary units) and contraction displacement (pixels), respectively, were our index of contractility (Maddah et al., 2015). The beating signal extracted by Pulse showed that the peak height value was unaltered by BPA in all three concentrations, even though a slight downward trend compared to the vehicle can be observed (**Figure 16A, B**). Although without significant differences, the contraction displacement visibly depicts a downward trend of cellular shortening in hiPSC-CMs treated with BPA (**Figure 16C**).

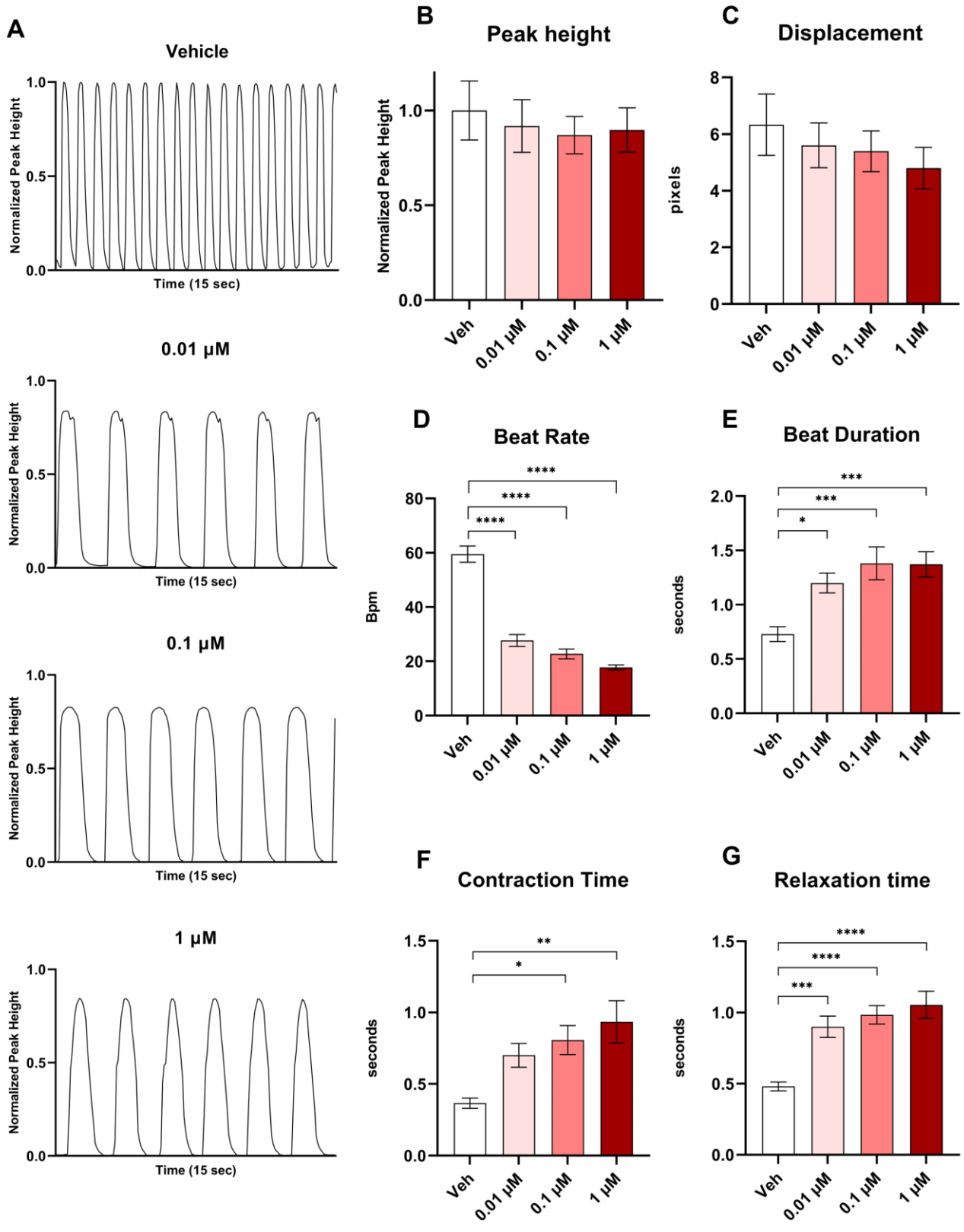

Figure 16. **Beating signals acquired by the Pulse software on hiPSC-CMs**. (**A**) Beating frequency and peak height of untreated (vehicle) and BPA-treated hiPSC-CMs. Peak height is normalized based on vehicle control. (**B**) Peak height of independent experiments normalized on vehicle control. (**C**) Contraction displacement analysis in pixels. (**D**) Beat rate (frequency) per minute of untreated and BPA-treated hiPSC-CMs. (**E**) Beat duration followed by (**F**) contraction and (**G**) relaxation time per second of untreated and BPA-treated hiPSC-CMs. Results show independent experiments (n = 16); error bars represent ±SEM. Two-way ANOVA with Dunnett's post-hoc test was used for comparisons between untreated control

(vehicle) and the three BPA concentrations (adjusted p-value *< 0.05, **< 0.01, ***< 0.001, ****< 0.0001.). Veh: vehicle.

Additionally, we did not claim an arrhythmic beating profile due to the regular contractions over time. However, the beat rate of hiPSC CMs treated with BPA showed a remarkable slowdown in a concentration-dependent manner, with a 70% reduction of beats per minute at the highest dose of BPA (**Figure 16D**). The treatment with BPA also led to a significant increase in the beat duration but without longer diastolic intervals between two consecutive beats (**Figure 16A, E**). Accordingly, the contraction and relaxation times were prolonged in a concentration-dependent manner (**Figure 16F, G**). Finally, BPA treatment significantly decreased the beating velocity of hiPSC-CMs. This vector analysis showed that the speed of elongation and shortening of hiPSC-CMs decreased as the concentration of BPA increased (**Figure 17A, B**)

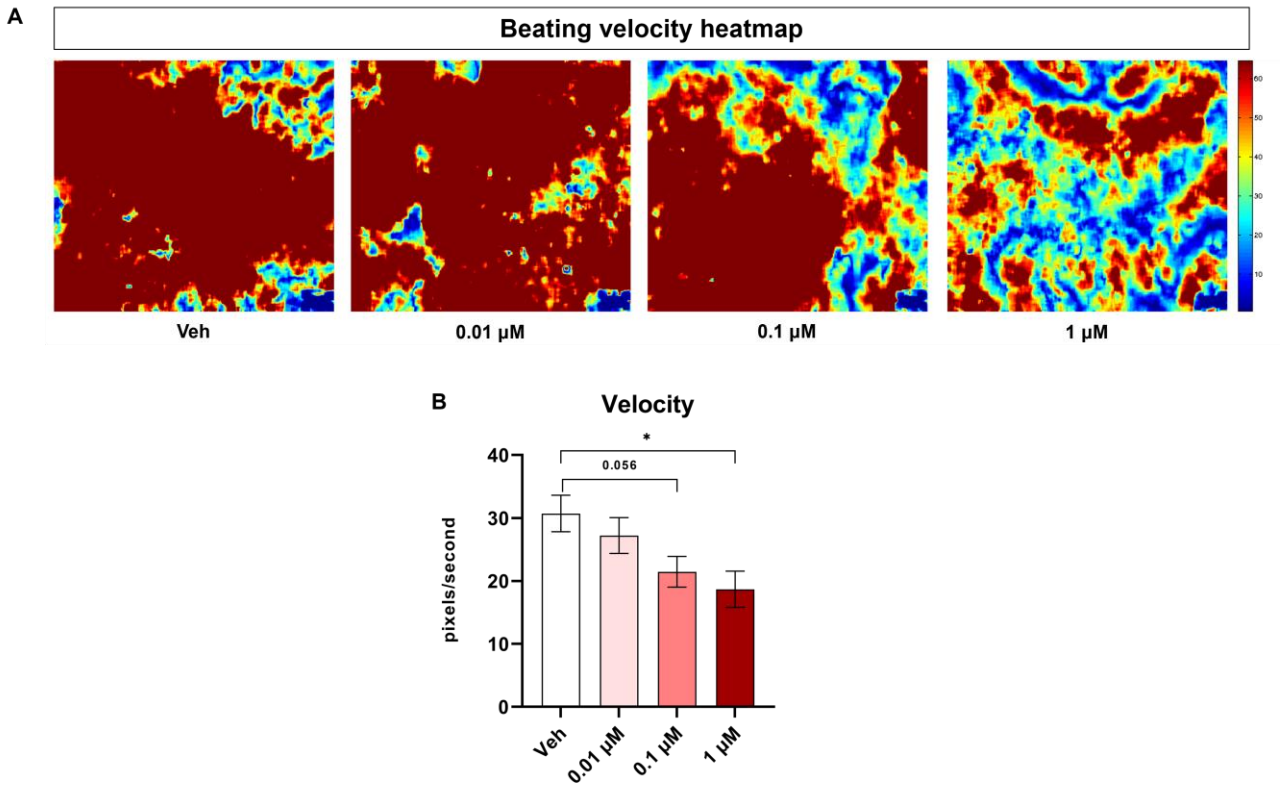

Figure 17: Velocity of elongation and shortening of hiPSC-CMs measured by Pulse. (**A**) Heatmap representing the areas of beating cells. The colour intensity represents higher (red) or lower (blue) beating velocity. (**B**) Quantification of beating velocity in pixels per second.

4.4 The proteome profile of hiPSC-CMs was altered after 21 days of Bisphenol A exposure

To investigate the effect of BPA exposure on hiPSC-CM proteome remodelling in a comprehensive and unbiased manner, we performed a label-free LC-MS/MS of cardiomyocytes at day 21 exposed to repeated doses of 0 µM (vehicle), 0.01 µM, 0.1 µM and 1 µM BPA for the

duration of cardiac differentiation. The abundance of multiple proteins was altered in hiPSC-CMs upon treatment with BPA, as shown by volcano plot visualization (**Figure 18A-C**).

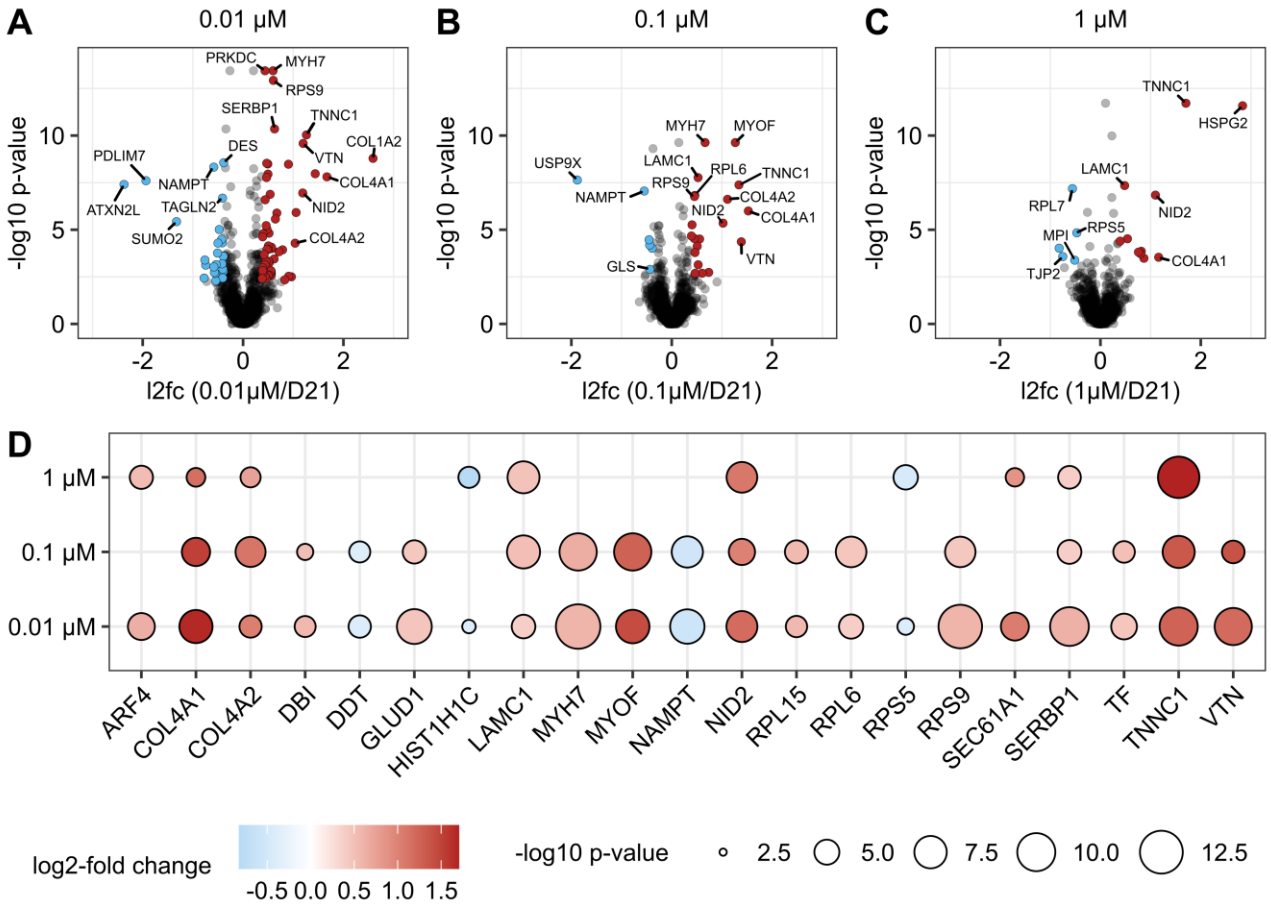

Figure 18. **Proteome analysis after 21 days of BPA-treated cardiac induction**. Volcano plot visualization of proteome alterations in hiPSC-CMs treated with (**A**) 0.01 µM (n = 4), (**B**) 0.1 µM (n = 4) and (**C**) 1 µM (n = 4) BPA for 21 days. The vehicle control is marked as D21 (n = 4). (**D**) Bubble plot of proteins significantly changed (adjusted p-value <0.05 and fold change >1.3) in at least two comparisons (0.01 µM versus D21; 0.1 µM versus D21; 1 µM versus D21). The colour and the size of the bubble correspond to log2 fold-change (red increased abundance, blue decreased abundance) and the significance of protein change, respectively.

In accordance with the consistently changed proteins, enrichment analysis displayed altered pathways related to muscle contraction, ECM, and translational regulation (**Supplementary Figure 1**), regardless of the BPA dose. Compared to the vehicle group, 81, 26 and 16 proteins were changed in abundance in 0.01 µM, 0.1 µM and 1 µM BPA-treated groups, respectively (**Supplementary table 5-7**). While twenty-one proteins were altered in at least two groups, six of them were increased in abundance in all three BPA concentrations (**Figure 18D**). These proteins are COL4A1, COL4A2, LAMC1 and NID2, components of the basement membrane (BM), (Boland et al., 2021), TNNC1, pivotal for muscle contraction (Li & Hwang, 2015) and SERBP1, involved in complex translational processes (Brown et al., 2018; Yan et al., 2021). The largest

number of differentially abundant BM proteins, together with LAMB1, LAMA1 and HSPG2, was identified in 1 µM BPA-treated group (**Supplementary table 7**). In 0.01 µM and 0.1 µM BPA-treated groups, we also observed an increase of MYH7, a component of the cardiomyocyte contraction machinery (Homburger et al., 2016). Furthermore, ribosomal proteins (e.g., RPS5, RPL15, RPL6, RPS9) were differentially abundant and predominantly upregulated after BPA treatment, which, together with SERBP1, belong to the dynamic protein synthesis regulation (Brown et al., 2018; Yan et al., 2021).

4.5 Network analysis of the proteomics dataset supports alterations in extracellular matrix remodelling

To investigate the correlations of the differentially abundant proteins with molecular pathways and diseases, firstly we compared them to a set of expert-curated gene-BPA annotations in humans from The Comparative Toxicogenomic Database (CTD) (https://ctdbase.org/) (Davis et al., 2023), observing a statistically significant overlap (p: 6e-05, Fisher's exact test). Thereafter, we mapped them in a human protein-protein interaction (PPI) network that consisted of 18,816 proteins and 478,353 physical interactions (Alanis-Lobato et al., 2017; Luck et al., 2020; Menche et al., 2015). Overall, we observed that the altered proteins in each BPA condition tended to be more connected than random in the PPI (**Figure 19A**), meaning that they contribute to the same molecular processes. The number of interactions was mainly driven by the upregulated proteins (**Figure 19B**).

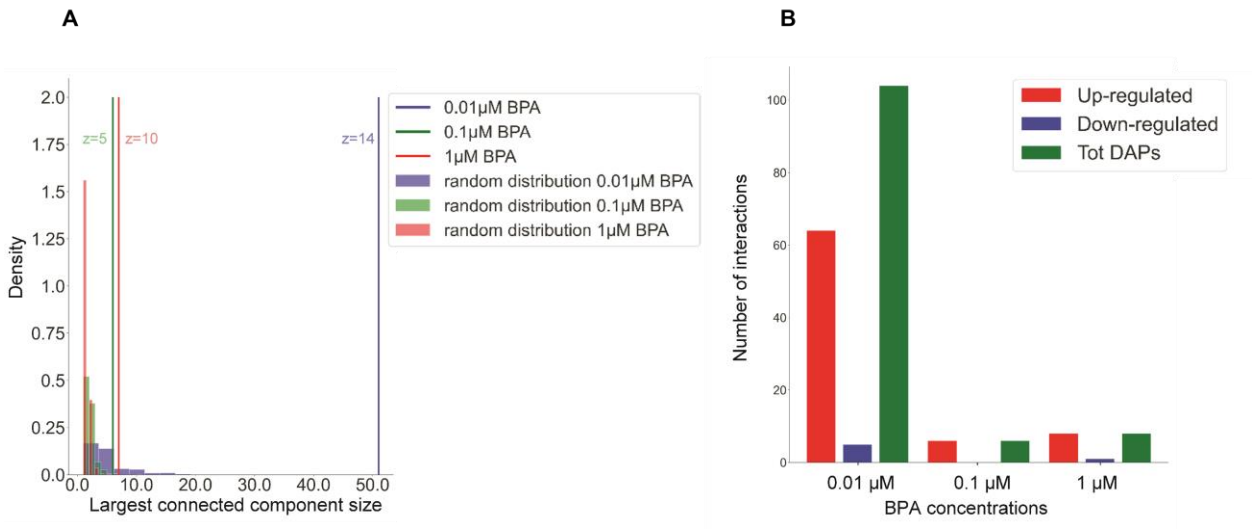

Figure 19. (**A**) Distribution of the size of the largest connected component of the differentially abundant proteins in the human Protein-Protein Interactions Network at 0.01 µM (blue), 0.1 µM (green), 1 µM (red) BPA concentration against 10,000 random protein sets of the same size. (**B**) Bar plot representing the number of interactions among the differentially abundant proteins for each BPA condition, distinguishing global signature (green), only the up-regulated proteins (red), and only the down-regulated proteins (blue).

In the BPA groups, we identified a core interacting module consisting of four proteins (COL4A2, COL4A1, LAMC1, NID2) (**Figure 20A**, p: 6e-39). These proteins will be referred to as the BPA-upregulated core (**Figure 20A**), which was associated with the ECM receptor-interaction (FDR: 2e-06, **Figure 20B**).

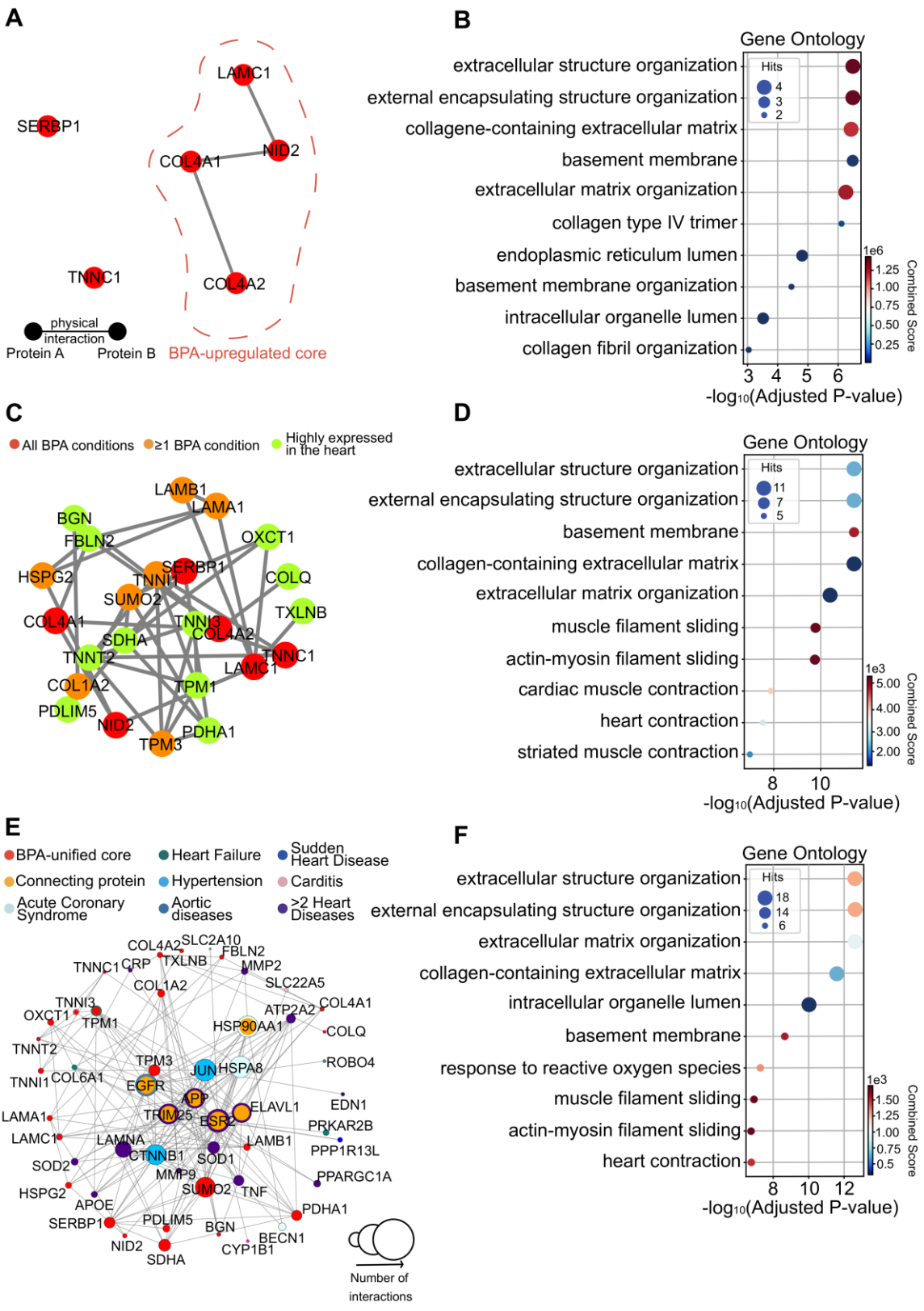

Figure 20. **Network analysis after 21 days of BPA treatment**. (**A**) Protein-Protein Interactions Network (PPI) of the 6 differentially abundant proteins in common with the three BPA-treated groups. The BPA-upregulated core is grouped by a dashed line. (**B**) Bubble plot of the top 10 enriched terms of the 6 BPA-upregulated core proteins with the gene ontology (GO). (**C**) PPI Network of the BPA-unified core. Red nodes are proteins perturbed in all three BPA conditions, orange nodes in one BPA condition, and green nodes are linker genes not perturbed by BPA, but highly expressed in the heart from the Human Protein Atlas (HPA). (**D**) Bubble plot of the top 10 enriched terms of the 24 unified BPA-upregulated core proteins with the GO. (**E**) PPI Network of the BPA unified core proteins and interacting heart disease proteins. The

size of each node is given by the degree in the heart-specific PPI, calculated by the network expansion of the proteins highly expressed in the heart from HPA. The inner colour of each node represents whether that protein belongs to the unified BPA core proteins (red), or a connecting protein (orange) or a disease-associated protein (colour-specific for each disease). If a protein is associated with more than 2 diseases, then the colour indigo will be used. The edge colour is used for BPA unified core proteins and connecting proteins that have been already observed to be associated with one or more diseases. (**F**) Bubble plot of the top 10 enriched terms of the BPA unified core proteins and connecting disease proteins with the GO. In (**B**), (**D**) and (**F**) bubbles are placed based on their -log10 p-value. Bubble size corresponds to the number of proteins that are found in each term, while their colour reflects the enrichment combined score.

Thereafter, we investigated the underlying interactions of the BPA-upregulated core with SERBP1 and TNNC1, through highly expressed proteins in the heart. We obtained an extended unified core of 24 proteins (BPA-unified core, **Figure 20C**), which was enriched in the ECM-receptor interaction and in pathological heart conditions, such as hypertrophic and dilated cardiomyopathy (**Figure 20D, Supplementary table 8**). To further investigate the possible association with heart-related diseases, we analysed its representation on a DisGeNET list of 11,099 diseases (Piñero et al., 2015), and we calculated a Jaccard Index which computed their genetic overlap with the BPA-unified core. We found a positive association with heart pathological conditions such as "Hypertrophic cardiomyopathy" (FDR: 5e-05) and "Idiopathic hypertrophic subaortic stenosis" (FDR: 0.0001) (**Supplementary table 9**).

Afterwards, to implement topological network traits on the gene sets overlap, we used the network proximity measure (Guney et al., 2016), which identified 1806 diseases associated with the BPA-unified core, including "Acute Coronary Syndrome" (FDR: 1e-19), "Heart Failure, Right-sided" (FDR: 4e-11), and "Cardiomyopathies" (FDR:4e-09) (data not shown). Due to the large number of associated heart diseases, we curated nine phenotypical groups, gathering them based on their common physiopathology. In this regard, we identified the closest interacting proteins that link the BPA-unified core to these diseases (**Figure 20E**). These are considered hub markers in the PPI, such as ESR1/2, EGFR and SOD1/2. The enrichment analysis of this network showed alterations in the ECM organization/interaction, and in the response to reactive oxygen species (ROS) (**Figure 20F, Supplementary table 10**). Due to these results, further investigations have been performed treating the hiPSC-CMs to a hypoxia/reoxygenation (H/R) insult. Indeed, alterations to ROS response can also be a contributing factor affecting the antioxidant defences during H/R (Li & Jackson, 2002). The integration of this stress factor, which can easily occur during early development, aimed to deeper evaluate the BPA's toxicity on early developing cardiomyocytes.

4.6 Effects of Bisphenol A upon hypoxia-reoxygenation challenge

After 21 days of BPA treatment, the hiPSC-CMs were subjected to a hypoxia/reoxygenation (H/R) challenge. The hiPSC-CMs were first exposed to 8 hours of hypoxia, followed by 15 hours of reoxygenation (**Figure 21A**).

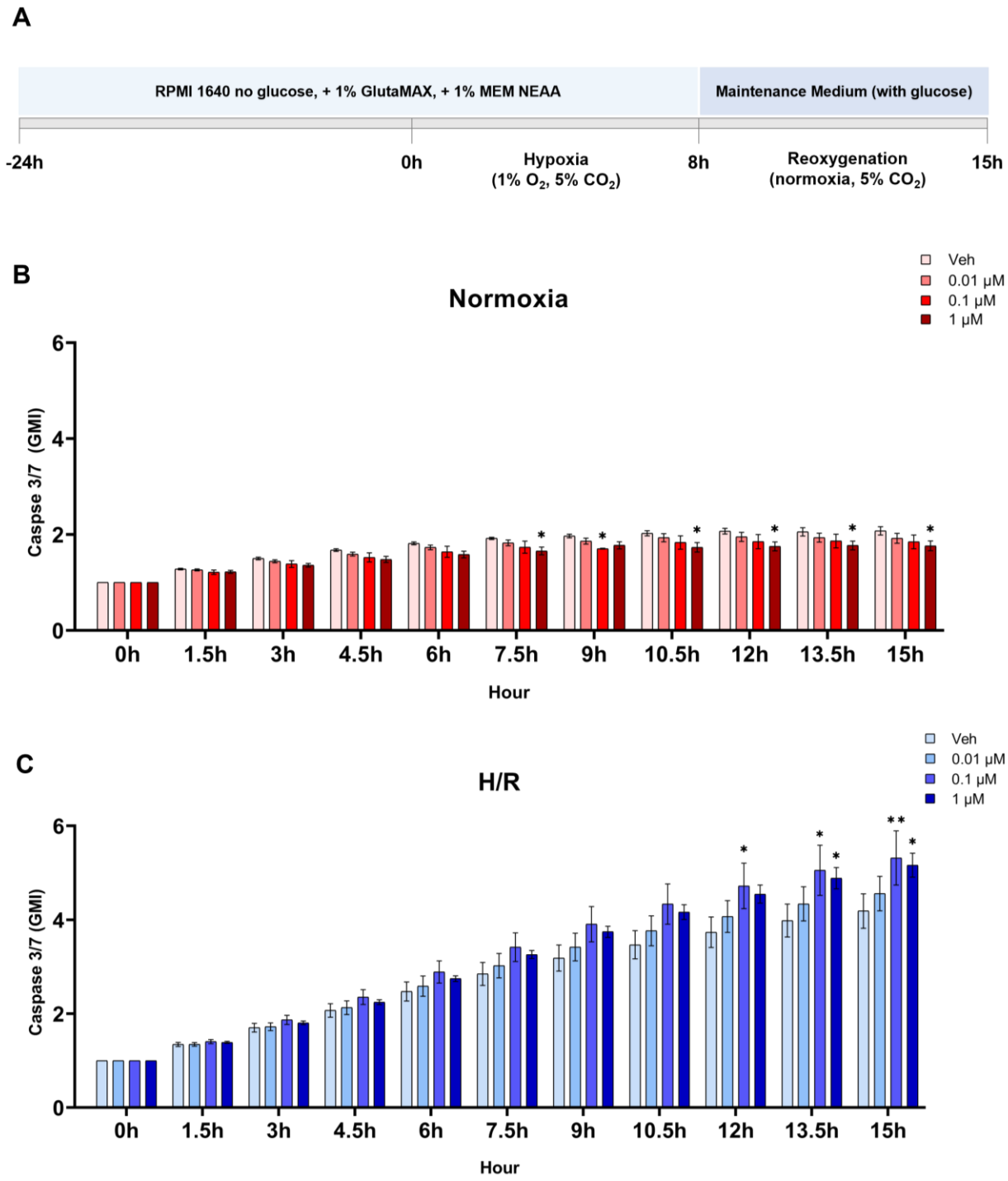

Figure 21. **Hypoxia and reoxygenation (H/R) induction on hiPSC-CMs treated with BPA**. (**A**) Schematic overview of H/R experiment. Apoptotic events were measured with caspase 3/7 dye during normoxia (**B**) and (**C**) H/R induction. Data were normalized to the baseline (0h) value. Results show independent experiments (n = 3); error bars represent ±SEM. Two-way ANOVA with Dunnett's post-hoc test was used for comparisons between untreated control (vehicle) and the three BPA concentrations

(adjusted p-value *< 0.05, **< 0.01, ***< 0.001, ****< 0.0001.). H/R, hypoxia and reoxygenation; GMI, Green Mean Intensity; RMI, Red Mean Intensity; MEM NEAA, Minimum Essential Medium Non-Essential Amino Acids.

The standard culture conditions are referred to as "normoxia". During the reoxygenation time, Caspase 3/7 Green probe was used to detect apoptotic events over time. A significant increase of cellular death was observed in hiPSC-CMs subjected to the sequential periods of H/R, compared to hiPSC-CMs in normoxia (**Figure 21B, C**). Regardless of the BPA treatment, the caspase activity in normoxia exhibited an overall increase of 1.9 times compared to the starting point (0h). By contrast, the hiPSC-CMs exposed to H/R showed a remarkable increase of apoptosis, with an overall elevation of 4.8 times by the end of the period (**Figure 21B, C**). In normoxia, we claimed a lower caspase activity in hiPSC-CMs treated with BPA compared to the untreated control ($p < 0.05$* in 1 µM). On the other hand, the apoptosis trend was reversed after H/R induction, with higher caspase activity in BPA-treated groups than in the vehicle control, especially in the hiPSC-CMs treated with two highest concentrations (0.1 µM, $p < 0.01$**; 1 µM, $p < 0.05$* by the end of the reoxygenation period). In standard conditions, and regardless of the BPA treatment, the mitochondrial activity remained stable (**Figure 22A**). However, the overall effect of the H/R induction was a 25% reduction in the mitochondrial fluorescent signal across all groups (**Figure 22B**). After H/R, the mitochondrial activity decreased mildly in 0.1 µM BPA ($p < 0.05$*), compared to the vehicle control (**Figure 22B**).

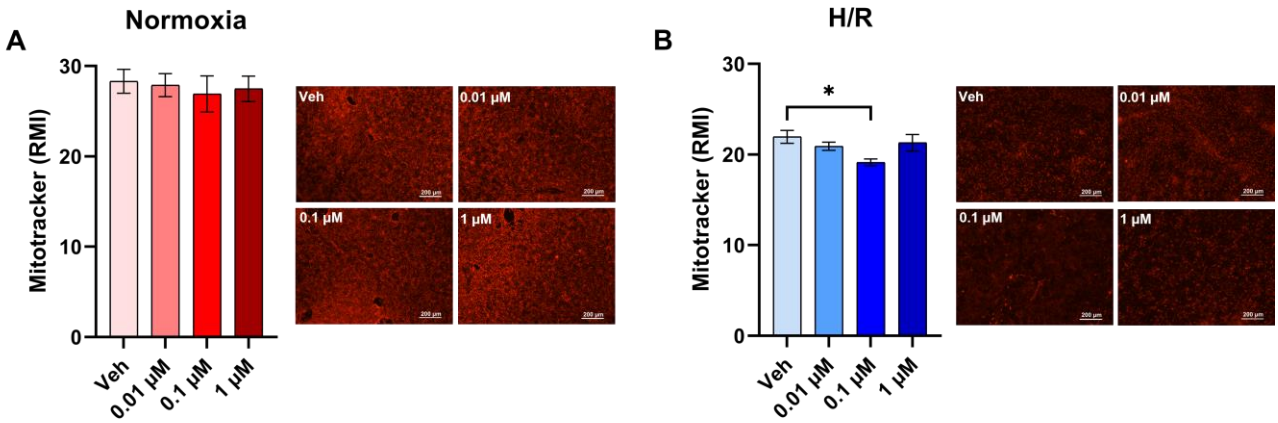

Figure 22. **Mitochondrial activity in normoxia and hypoxia/reoxygenation (H/R).** Mitochondrial activity was measured with MitoTracker™ Deep Red dye at the end of the considered period (15 h) after (**A**) normoxia and (**B**) H/R induction. Qualitative immunofluorescence pictures of MitoTracker™ Deep Red are displayed for (**A**) and (**B**), scale bar 200 µm. Results show independent experiments (n = 3); error bars represent ±SEM. Two-way ANOVA with Dunnett's post-hoc test was used for comparisons between untreated control (vehicle) and the three BPA concentrations (adjusted p-value *< 0.05, **< 0.01, ***< 0.001, ****< 0.0001.). H/R, hypoxia and reoxygenation; GMI, Green Mean Intensity; RMI, Red Mean Intensity.

5 NEW SCIENTIFIC RESULTS

In this research, the effects of a repeated-dose BPA exposure during the cardiomyocyte differentiation were investigated. Firstly, a 2D *in vitro* differentiation system to obtain cardiomyocytes from hiPSCs was established and characterised to provide a suitable model for the early stages of cardiac development. The model was suitable for cardiotoxicity investigations, providing reproducible dose-response effects from different DOHaD-related compounds, BPA included. Subsequently, functional, and molecular investigations were performed to identify the effects of environmentally relevant concentrations of BPA on hiPSC-CMs, and the potential implications with cardiovascular diseases. The research allowed the use of hiPSC-CMs to provide the following new scientific findings:

1. For the first time, I have provided a human *in vitro* model to investigate the effect of 21-day repeated-dose exposure to BPA. Of note, the BPA treatment was performed from the hiPSC stage to hiPSC-CMs, offering a new perspective of the BPA toxicity at the earliest stage of cardiomyocyte development.
2. I have presented data showing a significant change in functional features of hiPSC-CMs treated with BPA, such as the decreased contraction frequency and beating velocity, and the increased contraction and relaxation time, demonstrating that low doses of BPA significantly affect the function of hiPSC-CMs.
3. I have performed, for the first time, a proteomics-based analysis on hiPSC-CM treated with BPA for 21 days, and, together with network analysis, identified links between BPA-perturbed proteins and several cardiovascular alterations. Of note, the accumulation of BM components (COL4A2, COL4A1, LAMC1, NID2), TNNC1, and SERBP1 are potentially associated with the altered cellular functionality observed, and CVDs, such as heart failure and cardiomyopathies.
4. Finally, I have provided evidence that BPA potentially renders the hiPSC-CMs more vulnerable to additional challenges, such as the hypoxia-reoxygenation insult.

6 DISCUSSION

In the present study, we used a human-induced pluripotent stem cell-derived model to investigate the effects of repeated and low-dose BPA exposure on early developing cardiomyocytes. The hiPSC-derived cellular model used in the study consisted of human cardiomyocytes, which provide a well-established and suitable *in vitro* modelling system for studying cardiac toxicity mechanisms (Narkar et al., 2022). In line with the DOHaD field, we presented novel data which contribute to the current investigation of early biomarkers of cardiovascular alterations that can arise due to early-life chemical exposure.

Most of the currently available data on BPA toxicity originates from research done using animal models. While the resulting knowledge is extremely valuable and paved the way for further investigation in the field, our work with hiPSC-derived cardiomyocytes represents a valuable contribution, extending the work on animal models to the human cellular system. Since several stress conditions can alter the cardiovascular system and predispose to CVDs, progress has been made during the past decade in developing NAMs for cardiotoxicity to draw attention on the unique aspects of environmental toxicity assessment (Daley, 2022). Current advances in hiPSC-CM-based approaches showed the relevance of *in vitro* NAMs for accurately capturing impacts on human cardiovascular health. Therefore, as well as a paucity of data regarding BPA's toxicity on the developing human heart, in this work hiPSC-CMs were used to contribute to the current urgency of BPA's regulatory safety assessment, albeit the decision-making about a safe daily amount of BPA is rather complex due to the unique toxicity effects of this chemical and the varied nature of experimental conditions used for investigation (EFSA CEF Panel, 2015; EFSA CEP Panel, 2023; Heindel et al., 2020; Vandenberg et al., 2019; Vom Saal & Vandenberg, 2021).

Firstly, the pluripotency of the hiPSC line was determined before they were induced towards the cardiac lineage. To confirm whether the cells were fully reprogrammed, a spontaneous differentiation assay was performed to confirm their ability to generate EBs in culture and express markers of the three germ layers (Liu & Zheng, 2019). Therefore, following the cardiomyocyte differentiation, deep characterization of hiPSC-CMs was assessed to confirm the differentiation towards the cardiac lineage. The process involves the formation of endodermal and mesodermal cellular populations, leading cardiovascular progenitors into cardiomyocytes and other progenies (i.e., endothelial, fibroblast and smooth muscle cells) (Burridge et al., 2012). We obtained ~80% cTnT+ hiPSC-CMs, and, consistently with the gene expression profiles from other differentiation strategies (Lian et al., 2012, 2013; Lin & Zou, 2020), and with embryonic development, we obtained cells expressing key cardiac genes, closely resembling the embryonic day 9.5 *in vivo*

(Morita & Tohyama, 2020; Paige et al., 2015; Shimoji et al., 2010). Together with the distinctive contraction ability of hiPSC-CMs, the robust generation of cardiomyocytes was confirmed by LC–MS/MS analysis, which indicated a net increase of well-known cardiomyocyte markers (**Figure 11**). Since the goal of this study was to investigate the toxicity of BPA during the early stages of cardiac differentiation, the foetal phenotype of hiPSC-CMs represents an important aspect of this research. Compared to postnatal and adult cardiomyocytes, foetal cardiomyocytes exhibit a smaller size and disorganised structures (Karbassi et al., 2020), as observed for the generated hiPSC-CMs using immunocytochemistry. Additionally, our hiPSC-CM cultures showed genes predominantly expressed in the sarcomeres of the foetal heart and in early neonatal life (e.g., TNNI1, MYL2 and MYH6), conforming to the early-stage phenotype observed in other studies (Emanuelli et al., 2022; Ulmer & Eschenhagen, 2020).

Thereafter, we aimed to validate our cellular cultures as a NAM to study chemical exposures *in vitro*. The hiPSC-CMs have been widely used as models for investigating the effects of various chemicals. In this regard, our generated cells provided a robust and reproducible model to validate the cytotoxicity of well-known compounds (**Figure 12**). Doxorubicin is an anticancer agent which causes cardiotoxicity in many patients, and for this reason represents a well-established cardiotoxic standard *in vitro* (Zhao & Zhang, 2017). Acrylamide forms from food, particularly when cooked at high temperatures (Mottram et al., 2002), and menadione is commonly used as a nutritional supplement in animal feed (Prasad et al., 2018). All these compounds have been demonstrated to generate ROS, which can cause deleterious effects in many cell types, including cardiomyocytes (Asensio-López et al., 2017; Huang et al., 2018; Loor et al., 2010; Yang et al., 2021). Our results demonstrated that 24-hour treatment with doxorubicin and menadione induced a dose-dependent ROS production in hiPSC-CMs cultures, even at concentrations lower than the EC50 (**Figure 13A, B**). An upward trend of ROS production was observed even after acrylamide treatment, although this compound was significantly less cytotoxic after 24 hours, compared to doxorubicin and menadione (**Figure 13C**). Altogether, these results demonstrated that our model facilitated the generation of repeatable dose-response effects with well-known compounds and DOHaD-related, thus suitable for further *in vitro* cardiotoxicity assessments.

Therefore, to investigate the effects of environmentally relevant concentrations of BPA on human foetal cardiomyocytes, firstly a short treatment (24- and 72-hour) was performed to evaluate the acute toxicity of the chemical using a wider concentration range on differentiated cardiomyocytes. There was no relevant impact on the cellular viability, except for the supraphysiological dosage (100 µM) after 24- and 72-hour treatment. Low concentrations of interest (0.01 µM, 0.1 µM, 1 µM) did not elicit severe cytotoxicity, also after 72 hours of exposure (**Figure 14**). Later, a chronic

exposure scenario was mimicked, during which the cells were treated every second day of the differentiation process.

Firstly, the BPA's effect was investigated during the main time points of cardiomyocyte differentiation. Studies conducted *in vivo* revealed that intrauterine exposure to BPA impacts heart development, for example, compromising cardiomyocyte differentiation, the cardiac looping process, as well as the overall morphology and function of the heart (Chapalamadugu et al., 2014; Lombó et al., 2015, 2019; Rasdi et al., 2020). Knowing that changes in the number of cardiomyocytes are critical for the heart's functionality later in life (Corstius et al., 2005; Li et al., 1996), we hypothesized that BPA could affect the proportion of generated cardiomyocytes. The percentage of hiPSC-CMs (cTnT+) differentiated during the process was not altered by low-dose exposure to BPA, and the cellular viability remained unchanged upon the treatment (**Figure 15B, C**), suggesting that the chosen concentrations of BPA do not influence the proportion of cardiomyocytes. Likewise, the proliferation (percentage of Ki67-positive cells) and proportion of double-strand DNA breaks (percentage of γH2AX-positive cells) were not affected upon BPA treatment, meaning that low doses of BPA might not exert genotoxic effects on cardiomyocyte differentiation, in contrast to observations obtained from rat embryonic cardiomyoblasts (Escarda-Castro et al., 2021) and other cell types, such as hepatic cells (Eid et al., 2015), spermatozoa (Chianese et al., 2018; Liu et al., 2013) and human peripheral blood mononuclear cells (Di Pietro et al., 2020).

Although low doses of BPA did not elicit severe alterations of crucial differentiation features (i.e., quantity of cardiomyocytes generated, proliferation, and viability), we observed significant changes in the functionality of the hiPSC-CMs after 21-day treatment with BPA. Whereas mature atrial and ventricular cardiomyocytes display low automaticity, immature cardiomyocytes, and pluripotent stem cell-derived cardiomyocytes exhibit spontaneous beating activity, which is used to study alterations of cardiac health and excitability (Guo & Pu, 2020; Satin et al., 2004). In this work, BPA treatment significantly decreased the beat rate of hiPSC-CMs, and longer contraction and relaxation times were observed. These results suggest that repeated treatment with BPA elicits a chronotropic effect, as observed in neonatal rat cardiomyocytes (Ramadan et al., 2018), rat atrial preparations (Pant et al., 2011) and excised whole hearts from rats (Posnack et al., 2014), although after acute BPA exposure. Notably, observing the proteome profile of hiPSC-CMs treated with BPA, a higher abundance of TNNC1 was revealed (**Figure 18D**, **Supplementary table 5-7**). This is a key regulatory protein which binds calcium ions to initiate muscle contraction (Li & Hwang, 2015). Several studies reported that BPA has a negative impact on ion channel activity and calcium handling, either in cardiac cells and other cell types including neurons, pancreatic β-cells, and renal

tubular cells (Kuo et al., 2011; Tanabe et al., 2006; Villar-Pazos et al., 2017; Wang et al., 2019; Yan et al., 2011). In hiPSC-CMs, it has been demonstrated that acute BPA exposure at micromolar levels inhibits the L-type Ca^{2+} channels, which regulate the excitation-contraction coupling (Eisner et al., 2017; Hyun et al., 2021; Prudencio et al., 2021). Similarly, the chemical promoted the alteration of the Ca^{2+} release/reuptake kinetics of the sarcoplasmic reticulum in adult myocytes (Liang et al., 2014). These alterations may have an impact on the activation and deactivation rates of the myofilaments, which are mainly, but not exclusively, caused by altered Ca^{2+} binding and unbinding to TNNC1 (Chung et al., 2016). This provides a potential explanation for the higher levels of TNNC1 protein observed in hiPSC-CMs treated with BPA. Interestingly, we did not observe an arrhythmic beating profile, possibly related to the XY-karyotyped hiPSC-CMs used in this work. For instance, in the work of Cheng *et al.*, XX-karyotyped hESC-CMs displayed a higher susceptibility to low doses of BPA upon 3-day exposure, rather than XY-karyotyped cells (Cheng et al., 2020). Electrophysiological perturbations can be related to BPA's ability to target and activate ERs, leading to sex-specific alterations (Belcher et al., 2015; Raja et al., 2020; Xu et al., 2013; Zou et al., 2022). For example, BPA induced proarrhythmic effects in the female rodent and canine heart (Ma, et al., 2023; Yan et al., 2011), while in the male heart, the different sensitivity of myocytes to ERs resulted in unobservable responses (Belcher et al., 2012). Further studies would be relevant to investigate if XX-karyotyped hiPSC-CMs might exhibit different readouts.

Next, the proteomics analysis allowed us to identify additional molecular alterations induced by BPA. A higher number of altered proteins was observed for hiPSC-CMs treated with the two lowest BPA concentrations (0.01 μM and 0.1 μM). This result can be explained by the non-monotonic property of BPA (and other EDCs), which poses additional challenges when trying to agree on the effects of BPA exposure on cardiac development (Hill et al., 2018; Vandenberg et al., 2019). Nevertheless, an increased level of the BM components (COL4A1, COL4A2, LAMC1, NID2) was revealed in hiPSC-CMs treated with BPA in all three concentrations (**Figure 18D**). Notably, a higher number of ECM proteins was detected in the 1 μM BPA-treated group, in which LAMB1, LAMA1 and HSPG2 were significantly upregulated (**Supplementary table 7**). The BM has a wide range of biological functions, among which it provides structural and mechanical support to tissues (Boland et al., 2021). A pathological remodelling and deposition of the BM have been related to structural anomalies, such as fibrosis, either in the myocardium of animal models (Bahey et al., 2019; García-Arévalo et al., 2021; Rasdi et al., 2020) and in humans (Díez et al., 2002; Disertori et al., 2017; Heymans et al., 2005; Hinderer & Schenke-Layland, 2019). An excessive fibrosis can lead to detrimental effects on myocardial function, for example, anomalies in the contraction activity (Münch & Abdelilah-Seyfried, 2021). In this study, a clear slow-down

of the contraction frequency was observed after BPA treatment. Interestingly, a mild, although not significant, decrease in the contraction force (peak height) was recognized in hiPSC-CMs treated with BPA (**Figure 16B**). Moreover, the contraction displacement, and the beating velocity, representing vector features of the cellular movement, showed that both the speed and the range of cellular elongation-shortening were affected by BPA treatment (**Figure 16C, Figure 17**). In this context, a rigid environment can explain the increase of the contraction force and restrain the cell shortening distance, as observed in hESC-CMs (Ribeiro et al., 2020). At the same time, the stiff environment perturbs the beating frequency, demonstrated on avian cardiomyocytes (Engler et al., 2008), or on murine iPSC-CMs, which had an irregular beating profile on stiff hydrogels (Heras-Bautista et al., 2019). To counteract the stiffness of the niche, one of the possible adaptive responses of cardiomyocytes might be the increased production of contractile sarcomere proteins (Grossman & Paulus, 2013). This would explain the proteome profile of hiPSC-CMs treated with BPA, showing the upregulation of proteins related to muscle contraction, such as TNNC1 in all BPA concentrations and MYH7 in 0.01 µM- and 0.1 µM-treated groups (**Figure 18D, Supplementary table 5-7**). Additionally, higher rigidity of the cardiomyocyte niche has been linked to changes in the regulation of translational processes and protein synthesis (Simpson et al., 2020; Wu et al., 2020). In this study, proteins related to translational regulation were consistently changed in abundance in hiPSC-CMs after BPA treatment (**Figure 18D, Supplementary table 5-7**). We noticed the up- and down-regulation of the 60S and 40S ribosomal subunit components (e.g., RPL15, RPL6, RPS9, RPS5) in at least two BPA concentrations. In all BPA-treated groups, we observed the upregulation of SERBP1, which has been correlated with the translational inactivation of the 80S ribosomes in mammals, together with eEF2 (Brown et al., 2018). These results suggest that the ability to modulate global translation is required to maintain cardiomyocyte function and survival under cellular stress (Simpson et al., 2020).

Next, we explored the molecular interconnection between the genes involved in the ECM (BPA-upregulated core) and both TNNC1 and SERBP1. We obtained a unified network of 24 proteins, that were demonstrated to be modulated by BPA in at least one condition (**Figure 20C**). While examining the altered genetic pathways involved in CVDs, we have identified hub genes which, upon interaction with BPA-perturbed genes, could have different roles in heart pathologies (**Figure 20E**). For instance, ESR2, together with ESR1, is triggered by cardiac damage, mostly leading to ECM remodelling linked to pathological hypertrophy and heart failure in zebrafish and mouse models (McLellan et al., 2020; Xu et al., 2020). Conversely, other works demonstrated the interaction between ERs and ECM supporting the anti-fibrotic effect of ESR2 activation in female mice (Iorga et al., 2017; Pedram et al., 2016). Furthermore, we have identified connecting genes that are specifically associated with individual cardiovascular conditions. In this regard, EGFR

interaction with COL1A2 could potentially lead to localized changes in the ECM and, consequentially, blood pressure (Tian et al., 2016; Zheng et al., 2021).

Lastly, we examined the outcomes raised after BPA treatment exposing the hiPSC-CMs to a hypoxia-reoxygenation insult. Studies have investigated the pleiotropic effects of BPA in conjunction with other stressors such as hypoxia-reoxygenation (Cypher et al., 2015, 2018; Sonavane & Gassman, 2019). However, mixture exposures are difficult to perform and interpret since they are an additional confounding factor in understanding BPA impact. In normoxia, the caspase 3/7 activity was not remarkably affected in hiPSC-CMs treated with BPA, suggesting that the tested concentrations might not trigger substantial oxidative stress and cellular death, in line with the results of cellular viability (**Figure 15B**, **Figure 21B**). Conversely, over the hypoxic stress, the caspase 3/7 activity increased in hiPSC-CMs treated with BPA, alluding to an alteration of the cellular response (**Figure 21C**). One possible explanation could be the altered deposition of BM components in hiPSC-CMs treated with BPA. Perturbations in the BM network may deprive cardiomyocytes of crucial molecular signals that promote cardiomyocyte survival and function (Heras-Bautista et al., 2019; Sekiguchi & Yamada, 2018). For example, followed by stress stimuli, ECM remodelling and degradation can release latent growth factors and cytokines, and/or generate matrikines, through the proteolytic function of matrix metalloproteinases (Frangogiannis, 2019), with pro-apoptotic function, contributing to the cardiac cells' dysfunction (Chute et al., 2019; Frangogiannis, 2017; Mutgan et al., 2020). Otherwise, the toxicity of BPA has been previously linked to the destabilization of antioxidant defences *in vitro*, mainly through HIF-1α degradation (Kubo et al., 2004). Indeed, studies on zebrafish indicated that early cardiovascular development may be more susceptible to hypoxia under BPA exposure (Cypher et al., 2015, 2018). The analysis of the unified BPA-core disease network revealed a group of genes (e.g., JUN, TPM1, APOE, SOD2, MMP9, EGFR, SOD1) that may play a role in the ROS response, linking the BPA molecular signature to several CVDs, such as transient ischemic events (Kibel et al., 2020) and the acute coronary syndrome (Sugamura & Keaney, 2011). These conditions are also associated with the ECM remodelling, and the response to ROS (data not shown). Furthermore, a known response to hypoxia is the reduction of mitochondrial mass by mitophagy (Fuhrmann et al., 2013), in line with the decreased MitoTracker™ signal observed after H/R compared to normoxia, regardless of the BPA treatment (**Figure 22**). However, the MitoTracker™ and caspase 3/7 signals did not show a remarkable correlation in the time point analysed, although we observed lower mitochondrial activity in the 0.1 µM-treated group. This result could explain the higher levels of caspase 3/7 signal in the 0.1 µM compared to the other two BPA-treated groups, suggesting initiation of the apoptotic process through the mitochondria destabilization. Nevertheless, further investigations

are necessary to investigate the apoptotic pathway involved. A good avenue for future experiments could be the examination of the matrikines production (e.g., arresten, canstatin), and the Fas ligand-mediated apoptosis, a known target for BM matrikines (Panka & Mier, 2003; Verma et al., 2013). Since arresten and canstatin induce caspase-9 dependent mitochondrial apoptosis, quantification of this enzyme and cytochrome c release can elucidate the mechanism underlying the apoptotic events involved.

Despite the results obtained, which add a valuable contribution to the current information regarding the toxicity of BPA, the model used in this study does not lack limitations. Firstly, the use of one cell line limits the evaluation of BPA effects in a wider spectrum, and further studies will be needed to validate and expand our findings using other cell line models. Nevertheless, in the present study, an in-depth and comprehensive characterization of our cellular model was performed, and a deep investigation into the effects of BPA was addressed, obtaining results supported by previous studies and observed in human studies, animal models and *in vitro* investigations, thus making our data reliable. Secondly, stress exposure *in vitro*, for practical reasons, is different from the *in vivo* stress exposures, occurring over a longer period and in variable doses. Even if hiPSCs can be an effective model to reduce the use of experimental animals, which is costly and time-consuming, and involves numerous ethical issues, using hiPSCs instead of animals is still a controversial issue because it is difficult to predict the *in vivo* results with only *in vitro* data. For this reason, developing a more sophisticated *in vitro* model system, with longer differentiation time, might help to overcome the current limitations. Nevertheless, comparing the exposure effects in variable specific time points of the *in vitro* cardiac differentiation, and extrapolating to *in vivo* development, might allow to generate data comparable to the stress exposures occurring *in vivo*. Moreover, even if the features of hiPSC-CMs are improving due to numerous protocol developments, differentiation methods still need further improvement to reach the desired degree of maturity. Indeed, this represents a major difficulty to recapitulate the adult phenotype and, therefore, an adult disease modelling observed *in vivo*. On the other hand, the use of hiPSC from the pluripotency stage represents a unique opportunity to evaluate the disease progression from early stages of development to the adult tissue and to understand late-onset changes, as well.

In conclusion, we investigated, for the first time, the effects of a repeated-dose exposure with BPA for 21 days on early developing cardiomyocytes using an *in vitro* human-relevant iPSC-derived model, as a NAM for cardiotoxicity testing (Parish et al., 2020; Stucki et al., 2022; Zink et al., 2020). The results showed a significant reduction of the contraction frequency and beating velocity, as well as an increase of the contraction and relaxation times, concluding that BPA clearly

affects the function of hiPSC-CMs. The presence of a mixed cellular environment allowed us to show BPA's effects on the hiPSC-CMs niche, relevant for cardiomyogenesis and cardiomyocyte functionality (Fountoulaki et al., 2015). The proteome changes in hiPSC-CMs treated with BPA revealed the accumulation of BM components, which is considered an additional factor of hiPSC-CMs functional alteration also later in the development, contributing to CVDs, such as heart failure and cardiomyopathies (Larson et al., 2022; Silva et al., 2021). Moreover, BPA potentially renders the hiPSC-CMs more vulnerable to additional challenges, such as the hypoxia-reoxygenation insult. Indeed, we observed that hiPSC-CMs treated with BPA were more prone to apoptotic events, suggesting that their functional decline might be even more extended. In line with the DOHaD field, the above results add valuable insights to the current investigation of early biomarkers of cardiovascular alterations that can arise due to early-life chemical exposure.

7 SUMMARY

The hypothesis known as DOHaD asserts that, during early embryonic development, the foetus can be predisposed to stress conditions leading to the onset of NCDs after birth and/or later in life. Among these stressors, chemicals can negatively affect the embryo and organ development. Increasing evidence supports the requirement of NAMs that can generate human-relevant platforms for drug testing and *in vitro* toxicology models to study the effects of environmentally realistic doses of chemicals on foetal development. The goal of the present study was to investigate the BPA's toxicity over the early stages of cardiomyocyte development. BPA is a synthetic chemical widely used in plastics manufacturing, and it has been associated with heart developmental defects, even in low concentrations. The extent of BPA toxicity on human foetal heart development is still largely unexplored, and the information mostly comes from animal models, which include inter-species physiological differences with humans as a major limitation. Therefore, we have used hiPSCs to generate human foetal-like cardiomyocytes *in vitro* to provide a model relevant for toxicological applications, and to assess the effects of BPA in low doses on cardiac differentiation, resembling the main steps of embryonic heart development. Our experimental set-up mimics a chronic exposure scenario, showing that BPA significantly alters the functionality and cellular environment of hiPSC-CMs. The chemical significantly decreased the beat rate of hiPSC-CMs, extending the contraction and relaxation times in a dose-dependent manner. In hiPSC-CMs treated with BPA, quantitative proteomics analysis revealed a high abundance of BM components (e.g., COL4A1, COL4A2, LAMC1, NID2) and a significant increase in TNNC1 and SERBP1 proteins, suggesting that contractility alterations might result from increased ECM deposition. Network analysis of proteomics data supported altered ECM remodelling and provided a disease-gene association with well-known pathological conditions of the heart. Furthermore, upon the hypoxia-reoxygenation challenge, hiPSC-CMs treated with BPA showed a higher rate of apoptotic events. Network analysis revealed a group of genes (e.g., JUN, TPM1, APOE, SOD2, MMP9, EGFR, SOD1) that play a role in the ROS response and the ECM remodelling, supporting the observed results. Our work on hiPSC-CMs presents a valuable contribution to the DOHaD field, providing new insights about diseases that might arise upon early-life chemical exposure. The results of our study contribute to the current understanding of BPA effects on foetal cardiomyocytes, in correlation with human clinical observations and animal studies, and provide a suitable model for environmental chemical hazard and risk assessment.

8 BIBLIOGRAPHY

Alanis-Lobato, G., Andrade-Navarro, M. A., & Schaefer, M. H. (2017). HIPPIE v2.0: enhancing meaningfulness and reliability of protein–protein interaction networks. *Nucleic Acids Research*, *45*(Database issue), D408. https://doi.org/10.1093/NAR/GKW985

Alonso-Magdalena, P., Ropero, A. B., Soriano, S., García-Arévalo, M., Ripoll, C., Fuentes, E., Quesada, I., & Nadal, Á. (2012). Bisphenol-A acts as a potent estrogen via non-classical estrogen triggered pathways. *Molecular and Cellular Endocrinology*, *355*(2), 201–207. https://doi.org/10.1016/j.mce.2011.12.012

Altamirano, G. A., Ramos, J. G., Gomez, A. L., Luque, E. H., Muñoz-de-Toro, M., & Kass, L. (2017). Perinatal exposure to bisphenol A modifies the transcriptional regulation of the β-Casein gene during secretory activation of the rat mammary gland. *Molecular and Cellular Endocrinology*, *439*, 407–418. https://doi.org/10.1016/j.mce.2016.09.032

Ammar, C., Gruber, M., Csaba, G., & Zimmer, R. (2019). MS-EmpiRe Utilizes Peptide-level Noise Distributions for Ultra-sensitive Detection of Differentially Expressed Proteins. *Molecular & Cellular Proteomics : MCP*, *18*(9), 1880. https://doi.org/10.1074/MCP.RA119.001509

Ariemma, F., D'Esposito, V., Liguoro, D., Oriente, F., Cabaro, S., Liotti, A., Cimmino, I., Longo, M., Beguinot, F., Formisano, P., & Valentino, R. (2016). Low-Dose Bisphenol-A Impairs Adipogenesis and Generates Dysfunctional 3T3-L1 Adipocytes. *PLOS ONE*, *11*(3), e0150762. https://doi.org/10.1371/journal.pone.0150762

Asano, S., Tune, J. D., & Dick, G. M. (2010). Bisphenol A activates Maxi-K (K_{Ca} 1.1) channels in coronary smooth muscle. *British Journal of Pharmacology*, *160*(1), 160–170. https://doi.org/10.1111/j.1476-5381.2010.00687.x

Asensio-López, M. C., Soler, F., Pascual-Figal, D., Fernández-Belda, F., & Lax, A. (2017). Doxorubicin-induced oxidative stress: The protective effect of nicorandil on HL-1 cardiomyocytes. *PLOS ONE*, *12*(2), e0172803. https://doi.org/10.1371/journal.pone.0172803

Ashburner, M., Ball, C. A., Blake, J. A., Botstein, D., Butler, H., Cherry, J. M., Davis, A. P., Dolinski, K., Dwight, S. S., Eppig, J. T., Harris, M. A., Hill, D. P., Issel-Tarver, L., Kasarskis, A., Lewis, S., Matese, J. C., Richardson, J. E., Ringwald, M., Rubin, G. M., & Sherlock, G. (2000). Gene Ontology: tool for the unification of biology. *Nature Genetics*, *25*(1), 25. https://doi.org/10.1038/75556

Bae, S., & Hong, Y.-C. (2015). Exposure to Bisphenol A From Drinking Canned Beverages Increases Blood Pressure. *Hypertension*, *65*(2), 313–319. https://doi.org/10.1161/HYPERTENSIONAHA.114.04261

Bae, S., Lim, Y.-H., Lee, Y. A., Shin, C. H., Oh, S.-Y., & Hong, Y.-C. (2017). Maternal Urinary Bisphenol A Concentration During Midterm Pregnancy and Children's Blood Pressure at Age 4. *Hypertension*, *69*(2), 367–374. https://doi.org/10.1161/HYPERTENSIONAHA.116.08281

Bahey, N. G., Elaziz, H. O. A., & Gadalla, K. K. E. (2019). Potential Toxic Effect of Bisphenol A on the Cardiac Muscle of Adult Rat and the Possible Protective Effect of Omega-3: A Histological and Immunohistochemical Study. *Journal of Microscopy and Ultrastructure*, *7*(1), 1. https://doi.org/10.4103/JMAU.JMAU_53_18

Barker, D. J., & Osmond, C. (1988). Low birth weight and hypertension. *BMJ*, *297*(6641), 134–135. https://doi.org/10.1136/bmj.297.6641.134-b

BARKER, D. J. P. (1995). The fetal and infant origins of disease. *European Journal of Clinical Investigation*, *25*(7), 457–463. https://doi.org/10.1111/j.1365-2362.1995.tb01730.x

Barker, D. J. P., & Osmond, C. (1986). Infant Mortality, Childhood Nutrition, and Ischaemic Heart Disease in England and Wales. *The Lancet*, *327*(8489), 1077–1081. https://doi.org/10.1016/S0140-6736(86)91340-1

Barker, D. J. P., Osmond, C., Winter, P. D., Margetts, B., & Simmonds, S. J. (1989). WEIGHT IN INFANCY AND DEATH FROM ISCHAEMIC HEART DISEASE. *The Lancet*, *334*(8663), 577–580. https://doi.org/10.1016/S0140-6736(89)90710-1

Basma, H., Tatineni, S., Dhar, K., Qiu, F., Rennard, S., & Lowes, B. D. (2020). Electronic cigarette extract induced toxic effect in iPS-derived cardiomyocytes. *BMC Cardiovascular Disorders*, *20*(1). https://doi.org/10.1186/s12872-020-01629-4

Bedada, F. B., Chan, S. S. K., Metzger, S. K., Zhang, L., Zhang, J., Garry, D. J., Kamp, T. J., Kyba, M., & Metzger, J. M. (2014). Acquisition of a Quantitative, Stoichiometrically Conserved Ratiometric Marker of Maturation Status in Stem Cell-Derived Cardiac Myocytes. *Stem Cell Reports*, *3*(4), 594–605. https://doi.org/10.1016/J.STEMCR.2014.07.012

Belcher, S. M., Chen, Y., Yan, S., & Wang, H. S. (2012). Rapid Estrogen Receptor-Mediated Mechanisms Determine the Sexually Dimorphic Sensitivity of Ventricular Myocytes to 17β-Estradiol and the Environmental Endocrine Disruptor Bisphenol A. *Endocrinology*, *153*(2), 712. https://doi.org/10.1210/EN.2011-1772

Belcher, S. M., Gear, R. B., & Kendig, E. L. (2015). Bisphenol A Alters Autonomic Tone and Extracellular Matrix Structure and Induces Sex-Specific Effects on Cardiovascular Function in Male and Female CD-1 Mice. *Endocrinology*, *156*(3), 882–895. https://doi.org/10.1210/EN.2014-1847

Bellin, M., Marchetto, M. C., Gage, F. H., & Mummery, C. L. (2012). Induced pluripotent stem cells: the new patient? *Nature Reviews Molecular Cell Biology*, *13*(11), 713–726. https://doi.org/10.1038/nrm3448

Bergmann, O., Bhardwaj, R. D., Bernard, S., Zdunek, S., Barnabé-Heider, F., Walsh, S., Zupicich, J., Alkass, K., Buchholz, B. A., Druid, H., Jovinge, S., & Frisén, J. (2009). Evidence for cardiomyocyte renewal in humans. *Science (New York, N.Y.)*, *324*(5923), 98–102. https://doi.org/10.1126/science.1164680

Bers, D. M. (2002). Cardiac excitation–contraction coupling. *Nature*, *415*(6868), 198–205. https://doi.org/10.1038/415198a

Bi, X., Song, Y., Song, Y., Yuan, J., Cui, J., Zhao, S., & Qiao, S. (2021). Collagen Cross-Linking Is Associated With Cardiac Remodeling in Hypertrophic Obstructive Cardiomyopathy. *Journal of the American Heart Association*, *10*(1). https://doi.org/10.1161/JAHA.120.017752

Blackmore, H. L., & Ozanne, S. E. (2015). Programming of cardiovascular disease across the life-course. *Journal of Molecular and Cellular Cardiology*, *83*, 122–130. https://doi.org/10.1016/j.yjmcc.2014.12.006

Blanchette, A. D., Burnett, S. D., Grimm, F. A., Rusyn, I., & Chiu, W. A. (2020). A Bayesian Method for Population-wide Cardiotoxicity Hazard and Risk Characterization Using an *In Vitro* Human Model. *Toxicological Sciences*, *178*(2), 391–403. https://doi.org/10.1093/toxsci/kfaa151

Blin, G., Liand, M., Mauduit, C., Chehade, H., Benahmed, M., Simeoni, U., & Siddeek, B. (2020). Maternal exposure to high-fat diet induces long-term derepressive chromatin marks in the heart. *Nutrients*, *12*(1), 1–14. https://doi.org/10.3390/nu12010181

Block, T., Creech, J., da Rocha, A. M., Marinkovic, M., Ponce-Balbuena, D., Jiménez-Vázquez, E. N., Griffey, S., & Herron, T. J. (2020). Human perinatal stem cell derived extracellular matrix enables rapid maturation of hiPSC-CM structural and functional phenotypes. *Scientific Reports*, *10*(1), 19071. https://doi.org/10.1038/s41598-020-76052-y

Boland, E., Quondamatteo, F., & Van Agtmael, T. (2021). The role of basement membranes in cardiac biology and disease. *Bioscience Reports*, *41*(8), 20204185. https://doi.org/10.1042/BSR20204185

Brette, F., & Orchard, C. (2003). T-Tubule Function in Mammalian Cardiac Myocytes. *Circulation Research*, *92*(11), 1182–1192. https://doi.org/10.1161/01.RES.0000074908.17214.FD

Brown, A., Baird, M. R., Yip, M. C. J., Murray, J., & Shao, S. (2018). Structures of translationally inactive mammalian ribosomes. *ELife*, *7*. https://doi.org/10.7554/ELIFE.40486

Bruno, K. A., Mathews, J. E., Yang, A. L., Frisancho, J. A., Scott, A. J., Greyner, H. D., Molina, F. A., Greenaway, M. S., Cooper, G. M., Bucek, A., Morales-Lara, A. C., Hill, A. R., Mease, A. A., Di Florio, D. N., Sousou, J. M., Coronado, A. C., Stafford, A. R., & Fairweather, D. (2019). BPA Alters Estrogen Receptor Expression in the Heart After Viral Infection Activating Cardiac Mast Cells and T Cells Leading to Perimyocarditis and Fibrosis. *Frontiers in Endocrinology*, *10*. https://doi.org/10.3389/fendo.2019.00598

Burnett, S. D., Blanchette, A. D., Chiu, W. A., & Rusyn, I. (2021a). Cardiotoxicity Hazard and Risk Characterization of ToxCast Chemicals Using Human Induced Pluripotent Stem Cell-Derived Cardiomyocytes from Multiple Donors. *Chemical Research in Toxicology*, *34*(9), 2110–2124. https://doi.org/10.1021/ACS.CHEMRESTOX.1C00203/SUPPL_FILE/TX1C00203_SI_001.PDF

Burnett, S. D., Blanchette, A. D., Chiu, W. A., & Rusyn, I. (2021b). Human induced pluripotent stem cell (iPSC)-derived cardiomyocytes as an in vitro model in toxicology: strengths and weaknesses for hazard identification and risk characterization. *Expert Opinion on Drug Metabolism & Toxicology*, *17*(8), 887–902. https://doi.org/10.1080/17425255.2021.1894122

Burrage, D. M., Braddick, L., Cleal, J. K., Costello, P., Noakes, D. E., Hanson, M. A., & Green, L. R. (2009). The late gestation fetal cardiovascular response to hypoglycaemia is modified by prior peri-implantation undernutrition in sheep. *Journal of Physiology*, *587*(3), 611–624. https://doi.org/10.1113/jphysiol.2008.165944

Burridge, P. W., Keller, G., Gold, J. D., & Wu, J. C. (2012). Production of de novo cardiomyocytes: Human pluripotent stem cell differentiation and direct reprogramming. *Cell Stem Cell*, *10*(1), 16–28. https://doi.org/10.1016/j.stem.2011.12.013

Burridge, P. W., Matsa, E., Shukla, P., Lin, Z. C., Churko, J. M., Ebert, A. D., Lan, F., Diecke, S., Huber, B., Mordwinkin, N. M., Plews, J. R., Abilez, O. J., Cui, B., Gold, J. D., & Wu, J. C. (2014). Chemically defned generation of human cardiomyocytes. *Nature Methods*, *11*(8), 855–860. https://doi.org/10.1038/nMeth.2999

Bygren, L. O., Kaati, G., & Edvinsson, S. (2001). Longevity determined by paternal ancestors' nutrition during their slow growth period. *Acta Biotheoretica*, *49*(1), 53–59. https://doi.org/10.1023/A:1010241825519

Cai, S., Rao, X., Ye, J., Ling, Y., Mi, S., Chen, H., Fan, C., & Li, Y. (2020). Relationship between urinary bisphenol a levels and cardiovascular diseases in the U.S. adult population, 2003–2014. *Ecotoxicology and Environmental Safety*, *192*, 110300. https://doi.org/10.1016/j.ecoenv.2020.110300

Campostrini, G., Windt, L. M., van Meer, B. J., Bellin, M., & Mummery, C. L. (2021). Cardiac Tissues From Stem Cells. *Circulation Research*, *128*(6), 775–801. https://doi.org/10.1161/CIRCRESAHA.121.318183

Cardiovascular diseases (CVDs). (n.d.). Retrieved December 8, 2023, from https://www.who.int/en/news-room/fact-sheets/detail/cardiovascular-diseases-(cvds)

Chapalamadugu, K. C., VandeVoort, C. A., Settles, M. L., Robison, B. D., & Murdoch, G. K. (2014). Maternal bisphenol a exposure impacts the fetal heart transcriptome. *PloS One*, *9*(2). https://doi.org/10.1371/JOURNAL.PONE.0089096

Chen, L., Wang, Z., Gu, W., Zhang, X. X., Ren, H., & Wu, B. (2020). Single-Cell Sequencing Reveals Heterogeneity Effects of Bisphenol A on Zebrafish Embryonic Development. *Environmental Science and Technology*, *54*(15), 9537–9546. https://doi.org/10.1021/ACS.EST.0C02428/SUPPL_FILE/ES0C02428_SI_005.XLSX

Cheng, W., Yang, S., Li, X., Liang, F., Zhou, R., Wang, H., Feng, Y., & Wang, Y. (2020). Low doses of BPA induced abnormal mitochondrial fission and hypertrophy in human embryonic stem cell-derived cardiomyocytes via the calcineurin-DRP1 signaling pathway: A comparison between XX and XY

cardiomyocytes. *Toxicology and Applied Pharmacology*, *388*. https://doi.org/10.1016/J.TAAP.2019.114850

Chianese, R., Viggiano, A., Urbanek, K., Cappetta, D., Troisi, J., Scafuro, M., Guida, M., Esposito, G., Ciuffreda, L. P., Rossi, F., Berrino, L., Fasano, S., Pierantoni, R., De Angelis, A., & Meccariello, R. (2018). Chronic exposure to low dose of bisphenol A impacts on the first round of spermatogenesis via SIRT1 modulation. *Scientific Reports 2018 8:1*, *8*(1), 1–12. https://doi.org/10.1038/s41598-018-21076-8

Cho, Y. J., Park, S. Bin, Park, J. W., Oh, S. R., & Han, M. (2018). Bisphenol A modulates inflammation and proliferation pathway in human endometrial stromal cells by inducing oxidative stress. *Reproductive Toxicology*, *81*, 41–49. https://doi.org/10.1016/j.reprotox.2018.06.016

Chung, J. H., Biesiadecki, B. J., Ziolo, M. T., Davis, J. P., & Janssen, P. M. L. (2016). Myofilament calcium sensitivity: Role in regulation of in vivo cardiac contraction and relaxation. *Frontiers in Physiology*, *7*(DEC), 562. https://doi.org/10.3389/FPHYS.2016.00562/BIBTEX

Chute, M., Aujla, P., Jana, S., & Kassiri, Z. (2019). *The Non-Fibrillar Side of Fibrosis: Contribution of the Basement Membrane, Proteoglycans, and Glycoproteins to Myocardial Fibrosis*. https://doi.org/10.3390/jcdd6040035

Cimmino, I., Fiory, F., Perruolo, G., Miele, C., Beguinot, F., Formisano, P., & Oriente, F. (2020). Potential mechanisms of bisphenol a (BPA) contributing to human disease. In *International Journal of Molecular Sciences* (Vol. 21, Issue 16, pp. 1–22). MDPI AG. https://doi.org/10.3390/ijms21165761

Cooper, B. L., Salameh, S., & Posnack, N. G. (2023). Comparative cardiotoxicity assessment of bisphenol chemicals and estradiol using human induced pluripotent stem cell-derived cardiomyocytes. *BioRxiv : The Preprint Server for Biology*. https://doi.org/10.1101/2023.09.13.557564

Correia, C., Koshkin, A., Duarte, P., Hu, D., Teixeira, A., Domian, I., Serra, M., & Alves, P. M. (2017). Distinct carbon sources affect structural and functional maturation of cardiomyocytes derived from human pluripotent stem cells. *Scientific Reports*, *7*(1), 8590. https://doi.org/10.1038/s41598-017-08713-4

Corstius, H. B., Zimanyi, M. A., Maka, N., Herath, T., Thomas, W., Van Der Laarse, A., Wreford, N. G., & Black, M. J. (2005). Effect of Intrauterine Growth Restriction on the Number of Cardiomyocytes in Rat Hearts. *Pediatric Research 2005 57:6*, *57*(6), 796–800. https://doi.org/10.1203/01.pdr.0000157726.65492.cd

Cunningham, F., Allen, J. E., Allen, J., Alvarez-Jarreta, J., Amode, M. R., Armean, I. M., Austine-Orimoloye, O., Azov, A. G., Barnes, I., Bennett, R., Berry, A., Bhai, J., Bignell, A., Billis, K., Boddu, S., Brooks, L., Charkhchi, M., Cummins, C., Da Rin Fioretto, L., … Flicek, P. (2022). Ensembl 2022. *Nucleic Acids Research*, *50*(D1), D988–D995. https://doi.org/10.1093/NAR/GKAB1049

Cypher, A. D., Fetterman, B., & Bagatto, B. (2018). Vascular parameters continue to decrease post-exposure with simultaneous, but not individual exposure to BPA and hypoxia in zebrafish larvae. *Comparative Biochemistry and Physiology Part C: Toxicology & Pharmacology*, *206–207*, 11–16. https://doi.org/10.1016/J.CBPC.2018.02.002

Cypher, A. D., Ickes, J. R., & Bagatto, B. (2015). Bisphenol A alters the cardiovascular response to hypoxia in Danio rerio embryos. *Comparative Biochemistry and Physiology Part C: Toxicology & Pharmacology*, *174–175*, 39–45. https://doi.org/10.1016/J.CBPC.2015.06.006

Daley, M. (2022). Beyond pharmaceuticals: Fit-for-purpose new approach methodologies for environmental cardiotoxicity testing. *ALTEX*. https://doi.org/10.14573/altex.2109131

Davis, A. P., Wiegers, T. C., Johnson, R. J., Sciaky, D., Wiegers, J., & Mattingly, C. J. (2023). Comparative Toxicogenomics Database (CTD): update 2023. *Nucleic Acids Research*, *51*(D1), D1257–D1262. https://doi.org/10.1093/NAR/GKAC833

Deutschmann, A., Hans, M., Meyer, R., Häberlein, H., & Swandulla, D. (2013). Bisphenol A Inhibits Voltage-Activated Ca $^{2+}$ Channels in Vitro: Mechanisms and Structural Requirements. *Molecular Pharmacology*, *83*(2), 501–511. https://doi.org/10.1124/mol.112.081372

Devalla, H. D., Schwach, V., Ford, J. W., Milnes, J. T., El-Haou, S., Jackson, C., Gkatzis, K., Elliott, D. A., Lopes, S. M. C. de S., Mummery, C. L., Verkerk, A. O., & Passier, R. (2015). Atrial-like cardiomyocytes from human pluripotent stem cells are a robust preclinical model for assessing atrial-selective pharmacology. *EMBO Molecular Medicine*, *7*(4), 394. https://doi.org/10.15252/EMMM.201404757

Di Pietro, P., D'Auria, R., Viggiano, A., Ciaglia, E., Meccariello, R., Russo, R. Dello, Puca, A. A., Vecchione, C., Nori, S. L., & Santoro, A. (2020). Bisphenol A induces DNA damage in cells exerting immune surveillance functions at peripheral and central level. *Chemosphere*, *254*, 126819. https://doi.org/10.1016/J.CHEMOSPHERE.2020.126819

Dickinson, H., Moss, T. J., Gatford, K. L., Moritz, K. M., Akison, L., Fullston, T., Hryciw, D. H., Maloney, C. A., Morris, M. J., Wooldridge, A. L., Schjenken, J. E., Robertson, S. A., Waddell, B. J., Mark, P. J., Wyrwoll, C. S., Ellery, S. J., Thornburg, K. L., Muhlhausler, B. S., & Morrison, J. L. (2016). A review of fundamental principles for animal models of DOHaD research: An Australian perspective. *Journal of Developmental Origins of Health and Disease*, *7*(5), 449–472. https://doi.org/10.1017/S2040174416000477

Díez, J., Querejeta, R., López, B., González, A., Larman, M., & Martínez Ubago, J. L. (2002). Losartan-Dependent Regression of Myocardial Fibrosis Is Associated With Reduction of Left Ventricular Chamber Stiffness in Hypertensive Patients. *Circulation*, *105*(21), 2512–2517. https://doi.org/10.1161/01.CIR.0000017264.66561.3D

Disertori, M., Masè, M., & Ravelli, F. (2017). Myocardial fibrosis predicts ventricular tachyarrhythmias. *Trends in Cardiovascular Medicine*, *27*(5), 363–372. https://doi.org/10.1016/J.TCM.2017.01.011

Dix, D. J., Houck, K. A., Martin, M. T., Richard, A. M., Setzer, R. W., & Kavlock, R. J. (2007). The ToxCast Program for Prioritizing Toxicity Testing of Environmental Chemicals. *Toxicological Sciences*, *95*(1), 5–12. https://doi.org/10.1093/TOXSCI/KFL103

Doss, M. X., & Sachinidis, A. (2019). Current Challenges of iPSC-Based Disease Modeling and Therapeutic Implications. *Cells*, *8*(5), 403. https://doi.org/10.3390/cells8050403

Eberle, C., Kirchner, M. F., Herden, R., & Stichling, S. (2020). Paternal metabolic and cardiovascular programming of their offspring: A systematic scoping review. *PLOS ONE*, *15*(12), e0244826. https://doi.org/10.1371/JOURNAL.PONE.0244826

Edwards, C. A., & Ferguson-Smith, A. C. (2007). Mechanisms regulating imprinted genes in clusters. *Current Opinion in Cell Biology*, *19*(3), 281–289. https://doi.org/10.1016/j.ceb.2007.04.013

EFSA CEF Panel, 2015. (2015). Scientific Opinion on the risks to public health related to the presence of bisphenol A (BPA) in foodstuffs. *EFSA Journal*, *13*(1), 3978. https://doi.org/10.2903/j.efsa.2015.3978

EFSA CEP Panel. (2023). Scientific Opinion on the re-evaluation of the risks to public health related to the presence of bisphenol A (BPA) in foodstuffs. *EFSA Journal*, *21*(4), 6857. https://doi.org/10.2903/j.efsa.2023.6857

Eid, J. I., Eissa, S. M., & El-Ghor, A. A. (2015). Bisphenol A induces oxidative stress and DNA damage in hepatic tissue of female rat offspring. *The Journal of Basic & Applied Zoology*, *71*, 10–19. https://doi.org/10.1016/J.JOBAZ.2015.01.006

Eisner, D. A., Caldwell, J. L., Kistamás, K., & Trafford, A. W. (2017). Calcium and Excitation-Contraction Coupling in the Heart. In *Circulation Research* (Vol. 121, Issue 2, pp. 181–195). Lippincott Williams and Wilkins. https://doi.org/10.1161/CIRCRESAHA.117.310230

Emanuelli, G., Zoccarato, A., Reumiller, C. M., Papadopoulos, A., Chong, M., Rebs, S., Betteridge, K., Beretta, M., Streckfuss-Bömeke, K., & Shah, A. M. (2022). A roadmap for the characterization of

energy metabolism in human cardiomyocytes derived from induced pluripotent stem cells. *Journal of Molecular and Cellular Cardiology*, *164*, 136–147. https://doi.org/10.1016/J.YJMCC.2021.12.001

Engler, A. J., Carag-Krieger, C., Johnson, C. P., Raab, M., Tang, H. Y., Speicher, D. W., Sanger, J. W., Sanger, J. M., & Discher, D. E. (2008). Embryonic cardiomyocytes beat best on a matrix with heart-like elasticity: scar-like rigidity inhibits beating. *Journal of Cell Science*, *121*(Pt 22), 3794. https://doi.org/10.1242/JCS.029678

Escarda-Castro, E., Herráez, M. P., & Lombó, M. (2021). Effects of bisphenol A exposure during cardiac cell differentiation. *Environmental Pollution*, *286*, 117567. https://doi.org/10.1016/J.ENVPOL.2021.117567

Fainberg, H. P., Almond, K. L., Li, D., Rauch, C., Bikker, P., Symonds, M. E., & Mostyn, A. (2014). Impact of maternal dietary fat supplementation during gestation upon skeletal muscle in neonatal pigs. *BMC Physiology*, *14*(1), 1–12. https://doi.org/10.1186/s12899-014-0006-0

Fan, L., Lindsley, S. R., Comstock, S. M., Takahashi, D. L., Evans, A. E., He, G. W., Thornburg, K. L., & Grove, K. L. (2013). Maternal high-fat diet impacts endothelial function in nonhuman primate offspring. *International Journal of Obesity*, *37*(2), 254–262. https://doi.org/10.1038/ijo.2012.42

Fang, Z., Liu, X., & Peltz, G. (2023). GSEApy: a comprehensive package for performing gene set enrichment analysis in Python. *Bioinformatics*, *39*(1). https://doi.org/10.1093/BIOINFORMATICS/BTAC757

Feuer, S., & Rinaudo, P. (2016). From Embryos to Adults: A DOHaD Perspective on In Vitro Fertilization and Other Assisted Reproductive Technologies. *Healthcare*, *4*(3), 51. https://doi.org/10.3390/healthcare4030051

Fischer, I., Milton, C., & Wallace, H. (2020). Toxicity testing is evolving! *Toxicology Research*, *9*(2), 67. https://doi.org/10.1093/TOXRES/TFAA011

Fleming, T. P., Watkins, A. J., Sun, C., Velazquez, M. A., Smyth, N. R., & Eckert, J. J. (2015). Do little embryos make big decisions? How maternal dietary protein restriction can permanently change an embryo's potential, affecting adult health. *Reproduction, Fertility and Development*, *27*(4), 684. https://doi.org/10.1071/RD14455

Fleming, T. P., Watkins, A. J., Velazquez, M. A., Mathers, J. C., Prentice, A. M., Stephenson, J., Barker, M., Saffery, R., Yajnik, C. S., Eckert, J. J., Hanson, M. A., Forrester, T., Gluckman, P. D., & Godfrey, K. M. (2018). Origins of Lifetime Health Around the Time of Conception: Causes and Consequences. *Obstetrical and Gynecological Survey*, *73*(10), 555–557. https://doi.org/10.1097/OGX.0000000000000612

Flenkenthaler, F., Ländström, E., Shashikadze, B., Backman, M., Blutke, A., Philippou-Massier, J., Renner, S., Hrabe de Angelis, M., Wanke, R., Blum, H., Arnold, G. J., Wolf, E., & Fröhlich, T. (2021). Differential Effects of Insulin-Deficient Diabetes Mellitus on Visceral vs. Subcutaneous Adipose Tissue—Multi-omics Insights From the Munich MIDY Pig Model. *Frontiers in Medicine*, *8*, 751277. https://doi.org/10.3389/FMED.2021.751277/FULL

Fonseca, M. I., Lorigo, M., & Cairrao, E. (2022). Endocrine-Disrupting Effects of Bisphenol A on the Cardiovascular System: A Review. *Journal of Xenobiotics 2022, Vol. 12, Pages 181-213*, *12*(3), 181–213. https://doi.org/10.3390/JOX12030015

Fountoulaki, K., Dagres, N., & Iliodromitis, E. K. (2015). Cellular Communications in the Heart. *Cardiac Failure Review*, *1*(2), 64. https://doi.org/10.15420/CFR.2015.1.2.64

Frangogiannis, N. G. (2017). The extracellular matrix in myocardial injury, repair, and remodeling. *The Journal of Clinical Investigation*, *127*(5), 1600. https://doi.org/10.1172/JCI87491

Frangogiannis, N. G. (2019). The Extracellular Matrix in Ischemic and Nonischemic Heart Failure. *Circulation Research*, *125*(1), 117–146. https://doi.org/10.1161/CIRCRESAHA.119.311148

Freitas, J., Cano, P., Craig-Veit, C., Goodson, M. L., David Furlow, J., & Murk, A. J. (2011). Detection of thyroid hormone receptor disruptors by a novel stable in vitro reporter gene assay. *Toxicology in Vitro*, *25*(1), 257–266. https://doi.org/10.1016/j.tiv.2010.08.013

Fuhrmann, D. C., Wittig, I., Heide, H., Dehne, N., & Brüne, B. (2013). Chronic hypoxia alters mitochondrial composition in human macrophages. *Biochimica et Biophysica Acta (BBA) - Proteins and Proteomics*, *1834*(12), 2750–2760. https://doi.org/10.1016/J.BBAPAP.2013.09.023

Gao, X., Liang, Q., Chen, Y., & Wang, H. S. (2013). Molecular Mechanisms Underlying the Rapid Arrhythmogenic Action of Bisphenol A in Female Rat Hearts. *Endocrinology*, *154*(12), 4607. https://doi.org/10.1210/EN.2013-1737

Gao, X., & Wang, H. S. (2014). Impact of Bisphenol A on the Cardiovascular System — Epidemiological and Experimental Evidence and Molecular Mechanisms. *International Journal of Environmental Research and Public Health 2014, Vol. 11, Pages 8399-8413*, *11*(8), 8399–8413. https://doi.org/10.3390/IJERPH110808399

García-Arévalo, M., Lorza-Gil, E., Cardoso, L., Batista, T. M., Araujo, T. R., Ramos, L. A. F., Areas, M. A., Nadal, A., Carneiro, E. M., & Davel, A. P. (2021). Ventricular Fibrosis and Coronary Remodeling Following Short-Term Exposure of Healthy and Malnourished Mice to Bisphenol A. *Frontiers in Physiology*, *12*, 367. https://doi.org/10.3389/FPHYS.2021.638506/BIBTEX

Geneva: World Health Organization. (2020). Noncommunicable diseases progress monitor 2020. In *World Health* (Issues 978-92-4-000049–0). https://doi.org/10.5005/jp/books/11410_18

Ghassabian, A., Vandenberg, L., Kannan, K., & Trasande, L. (2022). Endocrine-Disrupting Chemicals and Child Health. *Annual Review of Pharmacology and Toxicology*, *62*(1), 573–594. https://doi.org/10.1146/annurev-pharmtox-021921-093352

Giacomelli, E., Bellin, M., Sala, L., van Meer, B. J., Tertoolen, L. G. J., Orlova, V. V., & Mummery, C. L. (2017). Three-dimensional cardiac microtissues composed of cardiomyocytes and endothelial cells co-differentiated from human pluripotent stem cells. *Development (Cambridge)*, *144*(6), 1008–1017. https://doi.org/10.1242/dev.143438

Giacomelli, E., Meraviglia, V., Campostrini, G., Cochrane, A., Cao, X., van Helden, R. W. J., Krotenberg Garcia, A., Mircea, M., Kostidis, S., Davis, R. P., van Meer, B. J., Jost, C. R., Koster, A. J., Mei, H., Míguez, D. G., Mulder, A. A., Ledesma-Terrón, M., Pompilio, G., Sala, L., … Mummery, C. L. (2020). Human-iPSC-Derived Cardiac Stromal Cells Enhance Maturation in 3D Cardiac Microtissues and Reveal Non-cardiomyocyte Contributions to Heart Disease. *Cell Stem Cell*, *26*(6), 862-879.e11. https://doi.org/10.1016/j.stem.2020.05.004

Gintant, G., Burridge, P., Gepstein, L., Harding, S., Herron, T., Hong, C., Jalife, J., & Wu, J. C. (2019). Use of Human Induced Pluripotent Stem Cell–Derived Cardiomyocytes in Preclinical Cancer Drug Cardiotoxicity Testing: A Scientific Statement From the American Heart Association. *Circulation Research*, *125*(10). https://doi.org/10.1161/RES.0000000000000291

Godfrey, K. M., Reynolds, R. M., Prescott, S. L., Nyirenda, M., Jaddoe, V. W. V., Eriksson, J. G., & Broekman, B. F. P. (2017). Influence of maternal obesity on the long-term health of offspring. *The Lancet Diabetes and Endocrinology*, *5*(1), 53–64. https://doi.org/10.1016/S2213-8587(16)30107-3

Goh, J. M., Bensley, J. G., Kenna, K., Sozo, F., Bocking, A. D., Brien, J., Walker, D., Harding, R., & Black, M. J. (2011). Alcohol exposure during late gestation adversely affects myocardial development with implications for postnatal cardiac function. *American Journal of Physiology - Heart and Circulatory Physiology*, *300*(2), 645–651. https://doi.org/10.1152/ajpheart.00689.2010

Goldfracht, I., Protze, S., Shiti, A., Setter, N., Gruber, A., Shaheen, N., Nartiss, Y., Keller, G., & Gepstein, L. (2020). Generating ring-shaped engineered heart tissues from ventricular and atrial human pluripotent stem cell-derived cardiomyocytes. *Nature Communications 2020 11:1*, *11*(1), 1–15. https://doi.org/10.1038/s41467-019-13868-x

Gore, A. C., Chappell, V. A., Fenton, S. E., Flaws, J. A., Nadal, A., Prins, G. S., Toppari, J., & Zoeller, R. T. (2015). EDC-2: The Endocrine Society's Second Scientific Statement on Endocrine-Disrupting Chemicals. *Endocrine Reviews*, *36*(6), E1. https://doi.org/10.1210/ER.2015-1010

Grossman, W., & Paulus, W. J. (2013). Myocardial stress and hypertrophy: a complex interface between biophysics and cardiac remodeling. *The Journal of Clinical Investigation*, *123*(9), 3701–3703. https://doi.org/10.1172/JCI69830

Gu, Z., Eils, R., & Schlesner, M. (2016). Complex heatmaps reveal patterns and correlations in multidimensional genomic data. *Bioinformatics*, *32*(18), 2847–2849. https://doi.org/10.1093/BIOINFORMATICS/BTW313

Guney, E., Menche, J., Vidal, M., & Barábasi, A. L. (2016). Network-based in silico drug efficacy screening. *Nature Communications 2016 7:1*, *7*(1), 1–13. https://doi.org/10.1038/ncomms10331

Guo, H., Tian, L., Zhang, J. Z., Kitani, T., Paik, D. T., Lee, W. H., & Wu, J. C. (2019). Single-Cell RNA Sequencing of Human Embryonic Stem Cell Differentiation Delineates Adverse Effects of Nicotine on Embryonic Development. *Stem Cell Reports*, *12*(4), 772–786. https://doi.org/10.1016/j.stemcr.2019.01.022

Guo, Y., & Pu, W. T. (2020). Cardiomyocyte Maturation. *Circulation Research*, 1086–1106. https://doi.org/10.1161/CIRCRESAHA.119.315862

Häkli, M., Kreutzer, J., Mäki, A. J., Välimäki, H., Lappi, H., Huhtala, H., Kallio, P., Aalto-Setälä, K., & Pekkanen-Mattila, M. (2021). Human induced pluripotent stem cell-based platform for modeling cardiac ischemia. *Scientific Reports 2021 11:1*, *11*(1), 1–13. https://doi.org/10.1038/s41598-021-83740-w

Hamad, S., Derichsweiler, D., Papadopoulos, S., Nguemo, F., Šarić, T., Sachinidis, A., Brockmeier, K., Hescheler, J., Boukens, B. J., & Pfannkuche, K. (2019). Generation of human induced pluripotent stem cell-derived cardiomyocytes in 2D monolayer and scalable 3D suspension bioreactor cultures with reduced batch-to-batch variations. *Theranostics*, *9*(24), 7222–7238. https://doi.org/10.7150/thno.32058

Hanson, M. A., & Gluckman, P. D. (2014). Early developmental conditioning of later health and disease: physiology or pathophysiology? *Physiological Reviews*, *94*(4), 1027–1076. https://doi.org/10.1152/physrev.00029.2013

Heindel, J. J., Belcher, S., Flaws, J. A., Prins, G. S., Ho, S. M., Mao, J., Patisaul, H. B., Ricke, W., Rosenfeld, C. S., Soto, A. M., vom Saal, F. S., & Zoeller, R. T. (2020). Data integration, analysis, and interpretation of eight academic CLARITY-BPA studies. *Reproductive Toxicology (Elmsford, N.y.)*, *98*, 29. https://doi.org/10.1016/J.REPROTOX.2020.05.014

Heras-Bautista, C. O., Mikhael, N., Lam, J., Shinde, V., Katsen-Globa, A., Dieluweit, S., Molcanyi, M., Uvarov, V., Jütten, P., Sahito, R. G. A., Mederos-Henry, F., Piechot, A., Brockmeier, K., Hescheler, J., Sachinidis, A., & Pfannkuche, K. (2019). Cardiomyocytes facing fibrotic conditions re-express extracellular matrix transcripts. *Acta Biomaterialia*, *89*, 180–192. https://doi.org/10.1016/J.ACTBIO.2019.03.017

Heymans, S., Schroen, B., Vermeersch, P., Milting, H., Gao, F., Kassner, A., Gillijns, H., Herijgers, P., Flameng, W., Carmeliet, P., Van De Werf, F., Pinto, Y. M., & Janssens, S. (2005). Increased Cardiac Expression of Tissue Inhibitor of Metalloproteinase-1 and Tissue Inhibitor of Metalloproteinase-2 Is Related to Cardiac Fibrosis and Dysfunction in the Chronic Pressure-Overloaded Human Heart. *Circulation*, *112*(8), 1136–1144. https://doi.org/10.1161/CIRCULATIONAHA.104.516963

Hill, C. E., Myers, J. P., & Vandenberg, L. N. (2018). Nonmonotonic Dose–Response Curves Occur in Dose Ranges That Are Relevant to Regulatory Decision-Making. *Dose-Response*, *16*(3), 155932581879828. https://doi.org/10.1177/1559325818798282

Hinderer, S., & Schenke-Layland, K. (2019). Cardiac fibrosis – A short review of causes and therapeutic strategies. *Advanced Drug Delivery Reviews*, *146*, 77–82. https://doi.org/10.1016/J.ADDR.2019.05.011

Hnatiuk, A. P., Briganti, F., Staudt, D. W., & Mercola, M. (2021). Human iPSC modeling of heart disease for drug development. *Cell Chemical Biology*, *28*(3), 271–282. https://doi.org/10.1016/j.chembiol.2021.02.016

Hofbauer, P., Jahnel, S. M., Papai, N., Giesshammer, M., Deyett, A., Schmidt, C., Penc, M., Tavernini, K., Grdseloff, N., Meledeth, C., Ginistrelli, L. C., Ctortecka, C., Šalic, Š., Novatchkova, M., & Mendjan, S. (2021). Cardioids reveal self-organizing principles of human cardiogenesis. *Cell*, *184*(12), 3299-3317.e22. https://doi.org/10.1016/j.cell.2021.04.034

Homburger, J. R., Green, E. M., Caleshu, C., Sunitha, M. S., Taylor, R. E., Ruppel, K. M., Metpally, R. P. R., Colan, S. D., Michels, M., Day, S. M., Olivotto, I., Bustamante, C. D., Dewey, F. E., Ho, C. Y., Spudich, J. A., & Ashley, E. A. (2016). Multidimensional structure-function relationships in human β-cardiac myosin from population-scale genetic variation. *Proceedings of the National Academy of Sciences of the United States of America*, *113*(24), 6701–6706. https://doi.org/10.1073/PNAS.1606950113/-/DCSUPPLEMENTAL

Huang, M., Jiao, J., Wang, J., Xia, Z., & Zhang, Y. (2018). Characterization of acrylamide-induced oxidative stress and cardiovascular toxicity in zebrafish embryos. *Journal of Hazardous Materials*, *347*, 451–460. https://doi.org/10.1016/j.jhazmat.2018.01.016

Hwang, H., Liu, R., Eldridge, R., Hu, X., Forghani, P., Jones, D. P., & Xu, C. (2023). Chronic ethanol exposure induces mitochondrial dysfunction and alters gene expression and metabolism in human cardiac spheroids. *Alcoholism: Clinical and Experimental Research*, *47*(4), 643–658. https://doi.org/10.1111/acer.15026

Hyun, S. A., Lee, C. Y., Ko, M. Y., Chon, S. H., Kim, Y. J., Seo, J. W., Kim, K. K., & Ka, M. (2021). Cardiac toxicity from bisphenol A exposure in human-induced pluripotent stem cell-derived cardiomyocytes. *Toxicology and Applied Pharmacology*, *428*, 115696. https://doi.org/10.1016/J.TAAP.2021.115696

Ieda, M., Tsuchihashi, T., Ivey, K. N., Ross, R. S., Hong, T.-T., Shaw, R. M., & Srivastava, D. (2009). Cardiac Fibroblasts Regulate Myocardial Proliferation through β1 Integrin Signaling. *Developmental Cell*, *16*(2), 233–244. https://doi.org/10.1016/j.devcel.2008.12.007

Iorga, A., Cunningham, C. M., Moazeni, S., Ruffenach, G., Umar, S., & Eghbali, M. (2017). The protective role of estrogen and estrogen receptors in cardiovascular disease and the controversial use of estrogen therapy. *Biology of Sex Differences*, *8*(1), 33. https://doi.org/10.1186/S13293-017-0152-8

Jha, R., Xu, R. H., & Xu, C. (2015). Efficient differentiation of cardiomyocytes from human pluripotent stem cells with growth factors. In *Cardiomyocytes: Methods and Protocols* (Vol. 1299, pp. 115–131). Springer New York. https://doi.org/10.1007/978-1-4939-2572-8_9

Judson, R., Richard, A., Dix, D. J., Houck, K., Martin, M., Kavlock, R., Dellarco, V., Henry, T., Holderman, T., Sayre, P., Tan, S., Carpenter, T., & Smith, E. (2009). The Toxicity Data Landscape for Environmental Chemicals. *Environmental Health Perspectives*, *117*(5), 685–695. https://doi.org/10.1289/ehp.0800168

Kaati, G., Bygren, L. O., & Edvinsson, S. (2002). Cardiovascular and diabetes mortality determined by nutrition during parents' and grandparents' slow growth period. *European Journal of Human Genetics*, *10*(11), 682–688. https://doi.org/10.1038/sj.ejhg.5200859

Kanehisa, M., & Goto, S. (2000). KEGG: kyoto encyclopedia of genes and genomes. *Nucleic Acids Research*, *28*(1), 27–30. https://doi.org/10.1093/NAR/28.1.27

Karbassi, E., Fenix, A., Marchiano, S., Muraoka, N., Nakamura, K., Yang, X., & Murry, C. E. (2020). Cardiomyocyte maturation: advances in knowledge and implications for regenerative medicine. *Nature Reviews Cardiology*, *Box 1*. https://doi.org/10.1038/s41569-019-0331-x

Kattman, S. J., Witty, A. D., Gagliardi, M., Dubois, N. C., Niapour, M., Hotta, A., Ellis, J., & Keller, G. (2011). Stage-Specific Optimization of Activin/Nodal and BMP Signaling Promotes Cardiac Differentiation of Mouse and Human Pluripotent Stem Cell Lines. *Cell Stem Cell*, *8*(2), 228–240. https://doi.org/10.1016/J.STEM.2010.12.008

Kehat, I., Kenyagin-Karsenti, D., Snir, M., Segev, H., Amit, M., Gepstein, A., Livne, E., Binah, O., Itskovitz-Eldor, J., & Gepstein, L. (2001). Human embryonic stem cells can differentiate into myocytes with structural and functional properties of cardiomyocytes. *Journal of Clinical Investigation*, *108*(3), 407–414. https://doi.org/10.1172/JCI200112131

Kibel, A., Lukinac, A. M., Dambic, V., Juric, I., & Relatic, K. S. (2020). Oxidative Stress in Ischemic Heart Disease. *Oxidative Medicine and Cellular Longevity*, *2020*. https://doi.org/10.1155/2020/6627144

Ko, E. B., Hwang, K. A., & Choi, K. C. (2019). Prenatal toxicity of the environmental pollutants on neuronal and cardiac development derived from embryonic stem cells. *Reproductive Toxicology*, *90*(June), 15–23. https://doi.org/10.1016/j.reprotox.2019.08.006

Kofron, C. M., Kim, T. Y., Munarin, F., Soepriatna, A. H., Kant, R. J., Mende, U., Choi, B.-R., & Coulombe, K. L. K. (2021). A predictive in vitro risk assessment platform for pro-arrhythmic toxicity using human 3D cardiac microtissues. *Scientific Reports*, *11*(1), 10228. https://doi.org/10.1038/s41598-021-89478-9

Krewski, D., Acosta, D., Andersen, M., Anderson, H., Bailar, J. C., Boekelheide, K., Brent, R., Charnley, G., Cheung, V. G., Green, S., Kelsey, K. T., Kerkvliet, N. I., Li, A. A., McCray, L., Meyer, O., Patterson, R. D., Pennie, W., Scala, R. A., Solomon, G. M., Stephens, M., Yager, J., Zeise, L., Staff of Committee on Toxicity Test. (2010). Toxicity Testing in the 21st Century: A Vision and a Strategy. *Journal of Toxicology and Environmental Health, Part B*, *13*(2–4), 51–138. https://doi.org/10.1080/10937404.2010.483176

Kroll, K., Chabria, M., Wang, K., Häusermann, F., Schuler, F., & Polonchuk, L. (2017). Electro-mechanical conditioning of human iPSC-derived cardiomyocytes for translational research. *Progress in Biophysics and Molecular Biology*, *130*, 212–222. https://doi.org/10.1016/j.pbiomolbio.2017.07.003

Krüger, M., Kohl, T., & Linke, W. A. (2006). Developmental changes in passive stiffness and myofilament Ca $^{2+}$ sensitivity due to titin and troponin-I isoform switching are not critically triggered by birth. *American Journal of Physiology-Heart and Circulatory Physiology*, *291*(2), H496–H506. https://doi.org/10.1152/ajpheart.00114.2006

Kubo, T., Maezawa, N., Osada, M., Katsumura, S., Funae, Y., & Imaoka, S. (2004). Bisphenol A, an environmental endocrine-disrupting chemical, inhibits hypoxic response via degradation of hypoxia-inducible factor 1α (HIF-1α): structural requirement of bisphenol A for degradation of HIF-1α. *Biochemical and Biophysical Research Communications*, *318*(4), 1006–1011. https://doi.org/10.1016/J.BBRC.2004.04.125

Kuo, C. C., Huang, J. K., Chou, C. T., Cheng, J. S., Tsai, J. Y., Fang, Y. C., Hsu, S. S., Liao, W. C., Chang, H. T., Ho, C. M., & Jan, C. R. (2011). Effect of bisphenol A on Ca2+ fluxes and viability in Madin-Darby canine renal tubular cells. *Http://Dx.Doi.Org/10.3109/01480545.2011.556645*, *34*(4), 454–461. https://doi.org/10.3109/01480545.2011.556645

Lacagnina, S. (2020). The Developmental Origins of Health and Disease (DOHaD). *American Journal of Lifestyle Medicine*, *14*(1), 47–50. https://doi.org/10.1177/1559827619879694

Lahmers, S., Wu, Y., Call, D. R., Labeit, S., & Granzier, H. (2004). Developmental Control of Titin Isoform Expression and Passive Stiffness in Fetal and Neonatal Myocardium. *Circulation Research*, *94*(4), 505–513. https://doi.org/10.1161/01.RES.0000115522.52554.86

LaKind, J. S., Goodman, M., & Mattison, D. R. (2014). Bisphenol A and indicators of obesity, glucose metabolism/type 2 diabetes and cardiovascular disease: A systematic review of epidemiologic research. *Critical Reviews in Toxicology*, *44*(2), 121–150. https://doi.org/10.3109/10408444.2013.860075

LaKind, J. S., Goodman, M., & Naiman, D. Q. (2012). Use of NHANES Data to Link Chemical Exposures to Chronic Diseases: A Cautionary Tale. *PLoS ONE*, *7*(12), e51086. https://doi.org/10.1371/journal.pone.0051086

Lang, I. A. (2008). Association of Urinary Bisphenol A Concentration With Medical Disorders and Laboratory Abnormalities in Adults. *JAMA*, *300*(11), 1303. https://doi.org/10.1001/jama.300.11.1303

Larson, A., Codden, C. J., Huggins, G. S., Rastegar, H., Chen, F. Y., Maron, B. J., Rowin, E. J., Maron, M. S., & Chin, M. T. (2022). Altered intercellular communication and extracellular matrix signaling as a potential disease mechanism in human hypertrophic cardiomyopathy. *Scientific Reports 2022 12:1*, *12*(1), 1–13. https://doi.org/10.1038/s41598-022-08561-x

Lazaraviciute, G., Kauser, M., Bhattacharya, S., Haggarty, P., & Bhattacharya, S. (2014). A systematic review and meta-analysis of DNA methylation levels and imprinting disorders in children conceived by IVF/ICSI compared with children conceived spontaneously. *Human Reproduction Update*, *20*(6), 840–852. https://doi.org/10.1093/humupd/dmu033

Lee, J.-H., Yoo, Y.-M., Jung, E.-M., Ahn, C. H., & Jeung, E.-B. (2019). Inhibitory effect of octyl-phenol and bisphenol A on calcium signaling in cardiomyocyte differentiation of mouse embryonic stem cells. *Journal of Physiology and Pharmacology : An Official Journal of the Polish Physiological Society*, *70*(3). https://doi.org/10.26402/jpp.2019.3.10

Li, C., & Jackson, R. M. (2002). Reactive species mechanisms of cellular hypoxia-reoxygenation injury. *American Journal of Physiology-Cell Physiology*, *282*(2), C227–C241. https://doi.org/10.1152/ajpcell.00112.2001

Li, F., Wang, X., Capasso, J. M., & Gerdes, A. M. (1996). Rapid transition of cardiac myocytes from hyperplasia to hypertrophy during postnatal development. *Journal of Molecular and Cellular Cardiology*, *28*(8), 1737–1746. https://doi.org/10.1006/jmcc.1996.0163

Li, M. X., & Hwang, P. M. (2015). Structure and function of cardiac troponin C (TNNC1): Implications for heart failure, cardiomyopathies, and troponin modulating drugs. *Gene*, *571*(2), 153–166. https://doi.org/10.1016/J.GENE.2015.07.074

Lian, X., Hsiao, C., Wilson, G., Zhu, K., Hazeltine, L. B., Azarin, S. M., Raval, K. K., Zhang, J., Kamp, T. J., & Palecek, S. P. (2012). Robust cardiomyocyte differentiation from human pluripotent stem cells via temporal modulation of canonical Wnt signaling. *Proceedings of the National Academy of Sciences of the United States of America*, *109*(27). https://doi.org/10.1073/pnas.1200250109

Lian, X., Zhang, J., Azarin, S. M., Zhu, K., Hazeltine, L. B., Bao, X., Hsiao, C., Kamp, T. J., & Palecek, S. P. (2013). Directed cardiomyocyte differentiation from human pluripotent stem cells by modulating Wnt/β-catenin signaling under fully defined conditions. *Nature Protocols*, *8*(1), 162–175. https://doi.org/10.1038/nprot.2012.150

Liang, Q., Gao, X., Chen, Y., Hong, K., & Wang, H. S. (2014). Cellular Mechanism of the Nonmonotonic Dose Response of Bisphenol A in Rat Cardiac Myocytes. *Environmental Health Perspectives*, *122*(6), 601. https://doi.org/10.1289/EHP.1307491

Liang, W., Han, P., Kim, E. H., Mak, J., Zhang, R., Torrente, A. G., Goldhaber, J. I., Marbán, E., & Cho, H. C. (2020). Canonical Wnt signaling promotes pacemaker cell specification of cardiac mesodermal cells derived from mouse and human embryonic stem cells. *STEM CELLS*, *38*(3), 352–368. https://doi.org/10.1002/STEM.3106

Liao, Y., Wang, J., Jaehnig, E. J., Shi, Z., & Zhang, B. (2019). WebGestalt 2019: gene set analysis toolkit with revamped UIs and APIs. *Nucleic Acids Research*, *47*(W1), W199–W205. https://doi.org/10.1093/NAR/GKZ401

Lin, Y., & Zou, J. (2020). Differentiation of Cardiomyocytes from Human Pluripotent Stem Cells in Fully Chemically Defined Conditions. *STAR Protocols*, *1*(1). https://doi.org/10.1016/J.XPRO.2020.100015

Lind, P. M., & Lind, L. (2011). Circulating levels of bisphenol A and phthalates are related to carotid atherosclerosis in the elderly. *Atherosclerosis*, *218*(1), 207–213. https://doi.org/10.1016/j.atherosclerosis.2011.05.001

Liu, C., Duan, W., Li, R., Xu, S., Zhang, L., Chen, C., He, M., Lu, Y., Wu, H., Pi, H., Luo, X., Zhang, Y., Zhong, M., Yu, Z., & Zhou, Z. (2013). Exposure to bisphenol A disrupts meiotic progression during spermatogenesis in adult rats through estrogen-like activity. *Cell Death & Disease*, *4*(6), e676. https://doi.org/10.1038/CDDIS.2013.203

Liu, L.-P., & Zheng, Y.-W. (2019). Predicting differentiation potential of human pluripotent stem cells: Possibilities and challenges. *World Journal of Stem Cells*, *11*(7), 375–382. https://doi.org/10.4252/wjsc.v11.i7.375

Liu, R., Sun, F., Armand, L. C., Wu, R., & Xu, C. (2021). Chronic Ethanol Exposure Induces Deleterious Changes in Cardiomyocytes Derived from Human Induced Pluripotent Stem Cells. *Stem Cell Reviews and Reports*, *17*(6), 2314–2331. https://doi.org/10.1007/s12015-021-10267-y

Lombó, M., Fernández-Díez, C., González-Rojo, S., Navarro, C., Robles, V., & Herráez, M. P. (2015). Transgenerational inheritance of heart disorders caused by paternal bisphenol A exposure. *Environmental Pollution*, *206*, 667–678. https://doi.org/10.1016/J.ENVPOL.2015.08.016

Lombó, M., González-Rojo, S., Fernández-Díez, C., & Herráez, M. P. (2019). Cardiogenesis impairment promoted by bisphenol A exposure is successfully counteracted by epigallocatechin gallate. *Environmental Pollution*, *246*, 1008–1019. https://doi.org/10.1016/J.ENVPOL.2019.01.004

Longmore, D. K., Barr, E. L. M., Lee, I. L., Barzi, F., Kirkwood, M., Whitbread, C., Hampton, V., Graham, S., Van Dokkum, P., Connors, C., Boyle, J. A., Catalano, P., Brown, A. D. H., O'Dea, K., Oats, J., McIntyre, H. D., Shaw, J. E., & Maple-Brown, L. J. (2019). Maternal body mass index, excess gestational weight gain, and diabetes are positively associated with neonatal adiposity in the Pregnancy and Neonatal Diabetes Outcomes in Remote Australia (PANDORA) study. *Pediatric Obesity*, *14*(4), 1–9. https://doi.org/10.1111/ijpo.12490

Loor, G., Kondapalli, J., Schriewer, J. M., Chandel, N. S., Vanden Hoek, T. L., & Schumacker, P. T. (2010). Menadione triggers cell death through ROS-dependent mechanisms involving PARP activation without requiring apoptosis. *Free Radical Biology and Medicine*, *49*(12), 1925–1936. https://doi.org/10.1016/j.freeradbiomed.2010.09.021

Lopaschuk, G. D., & Jaswal, J. S. (2010). Energy Metabolic Phenotype of the Cardiomyocyte During Development, Differentiation, and Postnatal Maturation. *Journal of Cardiovascular Pharmacology*, *56*(2), 130–140. https://doi.org/10.1097/FJC.0b013e3181e74a14

Luck, K., Kim, D. K., Lambourne, L., Spirohn, K., Begg, B. E., Bian, W., Brignall, R., Cafarelli, T., Campos-Laborie, F. J., Charloteaux, B., Choi, D., Coté, A. G., Daley, M., Deimling, S., Desbuleux, A., Dricot, A., Gebbia, M., Hardy, M. F., Kishore, N., Knapp, J. J., Kovács, I. A., Lemmens, I., Mee, M. W., Mellor, J. C., Pollis, C., Pons, C., Richardson, A. D., Schlabach, S., Teeking, B., Yadav, A., Babor, M., Balcha, D., Basha, O., Bowman-Colin, C., Chin, S.-F., Choi, S. G., Colabella, C., Coppin, G., D'Amata, C., De Ridder, D., De Rouck, S., Duran-Frigola, M., Ennajdaoui, H., Goebels, F., Goehring, L., Gopal, A., Haddad, G., Hatchi, E., Helmy, M., Jacob, Y., Kassa, Y., Landini, S., Li, R., van Lieshout, N., MacWilliams, A., Markey, D., Paulson, J. N., Rangarajan, S., Rasla, J., Rayhan, A., Rolland, T., San-Miguel, A., Shen, Y., Sheykhkarimli, D., Sheynkman, G. M., Simonovsky, E., Taşan, M., Tejeda, A., Tropepe, V., Twizere, J.-C., Wang, Y., Weatheritt, R. J., Weile, J., Xia, Y., Yang, X., Yeger-Lotem, E., Zhong, Q., Aloy, P., Bader, G. D., De Las Rivas, J., Gaudet, S., Hao, T., Rak, J., Tavernier, J., Hill, D. E., Vidal, M., Roth, F. P., Calderwood, M. A. (2020). A reference map of the human binary protein interactome. *Nature*, *580*(7803), 402–408. https://doi.org/10.1038/S41586-020-2188-X

Lurbe, E., & Ingelfinger, J. (2021). Developmental and Early Life Origins of Cardiometabolic Risk Factors: Novel Findings and Implications. In *Hypertension (Dallas, Tex. : 1979)* (Vol. 77, Issue 2, pp. 308–318). NLM (Medline). https://doi.org/10.1161/HYPERTENSIONAHA.120.14592

Ly, O. T., Brown, G. E., Han, Y. D., Darbar, D., & Khetani, S. R. (2021). Bioengineering approaches to mature induced pluripotent stem cell-derived atrial cardiomyocytes to model atrial fibrillation. *Experimental Biology and Medicine*, *246*(16), 1816–1828. https://doi.org/10.1177/15353702211009146

Ma, J., Niklewski, P. J., & Wang, H. S. (2023). Acute exposure to low-dose bisphenol A delays cardiac repolarization in female canine heart – Implication for proarrhythmic toxicity in large animals. *Food and Chemical Toxicology*, *172*, 113589. https://doi.org/10.1016/J.FCT.2022.113589

Ma, J., Wang, N. Y., Jagani, R., & Wang, H.-S. (2023). Proarrhythmic toxicity of low dose bisphenol A and its analogs in human iPSC-derived cardiomyocytes and human cardiac organoids through delay of cardiac repolarization. *Chemosphere*, *328*, 138562. https://doi.org/10.1016/j.chemosphere.2023.138562

Ma, Y., Liu, H., Wu, J., Yuan, L., Wang, Y., Du, X., Wang, R., Marwa, P. W., Petlulu, P., Chen, X., & Zhang, H. (2019). The adverse health effects of bisphenol A and related toxicity mechanisms. *Environmental Research*, *176*, 108575. https://doi.org/10.1016/J.ENVRES.2019.108575

Maddah, M., Heidmann, J. D., Mandegar, M. A., Walker, C. D., Bolouki, S., Conklin, B. R., & Loewke, K. E. (2015). A Non-invasive Platform for Functional Characterization of Stem-Cell-Derived Cardiomyocytes with Applications in Cardiotoxicity Testing. *Stem Cell Reports*, *4*(4), 621–631. https://doi.org/10.1016/J.STEMCR.2015.02.007

Magdy, T., Schuldt, A. J. T., Wu, J. C., Bernstein, D., & Burridge, P. W. (2018). Human Induced Pluripotent Stem Cell (hiPSC)-Derived Cells to Assess Drug Cardiotoxicity: Opportunities and Problems. *Annual Review of Pharmacology and Toxicology*, *58*(1), 83–103. https://doi.org/10.1146/annurev-pharmtox-010617-053110

McCurdy, C. E., Bishop, J. M., Williams, S. M., Grayson, B. E., Smith, M. S., Friedman, J. E., & Grove, K. L. (2009). Maternal high-fat diet triggers lipotoxicity in the fetal livers of nonhuman primates. *Journal of Clinical Investigation*, *119*(2), 323–335. https://doi.org/10.1172/JCI32661

McLellan, M. A., Skelly, D. A., Dona, M. S. I., Squiers, G. T., Farrugia, G. E., Gaynor, T. L., Cohen, C. D., Pandey, R., Diep, H., Vinh, A., Rosenthal, N. A., & Pinto, A. R. (2020). High-Resolution Transcriptomic Profiling of the Heart During Chronic Stress Reveals Cellular Drivers of Cardiac Fibrosis and Hypertrophy. *Circulation*, *142*(15), 1448–1463. https://doi.org/10.1161/CIRCULATIONAHA.119.045115

McMullen, S., & Mostyn, A. (2009). Animal models for the study of the developmental origins of health and disease. *Proceedings of the Nutrition Society*, *68*(3), 306–320. https://doi.org/10.1017/S0029665109001396

Melzer, D., Osborne, N. J., Henley, W. E., Cipelli, R., Young, A., Money, C., McCormack, P., Luben, R., Khaw, K. T., Wareham, N. J., & Galloway, T. S. (2012). Urinary bisphenol A concentration and risk of future coronary artery disease in apparently healthy men and women. *Circulation*, *125*(12), 1482–1490. https://doi.org/10.1161/CIRCULATIONAHA.111.069153

Melzer, D., Rice, N. E., Lewis, C., Henley, W. E., & Galloway, T. S. (2010). Association of Urinary Bisphenol A Concentration with Heart Disease: Evidence from NHANES 2003/06. *PLoS ONE*, *5*(1). https://doi.org/10.1371/JOURNAL.PONE.0008673

Menche, J., Sharma, A., Kitsak, M., Ghiassian, S. D., Vidal, M., Loscalzo, J., & Barabási, A. L. (2015). Uncovering disease-disease relationships through the incomplete human interactome. *Science (New York, N.Y.)*, *347*(6224), 1257601. https://doi.org/10.1126/SCIENCE.1257601

Mills, R. J., Titmarsh, D. M., Koenig, X., Parker, B. L., Ryall, J. G., Quaife-Ryan, G. A., Voges, H. K., Hodson, M. P., Ferguson, C., Drowley, L., Plowright, A. T., Needham, E. J., Wang, Q.-D., Gregorevic, P., Xin, M., Thomas, W. G., Parton, R. G., Nielsen, L. K., Launikonis, B. S., … Hudson, J. E. (2017). Functional screening in human cardiac organoids reveals a metabolic mechanism for cardiomyocyte cell cycle arrest. *Proceedings of the National Academy of Sciences*, *114*(40). https://doi.org/10.1073/pnas.1707316114

Moffat, J. G., Vincent, F., Lee, J. A., Eder, J., & Prunotto, M. (2017). Opportunities and challenges in phenotypic drug discovery: an industry perspective. *Nature Reviews Drug Discovery*, *16*(8), 531–543. https://doi.org/10.1038/nrd.2017.111

Moon, S., Yu, S. H., Lee, C. B., Park, Y. J., Yoo, H. J., & Kim, D. S. (2021). Effects of bisphenol A on cardiovascular disease: An epidemiological study using National Health and Nutrition Examination Survey 2003–2016 and meta-analysis. *Science of The Total Environment*, *763*, 142941. https://doi.org/10.1016/J.SCITOTENV.2020.142941

Morita, Y., & Tohyama, S. (2020). Metabolic Regulation of Cardiac Differentiation and Maturation in Pluripotent Stem Cells: A Lesson from Heart Development. *JMA Journal*, *3*(3), 193. https://doi.org/10.31662/JMAJ.2020-0036

Morrison, M., Klein, C., Clemann, N., Collier, D. A., Hardy, J., Heiβerer, B., Cader, M. Z., Graf, M., & Kaye, J. (2015). StemBANCC: Governing Access to Material and Data in a Large Stem Cell Research Consortium. *Stem Cell Reviews*, *11*(5), 681. https://doi.org/10.1007/S12015-015-9599-3

Mottram, D. S., Wedzicha, B. L., & Dodson, A. T. (2002). Acrylamide is formed in the Maillard reaction. *Nature*, *419*(6906), 448–449. https://doi.org/10.1038/419448a

Mummery, C., Ward-van Oostwaard, D., Doevendans, P., Spijker, R., van den Brink, S., Hassink, R., van der Heyden, M., Opthof, T., Pera, M., de la Riviere, A. B., Passier, R., & Tertoolen, L. (2003). Differentiation of Human Embryonic Stem Cells to Cardiomyocytes. *Circulation*, *107*(21), 2733–2740. https://doi.org/10.1161/01.CIR.0000068356.38592.68

Münch, J., & Abdelilah-Seyfried, S. (2021). Sensing and Responding of Cardiomyocytes to Changes of Tissue Stiffness in the Diseased Heart. *Frontiers in Cell and Developmental Biology*, *9*, 403. https://doi.org/10.3389/FCELL.2021.642840/BIBTEX

Murata, M., & Kang, J.-H. (2018). Bisphenol A (BPA) and cell signaling pathways. *Biotechnology Advances*, *36*(1), 311–327. https://doi.org/10.1016/j.biotechadv.2017.12.002

Murphy, S. A., Miyamoto, M., Kervadec, A., Kannan, S., Tampakakis, E., Kambhampati, S., Lin, B. L., Paek, S., Andersen, P., Lee, D.-I., Zhu, R., An, S. S., Kass, D. A., Uosaki, H., Colas, A. R., & Kwon, C. (2021). PGC1/PPAR drive cardiomyocyte maturation at single cell level via YAP1 and SF3B2. *Nature Communications*, *12*(1), 1648. https://doi.org/10.1038/s41467-021-21957-z

Mutgan, A. C., Jandl, K., & Kwapiszewska, G. (2020). Endothelial Basement Membrane Components and Their Products, Matrikines: Active Drivers of Pulmonary Hypertension? *Cells 2020, Vol. 9, Page 2029*, *9*(9), 2029. https://doi.org/10.3390/CELLS9092029

Nakano, H., Minami, I., Braas, D., Pappoe, H., Wu, X., Sagadevan, A., Vergnes, L., Fu, K., Morselli, M., Dunham, C., Ding, X., Stieg, A. Z., Gimzewski, J. K., Pellegrini, M., Clark, P. M., Reue, K., Lusis, A. J., Ribalet, B., Kurdistani, S. K., Christofk, H., Nakatsuji, N., Nakano, A. (2017). Glucose inhibits cardiac muscle maturation through nucleotide biosynthesis. *ELife*, *6*. https://doi.org/10.7554/eLife.29330

Nánási, P. P., Szabó, Z., Kistamás, K., Horváth, B., Virág, L., Jost, N., Bányász, T., Almássy, J., & Varró, A. (2020). Implication of frequency-dependent protocols in antiarrhythmic and proarrhythmic drug testing. *Progress in Biophysics and Molecular Biology*, *157*, 76–83. https://doi.org/10.1016/j.pbiomolbio.2019.11.001

Narkar, A., Willard, J. M., & Blinova, K. (2022). Chronic Cardiotoxicity Assays Using Human Induced Pluripotent Stem Cell-Derived Cardiomyocytes (hiPSC-CMs). *International Journal of Molecular Sciences 2022, Vol. 23, Page 3199*, *23*(6), 3199. https://doi.org/10.3390/IJMS23063199

Ng, K. M., Lau, Y. M., Dhandhania, V., Cai, Z. J., Lee, Y. K., Lai, W. H., Tse, H. F., & Siu, C. W. (2018). Empagliflozin Ammeliorates High Glucose Induced-Cardiac Dysfuntion in Human iPSC-Derived Cardiomyocytes. *Scientific Reports*, *8*(1), 1–13. https://doi.org/10.1038/s41598-018-33293-2

Niethammer, M., Burgdorf, T., Wistorf, E., Schönfelder, G., & Kleinsorge, M. (2022). *In vitro* models of human development and their potential application in developmental toxicity testing. *Development*, *149*(20). https://doi.org/10.1242/dev.200933

Ong, L. P., Bargehr, J., Knight-Schrijver, V. R., Lee, J., Colzani, M., Bayraktar, S., Bernard, W. G., Marchiano, S., Bertero, A., Murry, C. E., Gambardella, L., & Sinha, S. (2023). Epicardially secreted fibronectin drives cardiomyocyte maturation in 3D-engineered heart tissues. *Stem Cell Reports*, *18*(4), 936–951. https://doi.org/10.1016/j.stemcr.2023.03.002

O'Reilly, A. O., Eberhardt, E., Weidner, C., Alzheimer, C., Wallace, B. A., & Lampert, A. (2012). Bisphenol A Binds to the Local Anesthetic Receptor Site to Block the Human Cardiac Sodium Channel. *PLoS ONE*, *7*(7), e41667. https://doi.org/10.1371/journal.pone.0041667

Ottaviani, D., ter Huurne, M., Elliott, D. A., Bellin, M., & Mummery, C. L. (2023). Maturing differentiated human pluripotent stem cells *in vitro*: methods and challenges. *Development*, *150*(11). https://doi.org/10.1242/dev.201103

Paige, S. L., Plonowska, K., Xu, A., & Wu, S. M. (2015). Molecular Regulation of Cardiomyocyte Differentiation. *Circulation Research*, *116*(2), 341–353. https://doi.org/10.1161/CIRCRESAHA.116.302752

Panka, D. J., & Mier, J. W. (2003). Canstatin Inhibits Akt Activation and Induces Fas-dependent Apoptosis in Endothelial Cells. *Journal of Biological Chemistry*, *278*(39), 37632–37636. https://doi.org/10.1074/jbc.M307339200

Pant, J., Ranjan, P., & Deshpande, S. B. (2011). Bisphenol A decreases atrial contractility involving NO-dependent G-cyclase signaling pathway. *Journal of Applied Toxicology*, *31*(7), 698–702. https://doi.org/10.1002/jat.1647

Parish, S. T., Aschner, M., Casey, W., Corvaro, M., Embry, M. R., Fitzpatrick, S., Kidd, D., Kleinstreuer, N. C., Lima, B. S., Settivari, R. S., Wolf, D. C., Yamazaki, D., & Boobis, A. (2020). An evaluation framework for new approach methodologies (NAMs) for human health safety assessment. *Regulatory Toxicology and Pharmacology*, *112*, 104592. https://doi.org/10.1016/J.YRTPH.2020.104592

Patel, B. B., Raad, M., Sebag, I. A., & Chalifour, L. E. (2013). Lifelong Exposure to Bisphenol A Alters Cardiac Structure/Function, Protein Expression, and DNA Methylation in Adult Mice. *Toxicological Sciences*, *133*(1), 174–185. https://doi.org/10.1093/toxsci/kft026

Pedram, A., Razandi, M., Narayanan, R., & Levin, E. R. (2016). Estrogen receptor beta signals to inhibition of cardiac fibrosis. *Molecular and Cellular Endocrinology*, *434*, 57–68. https://doi.org/10.1016/J.MCE.2016.06.018

Pembrey, M. E., Bygren, L. O., Kaati, G., Edvinsson, S., Northstone, K., Sjöström, M., & Golding, J. (2006). Sex-specific, male-line transgenerational responses in humans. *European Journal of Human Genetics*, *14*(2), 159–166. https://doi.org/10.1038/sj.ejhg.5201538

Perez-Riverol, Y., Bai, J., Bandla, C., García-Seisdedos, D., Hewapathirana, S., Kamatchinathan, S., Kundu, D. J., Prakash, A., Frericks-Zipper, A., Eisenacher, M., Walzer, M., Wang, S., Brazma, A., & Vizcaíno, J. A. (2022). The PRIDE database resources in 2022: a hub for mass spectrometry-based proteomics evidences. *Nucleic Acids Research*, *50*(D1), D543. https://doi.org/10.1093/NAR/GKAB1038

Pfab, T., Slowinski, T., Godes, M., Halle, H., Priem;, F., & Hocher, B. (2006). Low Birth Weight, a Risk Factor for Cardiovascular Diseases in Later Life, Is Already Associated With Elevated Fetal Glycosylated Hemoglobin at Birth. *Circulation*, *114*(16), 1687–1692. https://doi.org/10.1161/CIRCULATIONAHA.106.625848

Piñero, J., Queralt-Rosinach, N., Bravo, À., Deu-Pons, J., Bauer-Mehren, A., Baron, M., Sanz, F., & Furlong, L. I. (2015). DisGeNET: a discovery platform for the dynamical exploration of human diseases and their genes. *Database : The Journal of Biological Databases and Curation*, *2015*. https://doi.org/10.1093/DATABASE/BAV028

Porrello, E. R., Mahmoud, A. I., Simpson, E., Hill, J. A., Richardson, J. A., Olson, E. N., & Sadek, H. A. (2011). Transient Regenerative Potential of the Neonatal Mouse Heart. *Science*, *331*(6020), 1078–1080. https://doi.org/10.1126/science.1200708

Posnack, N. G., Jaimes, R., Asfour, H., Swift, L. M., Wengrowski, A. M., Sarvazyan, N., & Kay, M. W. (2014). Bisphenol A exposure and cardiac electrical conduction in excised rat hearts. *Environmental Health Perspectives*, *122*(4), 384–390. https://doi.org/10.1289/ehp.1206157

Prasad, C. V., Nayak, V. L., Ramakrishna, S., & Mallavadhani, U. V. (2018). Novel menadione hybrids: Synthesis, anticancer activity, and cell-based studies. *Chemical Biology & Drug Design*, *91*(1), 220–233. https://doi.org/10.1111/cbdd.13073

Prudencio, T. M., Swift, L. M., Guerrelli, D., Cooper, B., Reilly, M., Ciccarelli, N., Sheng, J., Jaimes, R., & Posnack, N. G. (2021). Bisphenol S and Bisphenol F Are Less Disruptive to Cardiac Electrophysiology, as Compared With Bisphenol A. *Toxicological Sciences*, *183*(1), 214. https://doi.org/10.1093/TOXSCI/KFAB083

Raisi-Estabragh, Z., Cooper, J., Bethell, M. S., McCracken, C., Lewandowski, A. J., Leeson, P., Neubauer, S., Harvey, N. C., & Petersen, S. E. (2022). Lower birth weight is linked to poorer cardiovascular health in middle-aged population-based adults. *Heart*, heartjnl-2022-321733. https://doi.org/10.1136/heartjnl-2022-321733

Raja, G. L., Lite, C., Subhashree, K. D., Santosh, W., & Barathi, S. (2020). Prenatal bisphenol-A exposure altered exploratory and anxiety-like behaviour and induced non-monotonic, sex-specific changes in the cortical expression of CYP19A1, BDNF and intracellular signaling proteins in F1 rats. *Food and Chemical Toxicology*, *142*, 111442. https://doi.org/10.1016/J.FCT.2020.111442

Rajabzadeh, N., Fathi, E., & Farahzadi, R. (2019). Stem cell-based regenerative medicine. *Stem Cell Investigation*, *6*(July). https://doi.org/10.21037/sci.2019.06.04

Ramadan, M., Cooper, B., & Posnack, N. G. (2020). Bisphenols and phthalates: Plastic chemical exposures can contribute to adverse cardiovascular health outcomes. *Birth Defects Research*, *112*(17), 1362–1385. https://doi.org/10.1002/BDR2.1752

Ramadan, M., Sherman, M., Jaimes, R., Chaluvadi, A., Swift, L., & Posnack, N. G. (2018). Disruption of neonatal cardiomyocyte physiology following exposure to bisphenol-a. *Scientific Reports 2018 8:1*, *8*(1), 1–11. https://doi.org/10.1038/s41598-018-25719-8

Ramos, C., Ladeira, C., Zeferino, S., Dias, A., Faria, I., Cristovam, E., Gomes, M., & Ribeiro, E. (2019). Cytotoxic and genotoxic effects of environmental relevant concentrations of bisphenol A and interactions with doxorubicin. *Mutation Research/Genetic Toxicology and Environmental Mutagenesis*, *838*, 28–36. https://doi.org/10.1016/j.mrgentox.2018.11.009

Rampoldi, A., Singh, M., Wu, Q., Duan, M., Jha, R., Maxwell, J. T., Bradner, J. M., Zhang, X., Saraf, A., Miller, G. W., Gibson, G., Brown, L. A., & Xu, C. (2019). Cardiac toxicity from ethanol exposure in human-induced pluripotent stem cell-derived cardiomyocytes. *Toxicological Sciences*, *169*(1), 280–292. https://doi.org/10.1093/toxsci/kfz038

Rasdi, Z., Kamaludin, R., Ab. Rahim, S., Syed Ahmad Fuad, S. B., Othman, M. H. D., Siran, R., Mohd Nor, N. S., Abdul Hamid Hasani, N., & Sheikh Abdul Kadir, S. H. (2020). The impacts of intrauterine Bisphenol A exposure on pregnancy and expression of miRNAs related to heart development and diseases in animal model. *Scientific Reports 2020 10:1*, *10*(1), 1–13. https://doi.org/10.1038/s41598-020-62420-1

Ravelli, A. C. J., Van Der Meulen, J. H. P., Michels, R. P. J., Osmond, C., Barker, D. J. P., Hales, C. N., & Bleker, O. P. (1998). Glucose tolerance in adults after prenatal exposure to famine. *Lancet*, *351*(9097), 173–177. https://doi.org/10.1016/S0140-6736(97)07244-9

Ribeiro, M. C., Slaats, R. H., Schwach, V., Rivera-Arbelaez, J. M., Tertoolen, L. G. J., van Meer, B. J., Molenaar, R., Mummery, C. L., Claessens, M. M. A. E., & Passier, R. (2020). A cardiomyocyte show of force: A fluorescent alpha-actinin reporter line sheds light on human cardiomyocyte contractility

versus substrate stiffness. *Journal of Molecular and Cellular Cardiology*, *141*, 54–64. https://doi.org/10.1016/j.yjmcc.2020.03.008

Rodosthenous, R. S., Baccarelli, A. A., Mansour, A., Adir, M., Israel, A., Racowsky, C., Hauser, R., Bollati, V., & Machtinger, R. (2019). Supraphysiological Concentrations of Bisphenol A Alter the Expression of Extracellular Vesicle-Enriched miRNAs From Human Primary Granulosa Cells. *Toxicological Sciences*, *169*(1), 5–13. https://doi.org/10.1093/toxsci/kfz020

Rodríguez-Rodríguez, P., Ramiro-Cortijo, D., Reyes-Hernández, C. G., López de Pablo, A. L., Carmen González, M., & Arribas, S. M. (2018). Implication of oxidative stress in fetal programming of cardiovascular disease. *Frontiers in Physiology*, *9*(MAY), 1–13. https://doi.org/10.3389/fphys.2018.00602

Roseboom, T., de Rooij, S., & Painter, R. (2006). The Dutch famine and its long-term consequences for adult health. *Early Human Development*, *82*(8), 485–491. https://doi.org/10.1016/j.earlhumdev.2006.07.001

Roseboom, T. J. (2019). Epidemiological evidence for the developmental origins of health and disease: Effects of prenatal undernutrition in humans. *Journal of Endocrinology*, *242*(1), T135–T144. https://doi.org/10.1530/JOE-18-0683

Ross Brown, A., Green, J. M., Moreman, J., Gunnarsson, L. M., Mourabit, S., Ball, J., Winter, M. J., Trznadel, M., Correia, A., Hacker, C., Perry, A., Wood, M. E., Hetheridge, M. J., Currie, R. A., & Tyler, C. R. (2019). Cardiovascular Effects and Molecular Mechanisms of Bisphenol A and Its Metabolite MBP in Zebrafish. *Environmental Science and Technology*, *53*(1), 463–474. https://doi.org/10.1021/ACS.EST.8B04281/SUPPL_FILE/ES8B04281_SI_002.XLSX

Saleem, U., van Meer, B. J., Katili, P. A., Mohd Yusof, N. A. N., Mannhardt, I., Garcia, A. K., Tertoolen, L., de Korte, T., Vlaming, M. L. H., McGlynn, K., Nebel, J., Bahinski, A., Harris, K., Rossman, E., Xu, X., Burton, F. L., Smith, G. L., Clements, P., Mummery, C. L., … Denning, C. (2020). Blinded, Multicenter Evaluation of Drug-induced Changes in Contractility Using Human-induced Pluripotent Stem Cell-derived Cardiomyocytes. *Toxicological Sciences*, *176*(1), 103–123. https://doi.org/10.1093/toxsci/kfaa058

Satin, J., Kehat, I., Caspi, O., Huber, I., Arbel, G., Itzhaki, I., Magyar, J., Schroder, E. A., Perlman, I., & Gepstein, L. (2004). Mechanism of spontaneous excitability in human embryonic stem cell derived cardiomyocytes. *The Journal of Physiology*, *559*(Pt 2), 479. https://doi.org/10.1113/JPHYSIOL.2004.068213

Savoji, H., Mohammadi, M. H., Rafatian, N., Toroghi, M. K., Wang, E. Y., Zhao, Y., Korolj, A., Ahadian, S., & Radisic, M. (2019). Cardiovascular disease models: A game changing paradigm in drug discovery and screening. *Biomaterials*, *198*(May 2018), 3–26. https://doi.org/10.1016/j.biomaterials.2018.09.036

Schneider, C. A., Rasband, W. S., & Eliceiri, K. W. (2012). NIH Image to ImageJ: 25 years of image analysis. *Nature Methods*, *9*(7), 671–675. https://doi.org/10.1038/nmeth.2089

Schönfelder, G., Wittfoht, W., Hopp, H., Talsness, C. E., Paul, M., & Chahoud, I. (2002). Parent bisphenol A accumulation in the human maternal-fetal-placental unit. *Environmental Health Perspectives*, *110*(11). https://doi.org/10.1289/ehp.110-1241091

Sekiguchi, R., & Yamada, K. M. (2018). Basement membranes in development and disease. *Current Topics in Developmental Biology*, *130*, 143. https://doi.org/10.1016/BS.CTDB.2018.02.005

Shankar, A., & Teppala, S. (2012). Urinary Bisphenol A and Hypertension in a Multiethnic Sample of US Adults. *Journal of Environmental and Public Health*, *2012*, 1–5. https://doi.org/10.1155/2012/481641

Shankar, A., Teppala, S., & Sabanayagam, C. (2012). Bisphenol A and Peripheral Arterial Disease: Results from the NHANES. *Environmental Health Perspectives*, *120*(9), 1297–1300. https://doi.org/10.1289/ehp.1104114

Sharma, A., Sances, S., Workman, M. J., & Svendsen, C. N. (2020). Multi-lineage Human iPSC-Derived Platforms for Disease Modeling and Drug Discovery. *Cell Stem Cell*, *26*(3), 309–329. https://doi.org/10.1016/j.stem.2020.02.011

Sheng, Z.-G., Tang, Y., Liu, Y.-X., Yuan, Y., Zhao, B.-Q., Chao, X.-J., & Zhu, B.-Z. (2012). Low concentrations of bisphenol a suppress thyroid hormone receptor transcription through a nongenomic mechanism. *Toxicology and Applied Pharmacology*, *259*(1), 133–142. https://doi.org/10.1016/j.taap.2011.12.018

Shimoji, K., Yuasa, S., Onizuka, T., Hattori, F., Tanaka, T., Hara, M., Ohno, Y., Chen, H., Egasgira, T., Seki, T., Yae, K., Koshimizu, U., Ogawa, S., & Fukuda, K. (2010). G-CSF Promotes the Proliferation of Developing Cardiomyocytes In Vivo and in Derivation from ESCs and iPSCs. *Cell Stem Cell*, *6*(3), 227–237. https://doi.org/10.1016/j.stem.2010.01.002

Silva, A. C., Pereira, C., Fonseca, A. C. R. G., Pinto-do-Ó, P., & Nascimento, D. S. (2021). Bearing My Heart: The Role of Extracellular Matrix on Cardiac Development, Homeostasis, and Injury Response. *Frontiers in Cell and Developmental Biology*, *8*, 1705. https://doi.org/10.3389/FCELL.2020.621644/BIBTEX

Simpson, L. J., Reader, J. S., & Tzima, E. (2020). Mechanical Regulation of Protein Translation in the Cardiovascular System. *Frontiers in Cell and Developmental Biology*, *8*, 34. https://doi.org/10.3389/FCELL.2020.00034/BIBTEX

Sirenko, O., Grimm, F. A., Ryan, K. R., Iwata, Y., Chiu, W. A., Parham, F., Wignall, J. A., Anson, B., Cromwell, E. F., Behl, M., Rusyn, I., & Tice, R. R. (2017). In vitro cardiotoxicity assessment of environmental chemicals using an organotypic human induced pluripotent stem cell-derived model. *Toxicology and Applied Pharmacology*, *322*, 60–74. https://doi.org/10.1016/j.taap.2017.02.020

Smith, C. E. R., Pinali, C., Eisner, D. A., Trafford, A. W., & Dibb, K. M. (2022). Enhanced calcium release at specialised surface sites compensates for reduced t-tubule density in neonatal sheep atrial myocytes. *Journal of Molecular and Cellular Cardiology*, *173*, 61–70. https://doi.org/10.1016/j.yjmcc.2022.08.360

Snir, M., Kehat, I., Gepstein, A., Coleman, R., Itskovitz-Eldor, J., Livne, E., & Gepstein, L. (2003). Assessment of the ultrastructural and proliferative properties of human embryonic stem cell-derived cardiomyocytes. *American Journal of Physiology-Heart and Circulatory Physiology*, *285*(6), H2355–H2363. https://doi.org/10.1152/ajpheart.00020.2003

Sol, C. M., Santos, S., Asimakopoulos, A. G., Martinez-Moral, M.-P., Duijts, L., Kannan, K., Trasande, L., & Jaddoe, V. W. V. (2020). Associations of maternal phthalate and bisphenol urine concentrations during pregnancy with childhood blood pressure in a population-based prospective cohort study. *Environment International*, *138*, 105677. https://doi.org/10.1016/j.envint.2020.105677

Sonavane, M., & Gassman, N. R. (2019). Bisphenol A co-exposure effects: A key factor in understanding BPA's complex mechanism and health outcomes. *Critical Reviews in Toxicology*, *49*(5), 371. https://doi.org/10.1080/10408444.2019.1621263

Stucki, A. O., Barton-Maclaren, T. S., Bhuller, Y., Henriquez, J. E., Henry, T. R., Hirn, C., Miller-Holt, J., Nagy, E. G., Perron, M. M., Ratzlaff, D. E., Stedeford, T. J., & Clippinger, A. J. (2022). Use of new approach methodologies (NAMs) to meet regulatory requirements for the assessment of industrial chemicals and pesticides for effects on human health. *Frontiers in Toxicology*, *4*, 98. https://doi.org/10.3389/FTOX.2022.964553

Sugamura, K., & Keaney, J. F. (2011). Reactive Oxygen Species in Cardiovascular Disease. *Free Radical Biology & Medicine*, *51*(5), 978. https://doi.org/10.1016/J.FREERADBIOMED.2011.05.004

Sun, C., Burgner, D. P., Ponsonby, A. L., Saffery, R., Huang, R. C., Vuillermin, P. J., Cheung, M., & Craig, J. M. (2013). Effects of early-life environment and epigenetics on cardiovascular disease risk in children: Highlighting the role of twin studies. In *Pediatric Research* (Vol. 73, Issues 4–2, pp. 523–530). Nature Publishing Group. https://doi.org/10.1038/pr.2013.6

Symonds, M. E., Stephenson, T., Gardner, D. S., & Budge, H. (2007). Long-term effects of nutritional programming of the embryo and fetus: Mechanisms and critical windows. *Reproduction, Fertility and Development*, *19*(1), 53–63. https://doi.org/10.1071/RD06130

Takahashi, K., Tanabe, K., Ohnuki, M., Narita, M., Ichisaka, T., Tomoda, K., & Yamanaka, S. (2007). Induction of Pluripotent Stem Cells from Adult Human Fibroblasts by Defined Factors. *Cell*, *131*(5), 861–872. https://doi.org/10.1016/j.cell.2007.11.019

Tan, M. E., Li, J., Xu, H. E., Melcher, K., & Yong, E. (2015). Androgen receptor: structure, role in prostate cancer and drug discovery. *Acta Pharmacologica Sinica*, *36*(1), 3–23. https://doi.org/10.1038/aps.2014.18

Tanabe, N., Kimoto, T., & Kawato, S. (2006). Rapid Ca(2+) signaling induced by Bisphenol A in cultured rat hippocampal neurons. *Neuro Endocrinology Letters*, *27*(1–2), 97–104.

Tanwar, V., Bylund, J. B., Hu, J., Yan, J., Walthall, J. M., Mukherjee, A., Heaton, W. H., Wang, W.-D., Potet, F., Rai, M., Kupershmidt, S., Knapik, E. W., & Hatzopoulos, A. K. (2014). Gremlin 2 Promotes Differentiation of Embryonic Stem Cells to Atrial Fate by Activation of the JNK Signaling Pathway. *STEM CELLS*, *32*(7), 1774–1788. https://doi.org/10.1002/STEM.1703

Thomson, J. A. (1998). Embryonic stem cell lines derived from human blastocysts. *Science*, *282*(5391), 1145–1147. https://doi.org/10.1126/science.282.5391.1145

Tian, D. Z., Wei, W., & Dong, Y. J. (2016). Influence of COL1A2 gene variants on the incidence of hypertensive intracerebral hemorrhage in a Chinese population. *Genetics and Molecular Research*, *15*(1). https://doi.org/10.4238/GMR.15017369

Tiburcy, M., Hudson, J. E., Balfanz, P., Schlick, S., Meyer, T., Chang Liao, M.-L., Levent, E., Raad, F., Zeidler, S., Wingender, E., Riegler, J., Wang, M., Gold, J. D., Kehat, I., Wettwer, E., Ravens, U., Dierickx, P., van Laake, L. W., Goumans, M. J., … Zimmermann, W.-H. (2017). Defined Engineered Human Myocardium With Advanced Maturation for Applications in Heart Failure Modeling and Repair. *Circulation*, *135*(19), 1832–1847. https://doi.org/10.1161/CIRCULATIONAHA.116.024145

Tobi, E. W., Goeman, J. J., Monajemi, R., Gu, H., Putter, H., Zhang, Y., Slieker, R. C., Stok, A. P., Thijssen, P. E., Müller, F., Van Zwet, E. W., Bock, C., Meissner, A., Lumey, L. H., Eline Slagboom, P., & Heijmans, B. T. (2014). DNA methylation signatures link prenatal famine exposure to growth and metabolism. *Nature Communications*, *5*. https://doi.org/10.1038/ncomms6592

Torrens, C., Snelling, T. H., Chau, R., Shanmuganathan, M., Cleal, J. K., Poore, K. R., Noakes, D. E., Poston, L., Hanson, M. A., & Green, L. R. (2009). Effects of pre- and periconceptional undernutrition on arterial function in adult female sheep are vascular bed dependent. *Experimental Physiology*, *94*(9), 1024–1033. https://doi.org/10.1113/expphysiol.2009.047340

Truskey, G. A. (2018). Human Microphysiological Systems and Organoids as in Vitro Models for Toxicological Studies. *Frontiers in Public Health*, *6*. https://doi.org/10.3389/fpubh.2018.00185

Tyanova, S., Temu, T., & Cox, J. (2016). The MaxQuant computational platform for mass spectrometry-based shotgun proteomics. *Nature Protocols 2016 11:12*, *11*(12), 2301–2319. https://doi.org/10.1038/nprot.2016.136

Ulmer, B. M., & Eschenhagen, T. (2020). Human pluripotent stem cell-derived cardiomyocytes for studying energy metabolism. *Biochimica et Biophysica Acta. Molecular Cell Research*, *1867*(3). https://doi.org/10.1016/J.BBAMCR.2019.04.001

University of Hertfordshire, 2021. (2021). Implementation of the evidence-based risk assessment for the re-evaluation of Bisphenol A: preparatory work on Mode of Action studies in mammalian, human and/or in vitro models. *EFSA Supporting Publications*, *18*(12). https://doi.org/10.2903/sp.efsa.2021.EN-6995

Untergasser, A., Cutcutache, I., Koressaar, T., Ye, J., Faircloth, B. C., Remm, M., & Rozen, S. G. (2012). Primer3—new capabilities and interfaces. *Nucleic Acids Research*, *40*(15), e115–e115. https://doi.org/10.1093/NAR/GKS596

Vandenberg, L. N., Hauser, R., Marcus, M., Olea, N., & Welshons, W. V. (2007). Human exposure to bisphenol A (BPA). *Reproductive Toxicology*, *24*(2), 139–177. https://doi.org/10.1016/j.reprotox.2007.07.010

Vandenberg, L. N., Hunt, P. A., & Gore, A. C. (2019). Endocrine disruptors and the future of toxicology testing — lessons from CLARITY–BPA. *Nature Reviews Endocrinology 2019 15:6*, *15*(6), 366–374. https://doi.org/10.1038/s41574-019-0173-y

Veerman, C. C., Mengarelli, I., Lodder, E. M., Kosmidis, G., Bellin, M., Zhang, M., Dittmann, S., Guan, K., Wilde, A. A. M., Schulze-Bahr, E., Greber, B., Bezzina, C. R., & Verkerk, A. O. (2017). Switch From Fetal to Adult *SCN5A* Isoform in Human Induced Pluripotent Stem Cell–Derived Cardiomyocytes Unmasks the Cellular Phenotype of a Conduction Disease–Causing Mutation. *Journal of the American Heart Association*, *6*(7). https://doi.org/10.1161/JAHA.116.005135

Velazquez, M. A., Fleming, T. P., & Watkins, A. J. (2019). Periconceptional environment and the developmental origins of disease. *Journal of Endocrinology*, *242*(1), T33–T49. https://doi.org/10.1530/JOE-18-0676

Verma, R. K., Gunda, V., Pawar, S. C., & Sudhakar, Y. A. (2013). Extra Cellular Matrix Derived Metabolite Regulates Angiogenesis by FasL Mediated Apoptosis. *PLoS ONE*, *8*(12), e80555. https://doi.org/10.1371/journal.pone.0080555

Villar-Pazos, S., Martinez-Pinna, J., Castellano-Muñoz, M., Alonso-Magdalena, P., Marroqui, L., Quesada, I., Gustafsson, J.-A., & Nadal, A. (2017). Molecular mechanisms involved in the non-monotonic effect of bisphenol-a on Ca2+ entry in mouse pancreatic β-cells. *Scientific Reports*, *7*(1), 11770. https://doi.org/10.1038/s41598-017-11995-3

Vinnars, M.-T., Bixo, M., & Damdimopoulou, P. (2023). Pregnancy-related maternal physiological adaptations and fetal chemical exposure. *Molecular and Cellular Endocrinology*, *578*, 112064. https://doi.org/10.1016/j.mce.2023.112064

Vom Saal, F. S., & Vandenberg, L. N. (2021). Update on the Health Effects of Bisphenol A: Overwhelming Evidence of Harm. *Endocrinology*, *162*(3). https://doi.org/10.1210/ENDOCR/BQAA171

Vuguin, P. M. (2007). Animal Models for Small for Gestational Age and Fetal Programing of Adult Disease. *Hormone Research in Paediatrics*, *68*(3), 113–123. https://doi.org/10.1159/000100545

Wang, H., Zhao, P., Huang, Q., Chi, Y., Dong, S., & Fan, J. (2019). Bisphenol-A induces neurodegeneration through disturbance of intracellular calcium homeostasis in human embryonic stem cells-derived cortical neurons. *Chemosphere*, *229*, 618–630. https://doi.org/10.1016/j.chemosphere.2019.04.099

Wang, P. X., Wang, J. J., Lei, Y. X., Xiao, L., & Luo, Z. C. (2012). Impact of Fetal and Infant Exposure to the Chinese Great Famine on the Risk of Hypertension in Adulthood. *PLoS ONE*, *7*(11), 1–8. https://doi.org/10.1371/journal.pone.0049720

Wang, Z., Walker, G. W., Muir, D. C. G., & Nagatani-Yoshida, K. (2020). Toward a Global Understanding of Chemical Pollution: A First Comprehensive Analysis of National and Regional Chemical Inventories. *Environmental Science & Technology*, *54*(5), 2575–2584. https://doi.org/10.1021/acs.est.9b06379

Watkins, A. J., Rubini, E., Hosier, E. D., & Morgan, H. L. (2020). Paternal programming of offspring health. *Early Human Development*, *150*, 105185. https://doi.org/10.1016/j.earlhumdev.2020.105185

Watkins, A. J., & Sinclair, K. D. (2014). Paternal low protein diet affects adult offspring cardiovascular and metabolic function in mice. *Https://Doi.Org/10.1152/Ajpheart.00981.2013*, *306*(10), 1444–1452. https://doi.org/10.1152/AJPHEART.00981.2013

Watkins, A. J., Wilkins, A., Cunningham, C., Perry, V. H., Seet, M. J., Osmond, C., Eckert, J. J., Torrens, C., Cagampang, F. R. A., Cleal, J., Gray, W. P., Hanson, M. A., & Fleming, T. P. (2008). Low protein diet fed exclusively during mouse oocyte maturation leads to behavioural and cardiovascular abnormalities in offspring. *Journal of Physiology*, *586*(8), 2231–2244. https://doi.org/10.1113/jphysiol.2007.149229

WATSON, C., BULAYEVA, N., WOZNIAK, A., & FINNERTY, C. (2005). Signaling from the membrane via membrane estrogen receptor-α: Estrogens, xenoestrogens, and phytoestrogens. *Steroids*, *70*(5–7), 364–371. https://doi.org/10.1016/j.steroids.2005.03.002

Welch, C., & Mulligan, K. (2022). Does Bisphenol A Confer Risk of Neurodevelopmental Disorders? What We Have Learned from Developmental Neurotoxicity Studies in Animal Models. *International Journal of Molecular Sciences*, *23*(5), 2894. https://doi.org/10.3390/ijms23052894

Weng, Z., Kong, C. W., Ren, L., Karakikes, I., Geng, L., He, J., Chow, M. Z. Y., Mok, C. F., Harvey, C., Sarah, W., Keung, W., Chow, H., Andrew, M., Leung, A. Y. H., Hajjar, R. J., Li, R. A., & Chan, C. W. (2014). A simple, cost-effective but highly efficient system for deriving ventricular cardiomyocytes from human pluripotent stem cells. *Stem Cells and Development*, *23*(14), 1704–1716. https://doi.org/10.1089/SCD.2013.0509

WHO. (2022). Non-communicable diseases Progress Monitor 2022. *WHO*, *Oct*, 233. https://www.who.int/publications/i/item/9789240047761

Williams, A. J., Grulke, C. M., Edwards, J., McEachran, A. D., Mansouri, K., Baker, N. C., Patlewicz, G., Shah, I., Wambaugh, J. F., Judson, R. S., & Richard, A. M. (2017). The CompTox Chemistry Dashboard: a community data resource for environmental chemistry. *Journal of Cheminformatics*, *9*(1), 61. https://doi.org/10.1186/s13321-017-0247-6

Williams, L., Seki, Y., Vuguin, P. M., & Charron, M. J. (2014). Animal models of in utero exposure to a high fat diet: A review. *Biochimica et Biophysica Acta - Molecular Basis of Disease*, *1842*(3), 507–519. https://doi.org/10.1016/j.bbadis.2013.07.006

World Health Organization. (2011). Chapter 1: Burden : mortality , morbidity and risk factors. *Global Status Report on Non-Communicable Diseases 2010*, 9–31. https://doi.org/ISBN 978 92 4 068645 8

Wu, J., & Izpisua Belmonte, J. C. (2016). Stem Cells: A Renaissance in Human Biology Research. *Cell*, *165*(7), 1572–1585. https://doi.org/10.1016/j.cell.2016.05.043

Wu, J., Subbaiah, K. C. V., Xie, L. H., Jiang, F., Khor, E. S., Mickelsen, D., Myers, J. R., Tang, W. H. W., & Yao, P. (2020). Glutamyl-Prolyl-tRNA Synthetase Regulates Proline-Rich Pro-Fibrotic Protein Synthesis During Cardiac Fibrosis. *Circulation Research*, *127*(6), 827. https://doi.org/10.1161/CIRCRESAHA.119.315999

Xie, J., Wettschurack, K., & Yuan, C. (2020). Review: In vitro Cell Platform for Understanding Developmental Toxicity. *Frontiers in Genetics*, *11*. https://doi.org/10.3389/fgene.2020.623117

Xiong, Q., Liu, X., Shen, Y., Yu, P., Chen, S., Hu, J., Yu, J., Li, J., Wang, H.-S., Cheng, X., & Hong, K. (2015). Elevated Serum Bisphenol A Level in Patients with Dilated Cardiomyopathy. *International Journal of Environmental Research and Public Health*, *12*(5), 5329–5337. https://doi.org/10.3390/ijerph120505329

Xu, M., Che, L., Yang, Z., Zhang, P., Shi, J., Li, J., Lin, Y., Fang, Z., Che, L., Feng, B., Wu, D., & Xu, S. (2016). Effect of high fat dietary intake during maternal gestation on offspring ovarian health in a pig model. *Nutrients*, *8*(8). https://doi.org/10.3390/nu8080498

Xu, S., Xie, F., Tian, L., Fallah, S., Babaei, F., Manno, S. H. C., Manno, F. A. M., Zhu, L., Wong, K. F., Liang, Y., Ramalingam, R., Sun, L., Wang, X., Plumb, R., Gethings, L., Lam, Y. W., & Cheng, S. H. (2020). Estrogen accelerates heart regeneration by promoting the inflammatory response in zebrafish. *Journal of Endocrinology*, *245*(1), 39–51. https://doi.org/10.1530/JOE-19-0413

Xu, X., Liu, X., Zhang, Q., Zhang, G., Lu, Y., Ruan, Q., Dong, F., & Yang, Y. (2013). Sex-specific effects of bisphenol-A on memory and synaptic structural modification in hippocampus of adult mice. *Hormones and Behavior*, *63*(5), 766–775. https://doi.org/10.1016/J.YHBEH.2013.03.004

Yajnik, C., Ganpule-Rao, A., Limaye, T., & Rajgara, F. (2016). Developmental origins of non-communicable diseases. *Proceedings of the Indian National Science Academy*, *82*(5), 1465–1475. https://doi.org/10.16943/ptinsa/2016/48880

Yamada, H., Furuta, I., Kato, E. H., Kataoka, S., Usuki, Y., Kobashi, G., Sata, F., Kishi, R., & Fujimoto, S. (2002). Maternal serum and amniotic fluid bisphenol A concentrations in the early second trimester. *Reproductive Toxicology*, *16*(6), 735–739. https://doi.org/10.1016/S0890-6238(02)00051-5

Yan, S., Chen, Y., Dong, M., Song, W., Belcher, S. M., & Wang, H. S. (2011). Bisphenol A and 17β-Estradiol Promote Arrhythmia in the Female Heart via Alteration of Calcium Handling. *PLoS ONE*, *6*(9). https://doi.org/10.1371/JOURNAL.PONE.0025455

Yan, S., Song, W., Chen, Y., Hong, K., Rubinstein, J., & Wang, H.-S. (2013). Low-dose bisphenol A and estrogen increase ventricular arrhythmias following ischemia–reperfusion in female rat hearts. *Food and Chemical Toxicology*, *56*, 75–80. https://doi.org/10.1016/j.fct.2013.02.011

Yan, Y., Tang, R., Li, B., Cheng, L., Ye, S., Yang, T., Han, Y. C., Liu, C., Dong, Y., Qu, L. H., Lui, K. O., Yang, J. H., & Huang, Z. P. (2021). The cardiac translational landscape reveals that micropeptides are new players involved in cardiomyocyte hypertrophy. *Molecular Therapy*, *29*(7), 2253–2267. https://doi.org/10.1016/J.YMTHE.2021.03.004

Yang, L., Dong, L., Zhang, L., Bai, J., Chen, F., & Luo, Y. (2021). Acrylamide Induces Abnormal mtDNA Expression by Causing Mitochondrial ROS Accumulation, Biogenesis, and Dynamics Disorders. *Journal of Agricultural and Food Chemistry*, *69*(27), 7765–7776. https://doi.org/10.1021/acs.jafc.1c02569

Ye, Y., Tang, Y., Xiong, Y., Feng, L., & Li, X. (2019). Bisphenol A exposure alters placentation and causes preeclampsia-like features in pregnant mice involved in reprogramming of DNA methylation of *WNT2*. *The FASEB Journal*, *33*(2), 2732–2742. https://doi.org/10.1096/fj.201800934RRR

Yechikov, S., Kao, H. K. J., Chang, C. W., Pretto, D., Zhang, X. D., Sun, Y. H., Smithers, R., Sirish, P., Nolta, J. A., Chan, J. W., Chiamvimonvat, N., & Lieu, D. K. (2020). NODAL inhibition promotes differentiation of pacemaker-like cardiomyocytes from human induced pluripotent stem cells. *Stem Cell Research*, *49*, 102043. https://doi.org/10.1016/J.SCR.2020.102043

Yujiao, C., Meng, Z., Shanshan, L., Wei, W., Yipeng, W., & Chenghong, Y. (2023). Exposure to Bisphenol A induces abnormal fetal heart development by promoting ferroptosis. *Ecotoxicology and Environmental Safety*, *255*, 114753. https://doi.org/10.1016/J.ECOENV.2023.114753

Zhang, H., Pei, L., Ouyang, Z., Wang, H., Chen, X., Jiang, K., Huang, S., Jiang, R., Xiang, Y., & Wei, K. (2023). AP-1 activation mediates post-natal cardiomyocyte maturation. *Cardiovascular Research*, *119*(2), 536–550. https://doi.org/10.1093/cvr/cvac088

Zhang, Q., Jiang, J., Han, P., Yuan, Q., Zhang, J., Zhang, X., Xu, Y., Cao, H., Meng, Q., Chen, L., Tian, T., Wang, X., Li, P., Hescheler, J., Ji, G., & Ma, Y. (2011). Direct differentiation of atrial and ventricular myocytes from human embryonic stem cells by alternating retinoid signals. *Cell Research*, *21*(4), 579. https://doi.org/10.1038/CR.2010.163

Zhao, L., & Zhang, B. (2017). Doxorubicin induces cardiotoxicity through upregulation of death receptors mediated apoptosis in cardiomyocytes. *Scientific Reports*, *7*(1), 44735. https://doi.org/10.1038/srep44735

Zhao, M., Tang, Y., Zhou, Y., & Zhang, J. (2019). Deciphering Role of Wnt Signalling in Cardiac Mesoderm and Cardiomyocyte Differentiation from Human iPSCs: Four-dimensional control of Wnt pathway for hiPSC-CMs differentiation. *Scientific Reports 2019 9:1*, *9*(1), 1–15. https://doi.org/10.1038/s41598-019-55620-x

Zheng, Z., Chen, Y., Wang, Y., Li, Y., & Cheng, Q. (2021). MicroRNA-513b-5p targets COL1A1 and COL1A2 associated with the formation and rupture of intracranial aneurysm. *Scientific Reports 2021 11:1*, *11*(1), 1–17. https://doi.org/10.1038/s41598-021-94116-5

Zhou, R., Cheng, W., Feng, Y., Wang, W., Liang, F., Luo, F., Yang, S., & Wang, Y. (2020). Combined effects of BPA and PFOS on fetal cardiac development: In vitro and in vivo experiments. *Environmental Toxicology and Pharmacology*, *80*, 103434. https://doi.org/10.1016/J.ETAP.2020.103434

Zhou, R., Cheng, W., Feng, Y., Wei, H., Liang, F., & Wang, Y. (2017). Interactions between three typical endocrine-disrupting chemicals (EDCs) in binary mixtures exposure on myocardial differentiation of mouse embryonic stem cell. *Chemosphere*, *178*, 378–383. https://doi.org/10.1016/j.chemosphere.2017.03.040

Zhou, R., Xia, M., Zhang, L., Cheng, W., Yan, J., Sun, Y., Wang, Y., & Jiang, H. (2021). Individual and combined effects of BPA, BPS and BPAF on the cardiomyocyte differentiation of embryonic stem cells. *Ecotoxicology and Environmental Safety*, *220*, 112366. https://doi.org/10.1016/j.ecoenv.2021.112366

Zhu, W.-Z., Xie, Y., Moyes, K. W., Gold, J. D., Askari, B., & Laflamme, M. A. (2010). Neuregulin/ErbB Signaling Regulates Cardiac Subtype Specification in Differentiating Human Embryonic Stem Cells. *Circulation Research*, *107*(6), 776–786. https://doi.org/10.1161/CIRCRESAHA.110.223917

Zhu, Z., & Huangfu, D. (2013). Human pluripotent stem cells: An emerging model in developmental biology. *Development (Cambridge)*, *140*(4), 705–717. https://doi.org/10.1242/dev.086165

Zink, D., Chuah, J. K. C., & Ying, J. Y. (2020). Assessing Toxicity with Human Cell-Based In Vitro Methods. *Trends in Molecular Medicine*, *26*(6), 570–582. https://doi.org/10.1016/J.MOLMED.2020.01.008

Zou, Z., Harris, L. K., Forbes, K., & Heazell, A. E. P. (2022). Sex-specific effects of bisphenol A on the signaling pathway of ESRRG in the human placenta. *Biology of Reproduction*, *106*(6), 1278–1291. https://doi.org/10.1093/BIOLRE/IOAC044

Zuccarello, D., Sorrentino, U., Brasson, V., Marin, L., Piccolo, C., Capalbo, A., Andrisani, A., & Cassina, M. (2022). Epigenetics of pregnancy: looking beyond the DNA code. *Journal of Assisted Reproduction and Genetics*, *39*(4), 801–816. https://doi.org/10.1007/s10815-022-02451-x

9 PUBLICATIONS LIST

International paper publications:

- **Lamberto, F**., Peral-Sanchez, I., Muenthaisong, S., Zana, M., Willaime-Morawek, S., Dinnyés, A. (2021). *Environmental Alterations during Embryonic Development: Studying the Impact of Stressors on Pluripotent Stem Cell-Derived Cardiomyocytes*. Genes, 12, 1564. doi:10.3390/genes12101564.
- Mitrečić, D., Hribljan, V., Jagečić, D., Isaković, J., **Lamberto, F.,** Horánszky, A., Zana, M., Foldes, G., Zavan, B., Pivoriūnas, A., Martinez, S., Mazzini, L., Radenovic, L., Milasin, J., Chachques, J. C., Buzanska, L., Song, M. S., & Dinnyés, A. (2022). *Regenerative Neurology and Regenerative Cardiology: Shared Hurdles and Achievements.* International Journal of Molecular Sciences, 23(2). doi:10.3390/ijms23020855
- Kistamás, K., Müller, A., Muenthaisong, S., **Lamberto, F.**, Zana, M., Dulac, M., Leal, F., Maziz, A., Costa, P., Bernotiene, E., Bergaud, C., & Dinnyés, A. (2023). *Multifactorial approaches to enhance maturation of human iPSC-derived cardiomyocytes*. Journal of Molecular Liquids, 387, 122668. doi:10.1016/j.molliq.2023.122668.
- **Lamberto, F.**, Shashikadze, B., Elkhateib, R., Lombardo, S. D., Horánszky, A., Balogh, A., Kistamás, K., Zana, M., Menche, J., Fröhlich, T., & Dinnyés, A. (2023). *Low-dose Bisphenol A exposure alters the functionality and cellular environment in a human cardiomyocyte model*. Environmental Pollution, 335. doi:10.1016/j.envpol.2023.122359.
- Horánszky, A., Shashikadze, B., Elkhateib, R., Lombardo, S. D., **Lamberto, F.**, Zana, M., Menche, J., Fröhlich, T., & Dinnyés, A. (2023). *Proteomics and disease network associations evaluation of environmentally relevant Bisphenol A concentrations in a human 3D neural stem cell model*. Frontiers in Cell and Developmental Biology, 11. doi:10.3389/fcell.2023.1236243.

International abstract and poster presentations:

- **Lamberto, F.,** Zana M., Dinnyés, A. Impact of environmental exposures on cardiac differentiation of pluripotent stem cells. The 2nd conference of the Visegrád Group Society for developmental biology, September 2021, Szeged, Hungary.
- **Lamberto, F.,** Zana M., Dinnyés, A. Evaluation of the effects of Bisphenol A levels on cardiomyocytes differentiation of human iPSCs. Microsymposium on RNA Biology, April 2022, Wien, Austria.

- **Lamberto, F.,** Zana M., Dinnyés, A. Evaluation of the effects of Bisphenol A levels on cardiomyocytes differentiation of human iPSCs. Fiatal Biotechnológusok V. Országos Konferenciája (FIBOK) - 5th National Conference of Young Biotechnologists, April 2022, Gödöllő, Hungary.
- **Lamberto, F.**, Shashikadze, B., Lombardo, S. D., Horánszky, A., Balogh, A., Kistamás, K., Zana, M., Menche, J., Fröhlich, T., & Dinnyés, A. Repeated low-dose Bisphenol A exposure induced alterations in human induced pluripotent stem cell-derived cardiomyocytes. The 57th Congress of the European Toxicologists and European Societies of Toxicology (EUROTOX), September 2023, Ljubljana, Slovenia.

10 APPENDICES

Supplementary Table 1. Primary antibodies used in this work for immunocytochemistry (ICC) analysis.

Target	Host	Catalogue number and vendor	Working dilution
OCT3/4	Mouse	sc-5279 (Santa Cruz Biotechnology)	1:50
NANOG	Rabbit	sc-33760 (Santa Cruz Biotechnology)	1:1000
TRA1-81	Mouse	sc-21706 (Santa Cruz Biotechnology)	1:500
BRACHUYRY	Rabbit	sc-20109 (Santa Cruz Biotechnology)	1:50
TUBB3	Rabbit	802001 (Biolegend)	1:1000
NESTIN	Mouse	MAB5326 (Sigma-Aldrich)	1:1000
GATA4	Mouse	sc-25310 (Santa Cruz Biotechnology)	1:50
Cardiac TNT	Mouse	ab33589 (Abcam)	1:200
NKX2.5	Rabbit	PA5-49431 (Thermo Fisher Scientific)	1:100
MLC2a	Mouse	311011 (Synaptic Systems)	1:400
MLC2v	Rabbit	109061AP (ProteinTech)	1:200

Supplementary Table 2. Secondary antibodies used in this work for immunocytochemistry (ICC) analysis.

Antibody	Catalogue number	Working dilution
*AF® 488 donkey anti-mouse	A21202	1:1000
*AF® 594 donkey anti-rabbit	A21207	1:1000

*AF® = Alexa Fluor®; all Alexa Fluor® antibodies were purchased from Thermo Fisher Scientific

Supplementary Table 3. Primers used in this work for RT-qPCR analysis

Gene	Forward sequence	Reverse sequence
*GAPDH	CTCTCTGCTCCTCCTGTTCGAC	TGAGCGATGTGGCTCGGCT
OCT3/4	AAAGCGAACCAGTATCGAGAAC	GCCGGTTACAGAACCACACT
TBXT	TGAGCCTCGAATCCACATAGTG	GCTGTGATCTCCTCGTTCTGAT
HAND1	CAGCTACATCGCCTACCTGAT	CGGTGCGTCCTTTAATCCTCTT

GATA4	AATCTAAGACACCAGCAGCTCC	GTAGTGAGATGACAGGCCAGG
NKX2.5	CCTTCTATCCACGTGCCTACAG	TTTCGGCTCTAGGGTCCTTGG
TNNT2	AAGAAGAGGAAGCAAAGGAGGC	AAAGTCCACTCTCTCTCCATCG
TNNI3	GGTGGATGAAGAGAGATACGACA	CCGCTTAAACTTGCCTCGAAG
TNNI1	CCAAGGCCAAGGAATGCTG	AATGTCGTATCGCTCCTCATCC
MYH6	CCAACGCTCCCTCAATGATTTC	CCAACTCTCCATTCTCGGTCTG
MYH7	TTCTGTCAACGACCTCACCAG	GATCAGTGCCTCCTTCTCATCC
MYL2	GAGAAACTTAAGGGAGCGGACC	TTCCCGAACGTAATCAGCCTTC
MYL7	TCAACTTCACCGTCTTCCTCAC	AGCTGCTTGAACTCATCCTTGT

* GAPDH represents the housekeeping gene

Supplementary Table 4. Conjugated antibodies used in this work for flow cytometry analysis.

Antibody	Conjugated dye	Catalogue number and vendor	Working dilution
OCT3/4	PE	130-120-310 (Miltenyi Biotec)	1:50
NANOG	APC	130-120-704 (Miltenyi Biotec)	1:50
Cardiac TNT	FITC	130-119-575 (Miltenyi Biotec)	1:100
MLC2a	FITC	130-106-141 (Miltenyi Biotec)	1:10
MLC2v	PE	130-119-581 (Miltenyi Biotec)	1:50
Ki-67	PE	556027 (BD Bioscience)	1:500
Phospho-Histone H2AX (γH2AX)	PE	12-9865-42 (Invitrogen)	1:20

Supplementary Table 5. **Results of MS-EmpiRe-based quantitative proteomics of 0.01uM BPA D21 (D21L) vs D21. Only proteins showing significant differences in abundance between D21L and D21 (FDR < 0.05, fold-change > 1.3) are listed. False-discovery rate (FDR) was controlled using Benjamini-Hochberg (BH) method.**

Genes	log2 fold change (D21L vs D21)	p-value adjusted (BH)	Differentially abundant
COL1A2	2,59	2,72E-07	upregulated_in_Myoc_D21_L
COL4A1	1,67	1,24E-06	upregulated_in_Myoc_D21_L
MYOF	1,44	9,79E-07	upregulated_in_Myoc_D21_L
TNNC1	1,26	1,94E-08	upregulated_in_Myoc_D21_L
VTN	1,20	4,87E-08	upregulated_in_Myoc_D21_L
NID2	1,19	6,45E-06	upregulated_in_Myoc_D21_L
SEC61A1;SEC61A2	1,06	5,36E-05	upregulated_in_Myoc_D21_L
COL4A2	1,04	0,00137599	upregulated_in_Myoc_D21_L

CSTB	0,96	0,033434743	upregulated_in_Myoc_D21_L
MOGS	0,91	0,031413924	upregulated_in_Myoc_D21_L
SLC2A3	0,90	3,98E-07	upregulated_in_Myoc_D21_L
TNPO2	0,83	0,042802454	upregulated_in_Myoc_D21_L
PSMD8	0,79	0,002776157	upregulated_in_Myoc_D21_L
MGST3	0,72	0,0034741	upregulated_in_Myoc_D21_L
SURF4	0,67	5,56E-05	upregulated_in_Myoc_D21_L
ARF4	0,64	0,000110401	upregulated_in_Myoc_D21_L
SERBP1	0,63	1,06E-08	upregulated_in_Myoc_D21_L
SLC25A1	0,62	0,006401702	upregulated_in_Myoc_D21_L
RPS9	0,60	3,95E-11	upregulated_in_Myoc_D21_L
MYH7	0,60	0	upregulated_in_Myoc_D21_L
DBI	0,57	0,002506063	upregulated_in_Myoc_D21_L
RPL15	0,57	0,002160952	upregulated_in_Myoc_D21_L
GPS1	0,56	0,023830253	upregulated_in_Myoc_D21_L
SNRPD1	0,56	0,029208816	upregulated_in_Myoc_D21_L
HMGA1	0,56	0,019962068	upregulated_in_Myoc_D21_L
MYO6	0,55	0,019539395	upregulated_in_Myoc_D21_L
DHCR7	0,55	0,023346085	upregulated_in_Myoc_D21_L
APMAP	0,55	0,019539395	upregulated_in_Myoc_D21_L
RPN2	0,54	7,34E-06	upregulated_in_Myoc_D21_L
TOP1	0,52	0,009262964	upregulated_in_Myoc_D21_L
TMED4	0,52	0,028821604	upregulated_in_Myoc_D21_L
FAM162A	0,52	0,000491877	upregulated_in_Myoc_D21_L
MLEC	0,51	0,007999061	upregulated_in_Myoc_D21_L
STT3A	0,50	0,001858359	upregulated_in_Myoc_D21_L
MAGED2	0,50	0,002711836	upregulated_in_Myoc_D21_L
RPS16	0,50	9,79E-07	upregulated_in_Myoc_D21_L
FEN1	0,49	0,029208816	upregulated_in_Myoc_D21_L
CANX	0,49	3,98E-07	upregulated_in_Myoc_D21_L
TNNI1	0,48	0,000323899	upregulated_in_Myoc_D21_L
SLC16A3	0,47	0,002711836	upregulated_in_Myoc_D21_L
GLUD1	0,47	3,98E-07	upregulated_in_Myoc_D21_L
HIST1H4A	0,47	1,28E-06	upregulated_in_Myoc_D21_L
TF	0,46	0,000219024	upregulated_in_Myoc_D21_L
PCK2	0,46	0,037617732	upregulated_in_Myoc_D21_L
NDUFAB1	0,46	0,007999061	upregulated_in_Myoc_D21_L
ARF1;ARF3	0,44	1,26E-05	upregulated_in_Myoc_D21_L
PRKDC	0,44	0	upregulated_in_Myoc_D21_L
RPL24	0,44	0,031413924	upregulated_in_Myoc_D21_L
EIF4A2	0,43	0,011174573	upregulated_in_Myoc_D21_L
ATP1B1	0,42	0,004325646	upregulated_in_Myoc_D21_L
SLC25A4	0,40	0,017905677	upregulated_in_Myoc_D21_L
RPL6	0,40	0,000499373	upregulated_in_Myoc_D21_L
TPM3	0,39	0,023377823	upregulated_in_Myoc_D21_L
RPL22	0,39	0,014939029	upregulated_in_Myoc_D21_L
PGRMC2	0,39	0,019539395	upregulated_in_Myoc_D21_L
LAMC1	0,39	0,000686657	upregulated_in_Myoc_D21_L
RPL13A	0,38	0,03766848	upregulated_in_Myoc_D21_L
DES	-0,39	3,98E-07	downregulated_in_Myoc_D21_L

HIST1H1C	-0,39	0,019879602	downregulated_in_Myoc_D21_L
CIAPIN1	-0,39	0,005012432	downregulated_in_Myoc_D21_L
SERPINB6	-0,40	0,017356428	downregulated_in_Myoc_D21_L
ENAH	-0,41	0,036384574	downregulated_in_Myoc_D21_L
TAGLN2	-0,41	1,07E-05	downregulated_in_Myoc_D21_L
DDT;DDTL	-0,41	0,001358565	downregulated_in_Myoc_D21_L
RPS5	-0,42	0,010326854	downregulated_in_Myoc_D21_L
AKAP12	-0,43	0,000889287	downregulated_in_Myoc_D21_L
TPT1	-0,47	0,000324577	downregulated_in_Myoc_D21_L
PDLIM3	-0,50	0,00137599	downregulated_in_Myoc_D21_L
RBM3	-0,51	0,003955695	downregulated_in_Myoc_D21_L
CHMP4B	-0,54	0,011174573	downregulated_in_Myoc_D21_L
EPS15L1	-0,54	0,047261018	downregulated_in_Myoc_D21_L
STAM	-0,55	0,023830253	downregulated_in_Myoc_D21_L
LRP1	-0,57	0,022937225	downregulated_in_Myoc_D21_L
SYNE2	-0,58	0,013743955	downregulated_in_Myoc_D21_L
NAMPT	-0,58	5,30E-07	downregulated_in_Myoc_D21_L
TMSB10	-0,74	0,011655248	downregulated_in_Myoc_D21_L
EIF1	-0,76	0,007116014	downregulated_in_Myoc_D21_L
CSRP1	-0,78	0,036617238	downregulated_in_Myoc_D21_L
SUMO2	-1,33	0,000144475	downregulated_in_Myoc_D21_L
PDLIM7	-1,94	1,74E-06	downregulated_in_Myoc_D21_L
ATXN2L	-2,37	2,65E-06	downregulated_in_Myoc_D21_L

Supplementary Table 6. Results of MS-EmpiRe-based quantitative proteomics of 0.1uM BPA D21 (D21M) vs D21. Only proteins showing significant differences in abundance between D21M and D21 (FDR < 0.05, fold-change > 1.3) are listed. False-discovery rate (FDR) was controlled using Benjamini-Hochberg (BH) method.

Genes	log2 fold change (D21M vs D21)	p-value adjusted (BH)	Differentially abundant
COL4A1	1,53	0,000116559	upregulated_in_Myoc_D21_M
VTN	1,39	0,002271246	upregulated_in_Myoc_D21_M
TNNC1	1,34	9,64E-06	upregulated_in_Myoc_D21_M
MYOF	1,27	1,27E-07	upregulated_in_Myoc_D21_M
COL4A2	1,11	3,56E-05	upregulated_in_Myoc_D21_M
NID2	1,02	0,000453088	upregulated_in_Myoc_D21_M
DPP4	0,74	0,045560306	upregulated_in_Myoc_D21_M
MYH7	0,66	0	upregulated_in_Myoc_D21_M
C1QBP	0,61	0,04821489	upregulated_in_Myoc_D21_M
RPL15	0,56	0,001789695	upregulated_in_Myoc_D21_M
DBI	0,53	0,022067879	upregulated_in_Myoc_D21_M
LAMC1	0,52	5,51E-06	upregulated_in_Myoc_D21_M
TF	0,51	0,003445996	upregulated_in_Myoc_D21_M
CYB5A	0,46	0,04821489	upregulated_in_Myoc_D21_M
ACAA1	0,46	0,006435002	upregulated_in_Myoc_D21_M
RPL6	0,46	2,71E-05	upregulated_in_Myoc_D21_M

RPS9	0,45	2,79E-05	upregulated_in_Myoc_D21_M
GLUD1	0,45	0,001789695	upregulated_in_Myoc_D21_M
ANXA4	0,40	0,00052216	upregulated_in_Myoc_D21_M
SERBP1	0,39	0,001441933	upregulated_in_Myoc_D21_M
DDT;DDTL	-0,39	0,00421023	downregulated_in_Myoc_D21_M
GLS	-0,44	0,033058456	downregulated_in_Myoc_D21_M
COX5A	-0,44	0,003098105	downregulated_in_Myoc_D21_M
ENO2	-0,45	0,001892221	downregulated_in_Myoc_D21_M
NAMPT	-0,55	1,78E-05	downregulated_in_Myoc_D21_M
USP9X	-1,88	6,17E-06	downregulated_in_Myoc_D21_M

Supplementary Table 7. **Results of MS-EmpiRe-based quantitative proteomics of 1uM BPA D21 (D21H) vs D21. Only proteins showing significant differences in abundance between D21H and D21 (FDR < 0.05, fold-change > 1.3) are listed. False-discovery rate (FDR) was controlled using Benjamini-Hochberg (BH) method.**

Genes	log2 fold change (D21H vs D21)	p-value adjusted (BH)	Differentially abundant
HSPG2	2,83292	1,49E-09	upregulated_in_Myoc_D21_H
TNNC1	1,70409	0	upregulated_in_Myoc_D21_H
COL4A1	1,16073	0,021417575	upregulated_in_Myoc_D21_H
NID2	1,09665	3,52E-05	upregulated_in_Myoc_D21_H
SEC61A1;SEC61A2	0,86757	0,022784368	upregulated_in_Myoc_D21_H
LAMA1	0,81476	0,012438524	upregulated_in_Myoc_D21_H
LAMB1	0,79687	0,014918799	upregulated_in_Myoc_D21_H
COL4A2	0,75809	0,013148226	upregulated_in_Myoc_D21_H
ARF4	0,53899	0,00427456	upregulated_in_Myoc_D21_H
LAMC1	0,48250	1,54E-05	upregulated_in_Myoc_D21_H
SERBP1	0,39364	0,005273008	upregulated_in_Myoc_D21_H
RPS5	-0,46974	0,002244793	downregulated_in_Myoc_D21_H
MPI	-0,51182	0,025987128	downregulated_in_Myoc_D21_H
RPL7	-0,55775	1,86E-05	downregulated_in_Myoc_D21_H
TJP2	-0,74990	0,020523141	downregulated_in_Myoc_D21_H
HIST1H1C	-0,82208	0,009478341	downregulated_in_Myoc_D21_H

Supplementary Table 8. Enrichment analysis of BPA-Unified core. The list shows terms in KEGG Pathway Library. Fisher's exact test and Benjamini-Hochberg threshold=0.05 (correcting for multiple comparisons) were used.

KEGG_2021_Human_Term	p-value	Adjusted p-value	Combined Score
ECM-receptor interaction	8,2E-12	3,67E-10	2582.31
Hypertrophic cardiomyopathy	8,84E-10	1,97E-08	1645.56
Dilated cardiomyopathy	1,31E-09	1,97E-08	1506.41
Cardiac muscle contraction	5,52E-08	4,97E-07	1066.98
Focal adhesion	1,11E-07	7,11E-07	541.58
Adrenergic signaling in cardiomyocytes	8,41E-07	4,73E-06	503.47
PI3K-Akt signaling pathway	3,03E-06	1,36E-05	238.9
Diabetic cardiomyopathy	9,34E-05	3,50E-04	184.43
AGE-RAGE signaling pathway in diabetic complications	2,27E-04	7,87E-04	245.59
Relaxin signaling pathway	4,81E-04	1,35E-03	171.96
Citrate cycle (TCA cycle)	5,88E-04	1,56E-03	481.77
Synthesis and degradation of ketone bodies	1,19E-02	2,98E-02	427.12

Supplementary Table 9. Genetic overlap between group of proteins of interest and diseases calculated by a Fisher's exact test + Benjamini Hochberg correction for multiple comparisons.

Disease Name	FDR
Hypertrophic Cardiomyopathy	5.318130946626812e-05
Cardiomyopathy, Hypertrophic, Familial	0.0001010286818400429
Obstructive asymmetric septal hypertrophy	0.00017650428162827554
Idiopathic hypertrophic subaortic stenosis	0.00017650428162827554
Porencephaly, Familial	0.002884604763795208
Developmental Porencephaly	0.002884604763795208
Other restrictive cardiomyopathy	0.024667404626811808

Supplementary Table 10. Enrichment analysis of BPA-Unified core with Disease Proteins Network. The list shows terms in KEGG Pathway Library. Fisher's exact test and Benjamini-Hochberg threshold=0.05 (correcting for multiple comparisons) were used.

KEGG_2021_Human_Term	p-value	Adjusted p-value	Combined Score
Hypertrophic cardiomyopathy	2,76E-14	4,69E-12	1846.2
Dilated cardiomyopathy	2,86E-12	2,43E-10	1270.03
ECM-receptor interaction	6,52E-11	2,77E-09	1059.03
Focal adhesion	9,20E-11	3,13E-09	569.14
Relaxin signaling pathway	1,43E-09	4,04E-08	606.81

Fluid shear stress and atherosclerosis	2,58E-09	6,28E-08	543.87
AGE-RAGE signaling pathway in diabetic complications	7,03E-09	1,49E+09	623.48
Estrogen signaling pathway	6,27E-08	9,70E-07	393.27
Cardiac muscle contraction	9,86E-08	1,40E-06	516.09
PI3K-Akt signaling pathway	2,90E-07	3,79E-06	179.03
Diabetic cardiomyopathy	9,09E-07	1,10E-05	218.07
Adrenergic signaling in cardiomyocytes	2,47E-06	2,62E-05	231.64
IL-17 signaling pathway	4,50E-06	4,25E-05	292.27
Lipid and atherosclerosis	1,94E-05	1,65E-04	133.66
Arrhythmogenic right ventricular cardiomyopathy	4,78E-05	3,69E-04	225.72
TNF signaling pathway	2,05E-04	1,29E-03	130.0
Chemical carcinogenesis	3,84E-04	2,25E-03	70.48
Apoptosis	5,06E-04	2,87E-03	90.78
GnRH signaling pathway	1,82E-03	8,38E-03	85.2
cAMP signaling pathway	2,39E-03	1,04E-02	46.84
Citrate cycle (TCA cycle)	2,75E-03	1,17E-02	167.76
HIF-1 signaling pathway	2,87E-03	1,19E-02	67.1
MAPK signaling pathway	7,12E-03	2,63E-02	27.93
NOD-like receptor signaling pathway	1,16E-02	3,81E-02	30.28
Mitophagy	1,35E-02	4,10E-02	51.84
Adherens junction	1,47E-02	4,10E-02	48.63

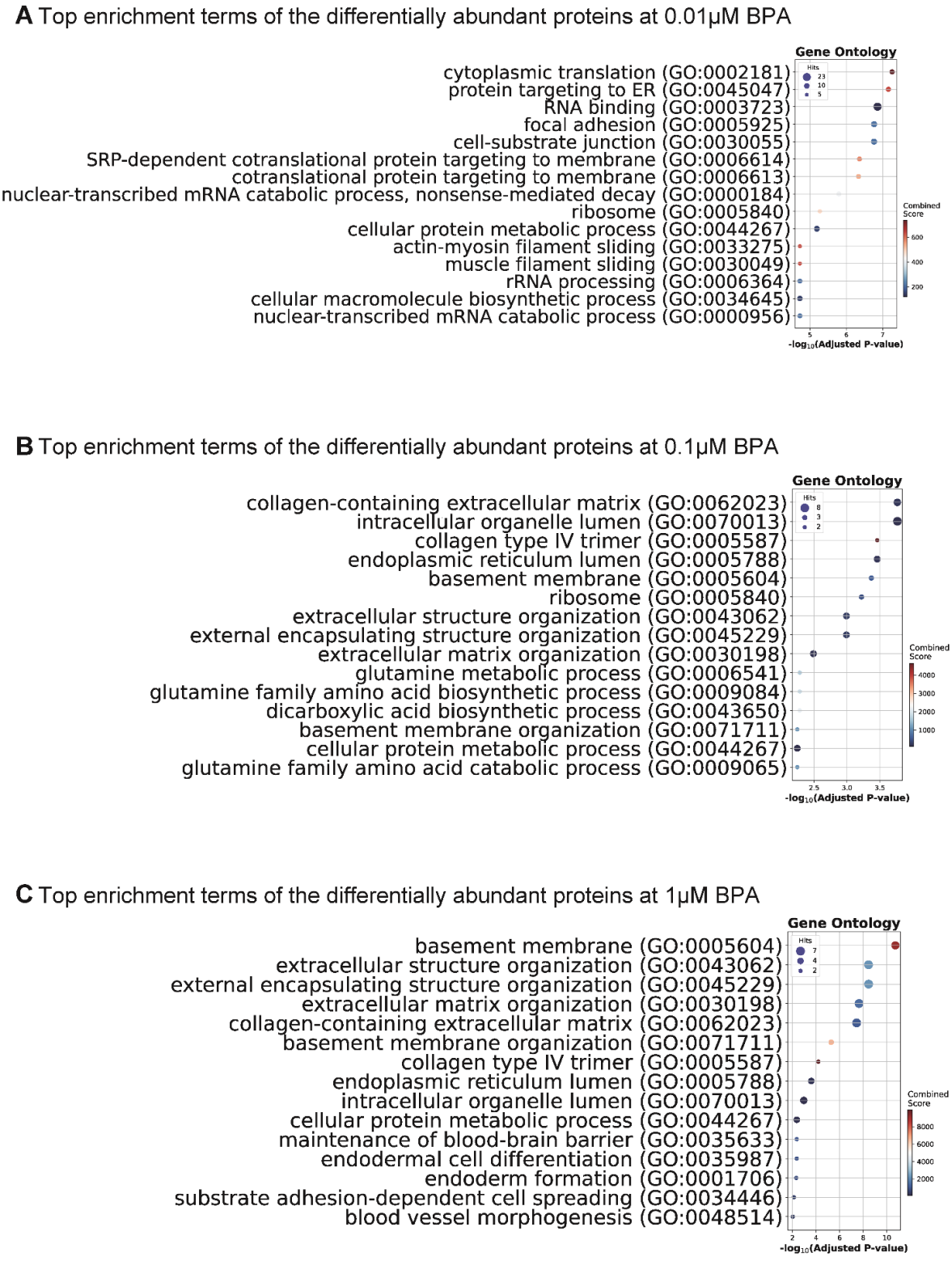

Supplementary Figure 1. Bubble plot of the top 10 enriched terms of the differentially abundant proteins at 0.01 µM (**A**), 0.1 µM (**B**), 1 µM (**C**) BPA concentration with the 3 main branches of the gene ontology (GO) (biological processes (BP), molecular functions (MF), and cellular components (CC). Bubbles are placed based on their -log10 p-value. Bubble size corresponds to the number of proteins that are found in each term, while their colour reflects the enrichment combined score.

11 ACKNOWLEDGEMENTS

I sincerely thank my supervisor Professor András Dinnyés, for the opportunity to carry out my doctoral study on this exciting, novel project. I would like to thank him for the valuable guidance, insights, and support on my research project, as well as for the opportunity to participate in several conferences and international meetings, which provided me the chance for networking with the scientific community, supporting my professional development.

My sincere gratitude to my co-supervisor Dr Melinda Zana, for her continuous support and encouragement during my PhD study. I am thankful for the hours spent together to discuss, plan, and investigate this research project, either to keep me on track, but also to provide me high scientific motivation. Her guidance and knowledge helped me in research, as well as writing articles and thesis.

I am extremely grateful to the DohART-NET consortium, including PIs of invaluable scientific expertise and highly motivated ESRs. Particularly, I would like to express my deepest gratitude to Irene Peral-Sanchez, Bachuki Shashikadze and Salvo Lombardo for the fruitful collaborations, their valuable scientific skills, and friendship. I thank Dr Sandrine Willaime-Morawek, my external co-supervisor, for the guidance and all the useful discussions, and Dr Thomas Frohlich, for the valuable opportunity to conduct my secondment at the Gene Center in Munich, performing the proteomics-based analysis. All the time spent together was a great experience and I sincerely wish all ESRs the best of luck in accomplish their careers and dreams in the future!

I am very grateful to Ms Zsuzsanna Tassy and Ms Edit Simáné Dolányi of MATE University, for their reliability and continuous assistance during the doctoral school studies.

I also would like to extend my sincere thanks to the whole Biotalentum team, especially to Emi Ivók for helping and guiding me the first time I arrived in Hungary; Pukky Polgari for introducing, training, and guiding me throughout the cell work; Marcsi Bódi-Jakus for being always ready to help; Andrea Balogh for her immense knowledge and all the help given during the darkest moments. I thank all my colleagues: Geta Serbana, Ingrid Csordás, János Farkas, Vivien Réka, Balázs Széky, Anita Fehér, Kornél Kistamás, and many others. I also thank Ildikó Nagy, Mariann Jakab, Edina Hajdu, Timea Halmosi and Katalin Bazan for their crucial work and support behind the research scene.

Words cannot express my gratitude to the friends that made my PhD experience unforgettable: Linda Francistiová and Kinga Vörös for the warm support, many de-stress coffee sessions, and a lasting friendship; Alex Horánszky for relieving the anxiety and stress over this journey.

A devoted and special thanks to Fabio, for always believing in me, being there for me during the brightest and darkest days, and for bringing light, wisdom and love every day.

Last, but not least, I want to thank my family for their solid trust, and deep love. Thanks to my mum Daniela and my dad Sergio for imparting some of their courage in me, for teaching me the value of the hard work and resilience, and for always supporting me beyond whatever physical distance.

This project has received funding from the European Union's Horizon 2020 research and innovation program under the Marie Skłodowska-Curie grant agreement No. 812660 (DohART-NET) and under grant agreements No. 953138 (EMAPS-Cardio), and the Hungarian Grants No. 2020–1.1.5-GYORSÍTÓSÁV-2021-00016 and No. TKP2021-EGA-28 from the National Research, Development and Innovation Fund.